Meteorological Adjustment of Western Washington and Northwest Oregon Surface Ozone Observations with investigation of Trends

Joel H. Reynolds Barnali Das Paul D. Sampson

Peter Guttorp

NRCSE

Technical Report Series

NRCSE-TRS No. 015

Meteorological Adjustment of Western Washington and Northwest Oregon Surface Ozone Observations with investigation of Trends*

Joel H. Reynolds Barnali Das Paul D. Sampson
Peter Guttorp
Dept. of Statistics, University of Washington
National Research Center for Statistics and the Environment

June 29, 1998

Abstract

Daily 1 and 8 hour maximum surface ozone records from 9 monitors in Western Washington and Northwest Oregon were used to construct a univariate regional daily composite of surface ozone activity which was then adjusted for both regional surface and mesoscale meteorology, and, subsequently, regional estimated emissions rates. The regional composites were derived from a Canonical Covariance Analysis. Both daily 1 and 8 hour maximum surface ozone regional composites displayed increasing long term trends after meteorological adjustment; neither revealed any association with the regional emissions composite after meteorological adjustment. The current results are contrasted with a previous analysis of a subset of the data ([Harris 94]).

1 Introduction

Tropospheric ozone is known to reduce both human and vegetation health as well as decrease visibility ([NRC 91], [Wax 91]). In response to this, the EPA has instituted air quality standards, with recently proposed revisions ([EPA 95]), that each state must meet or else face noncompliance. In order for a state to develop plans for controlling ozone exceedences, it must determine the extent to which historical trends in ozone levels can be attributed to increases in precursor emissions (NOx, VOC) rather than to increases in the occurrence of meteorological conditions conducive to the formation of ozone from these precursors ([NRC 91]).

Meteorologically-adjusted ozone is obtained by statistically modeling the association between surface ozone observations and meteorological variables generally collected nearby ([NRCSE 98]). Most trend analyses model meteorological data from a single location with

*Washington Dept. of Ecology Contract C9700093

ozone observations from a single monitor ([NRCSE 98]). In the cases where a spatial network of ozone monitors is available, the literature contains two basic approaches to modelling the association between ozone and meteorology ([NRCSE 98]): independently model the dependence of ozone response for each monitor or model the dependence of an ozone network summary (e.g., median daily 1 hour maximum ozone from the network ([Bloom 96])). Fitting ozone monitor- specific models directly to local surface meteorology ignores any information content on regional dynamics of meteorology and ozone in the simultaneous analysis of the whole ozone network (Figure 1); using an ozone network summary captures more of this regional information. The literature contains no trend analyses associating ozone network observations with a spatial network of meteorology observations. If spatial meteorological observations are available, using data from only a single location ignores information on regional-scale meteorological influences on ozone production.

Washington Department of Ecology has operated a network of surface ozone monitors along the Puget Sound corridor since the early 1970's (see Section 2). Recent work demonstrates regional-scale meteorology as a driving component of Western Washington's extreme ozone events ([Recker 97], [Mass 97]), either through non-local production and transport of ozone driven by regional-scale meteorology or via regional meteorology that acts to 'retain' locally produced ozone. The analysis reported here records our efforts to model the regional-scale association between the Western Washington ozone monitor network and selected meteorology variables (see Section 2).

The analysis determines the dominant patterns of association between the ozone network and the meteorology and emissions spatial fields by applying Canonical Covariance Analysis to their temporal cross-correlation matrix (see Section 3). Canonical Covariance Analysis provides the linear combination of ozone monitors and linear combination of meteorology and emissions variables which best represent, respectively, the dominant ozone and {meteorology, emissions} spatial patterns underlying the regional association. These univariate regional summaries are then analyzed with multiple linear regression to produce a meteorologically-adjusted regional ozone summary, which is further analyzed for both association with the regional emissions summary and for the presence of long-term trend.

2 Data Sources, Selection and Description

2.1 Ozone data

The ozone data consists of hourly measurements from eight Washington Department of Ecology ozone monitors in Western Washington, and one monitor from the Portland, Oregon region. A Washington monitor record was included if it had been active for eight or more seasons(Table 1, Figure 2).[1] The number of active monitors varied from season to season, with an average of seven active monitors during any season in the last decade (Table 2). A monitor was considered active during the ozone season (defined by Washington Department of Ecology as April 1 to October 31) if observations were available for at least half of the

[1]The Port Angeles monitor, while having a record of eight seasons, was excluded from the analysis due to its lack of signal and its distinct meteorological regime compared to that experienced by monitors found along the Puget Sound corridor.

Figure 1: Relationship of co-occurring daily maximum 1 hour ozone readings across each pair of monitors in the network. Stripes arise from monitor precision.

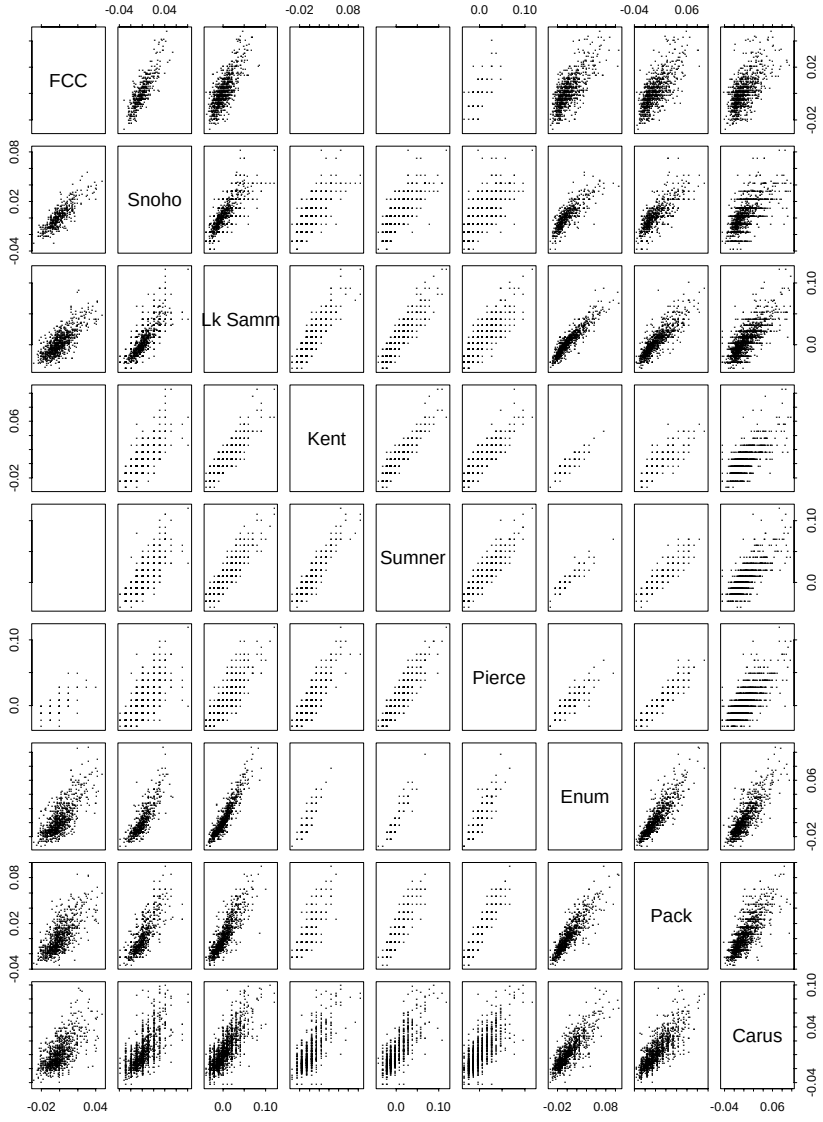

Table 1: Department of Ecology Monitors used in the analysis.

Name	County	ID	Record Period
FCC	Whatcom	3700006	4/89 - 7/96
Snohomish Fire Dist. 22	Snohomish	3100002	4/78 - 7/96
Lake Sammamish	King	1700002	1/76 - 7/96
Kent (86 Ave. South)	King	1740K63	7/74 - 10/86
Sumner Jr. High	Pierce	2780P12	6/78 - 10/88
Pierce County Fire Dist.	Pierce	2700002	6/78 - 10/89
Enumclaw (Weyerhauser)	King	1700007	8/85 - 7/96
Pack Forest	Pierce	2700007	5/85 - 7/96
Carus (Portland, OR)	Clackamas	-	5/77 - 7/96

days in the season. As a collection, the selected monitoring sites were active from 1974 (86 Ave. South, Kent) to October 1996 (Table 2). Given the sparseness of the network in the initial years, our analysis concentrated on the record period 1978 - 1996.

Maximum 1 hour and maximum 8 hour average ozone readings were calculated as daily summaries of each monitor's record. Following the EPA Region X guidelines, these daily maximum are defined over the following intervals:

maximum 1 hour average from 9 am - 9 pm PST

maximum 8 hour average from 7 am - 11 pm PST

Plots of daily ozone summaries across the April 1 - October 31 season clearly demonstrate the occurrence of two peaks: a spring peak during April - May and a late summer peak during July - August (Figure 3). Research has shown that spring peaks in surface ozone often occur due to vertical transport of stratospheric ozone down into the troposphere ([Logan 85], [Wool 97], [Harris 94]). The ozone season was redefined as June 1 - September 30 to avoid confounding the meteorological drivers of the spring nonanthropogenic ozone peaks with those of the mid- to late-summer anthropogenic peaks ([Wool 97]). October was dropped from the analysis as it represented a shift to a different weather regime and there was little ozone signal. The revised ozone season definition concurs with that chosen by Figuroa et al ([Fig 95]) as the period most conducive to ozone formation in Western Washington.

2.2 Surface Meteorology Data

Maximum daily temperature (degrees Fahrenheit) and precipitation (inches) from the active surface meteorology station nearest each ozone monitor were obtained from the Cooperative Observer Network Database of the National Climatic Data Center (NCDC) ([Hydro 95]) (Table 3). Surface meteorology was limited to these variables as they were the only measurements universally available across the surface meteorology monitoring sites.

The surface meteorology records vary in their completeness (Figure 4). Considered as a network, complete records (both temperature and precipitation) exist for 65% of the analysis period, (84% if Kent is dropped). Considering just surface temperature, the records are 72% complete for the period (84% if Kent is dropped). Precipitation is an indicator only of

Table 2: Ozone monitors active each year, 1974 - 1996.

Site	1974	75	76	77	78	79	80	81	82	83	84	85	86	87	88	89	90	91	92	93	94	95	96	**Total**
FCC																x	x	x	x	x	x	x	x	8
Snohomish					x	x	x	x	x	x	x	x	x	x	x					x	x	x	x	15
Lake Sammamish			x	x	x	x	x	x	x	x	x	x	x	x	x	x	x	x	x	x	x	x	x	21
Kent	x	x	x	x	x	x	x	x		x	x	x	x											12
Sumner					x	x	x	x	x	x		x	x		x									9
Pierce					x	x	x	x	x	x	x	x	x	x	x		x	x						12
Enumclaw													x	x		x	x	x	x	x	x	x	x	10
Pack Forest												x	x	x	x	x	x	x	x	x	x	x	x	12
Carus				x	x	x	x	x	x			x	x	x	x	x	x	x	x	x	x	x	x	18
Total	1	1	2	3	6	7	7	7	6	6	4	8	9	7	6	7	7	7	6	8	8	8	8	

Figure 2: Western Washington and Northwest Oregon ozone monitors (x) and surface meteorology sites (m) analyzed. See Table 1 for ozone monitor details, Table 3 for surface meteorology sites. The Columbia River forms the state boundary shown in the lower 1/3 of the map.

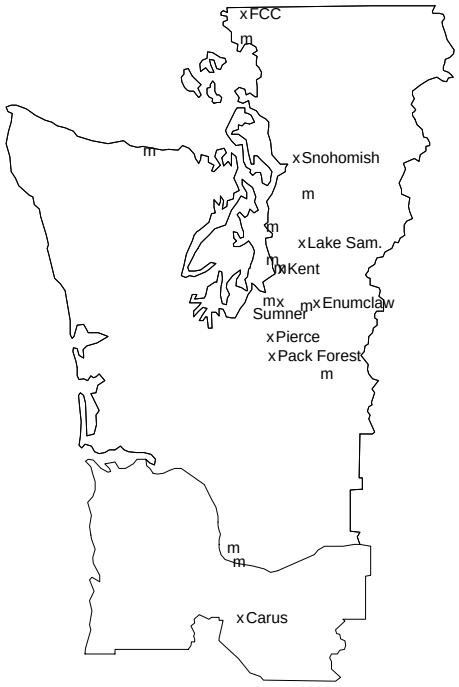

Table 3: Nearest National Weather Service/NOAA Cooperative Observer Network surface meteorology station.

Ozone Monitor	**Nearest Surface Station**	**Station ID**[a]
FCC	Bellingham Airport	574
Snohomish	State EMSU	7458
Lake Sammamish	State EMSU	7458
Kent	SeaTac Airport and Kent[b]	4169
Sumner	Puyallup 2 W exp	6803
Pierce	Puyallup 2 W exp	6803
Enumclaw	Buckley 1 NE	945
Pack Forest	Longmire Rainier	4764
Carus	Portland Airport[c]	6751

[a]Cooperative Observer Network ID

[b]Kent meteorology was later dropped due to missing observations.

[c]Surface meteorology from Vancouver, Washington is also used in the analysis.

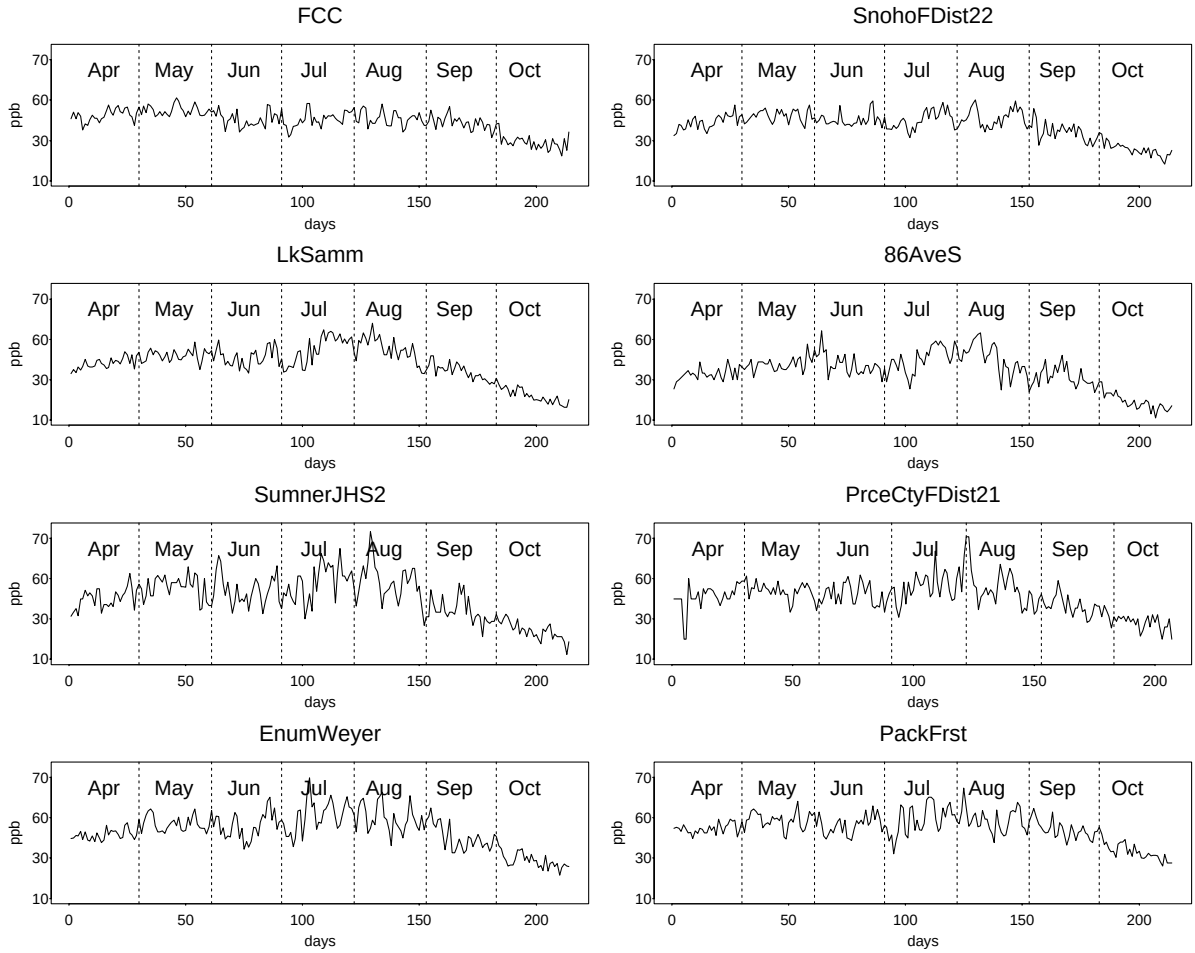

Figure 3: Median daily maximum 1 hour ozone reading, by monitor, taken across all available years for that day of year, (e.g., median June 1st reading).

Table 4: NCEP/NCAR Reanalysis Fields Selected for Analysis

Variable	Description (units) [a]	Grid [b]	Reliability [c]
Ht1000	Mean[d] geopotential height of 1000 mbar pressure field (m)	L	A
Ht850	Mean geopotential height of 850 mbar pressure filed (m)	L	A
T1000	Mean temperature of 1000 mbar pressure field (K)	L	A
T850	Mean temperature of 850 mbar pressure field (K)	L	A
T2m	Mean temperature 2 m from surface (K)	S	B
Wind Speed	Mean wind speed 10 m from surface (m/s)	S	B
Wind Direction	Mean wind direction 10 m from surface (from East)	S	B
Ppt	Daily mean precipitation (kg/m^2)	S	C

[a] All variables are spatial means over the grid cell.

[b] L - large: 2.5 degree latitude x 2.5 degree longitude grid; S - small: 'T62 Gaussian grid' 1.875 degree latitude x 1.9047 degree longitude.

[c] See Reliability Classifications in text.

[d] Daily means (0400, 1600 PST).

low ozone, which is also indicated by low surface temperature. Given the reduction in the network record caused by the missing precipitation values, surface precipitation was dropped from further consideration in the analysis.

2.3 Reanalysis Meteorology Data

Gridded tropospheric and surface boundary meteorological data were obtained from the National Center for Environmental Prediction (NCEP)/National Center for Atmospheric Research (NCAR) Reanalysis Project (http://www.cdc.noaa.gov) as representative measures of regional meteorology characteristics ([Kalnay 96]). The reanalysis project uses a state-of-the-art global atmospheric model combined with as complete a database as possible to provide a variety of spatially-gridded meteorological fields.

The predicted fields differ in their spatial and temporal resolution, as well as in their reliability ([Kalnay 96]). NCEP provides a four-level classification of variable reliability, though we are only concerned with the first three classifications:

A variables strongly influenced by observed data (and hence most reliable),

B variables partly defined by observations but which are strongly influenced by the model characteristics (and hence should be interpreted with caution),

C variables not directly observed whose values are derived solely from the model (and hence should be interpreted with caution),

D variables obtained from observed data with no dependence on the model.

The meteorological fields selected for analysis, their spatial grid dimension, temporal resolution, and reliability are given in Table 4. The spatial grids of the reanalysis data are shown in Figure 5.

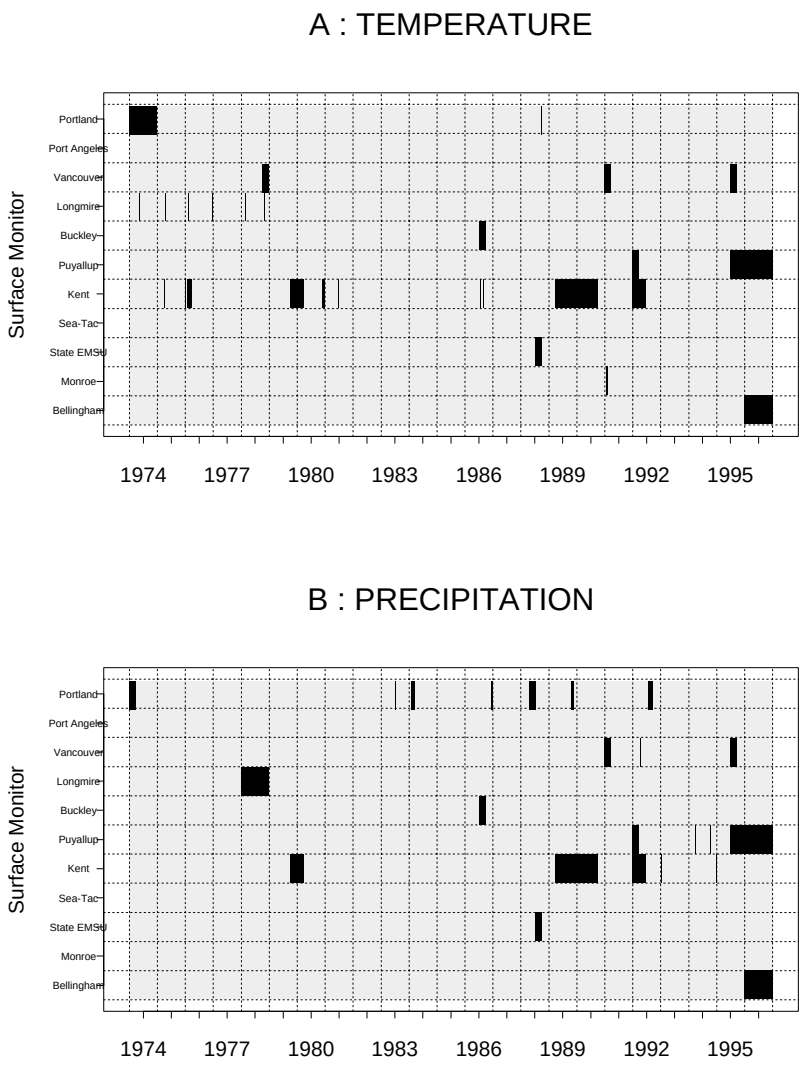

Figure 4: Availability of surface meteorology records, by site, for June 1 - September 30 each year. Black denotes missing records.

Figure 5: Study region with Reanalysis Meteorology grids overlain. Solid lines demarcate the inner core of the large grid (3x3), dashed lines demarcate the inner core of the smaller grid (4x4). Not shown is the horizontal boundary for the smaller grid which occurs directly above the U.S. - Canada border.

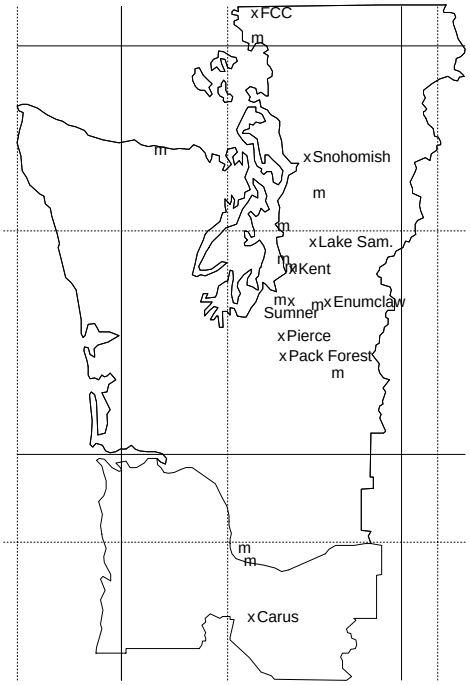

Discussion of known problems or caveats regarding the reanalysis project predictions can be found at http://www.cdc.noaa.gov/cdc/reanalysis/problems.htm. Those of importance to this analysis concern the calculation of the near surface variables T2m, Wind Magnitude, Wind Direction, and Ppt (Table 4). Based on exploratory data analysis, and in light of both the extreme uncertainty surrounding the reanalysis precipitation data and the fact that is associated only with low ozone (which is again revealed by low 2m temperature (T2m)), precipitation was dropped from the reanalysis variables under consideration.

2.4 Emissions Estimates

Estimates of daily total NO_x and VOC (grams) emissions on a 100 x 100 km grid (Figure 6) were provided by Sally Otterson of Washington Department of Ecology. The daily totals were developed from estimates from each of the five major source categories: onroad mobile, stationary area sources, nonroad mobile sources, large point sources, and biogenic sources. The details of the temporal and spatial interpolation required to generate estimates on the time and space scales appropriate to this analysis are given in Appendix E.

Figure 6: Study region with emission estimation grid overlain. The northernmost grid boundary, directly above the U.S. - Canada border, is not shown.

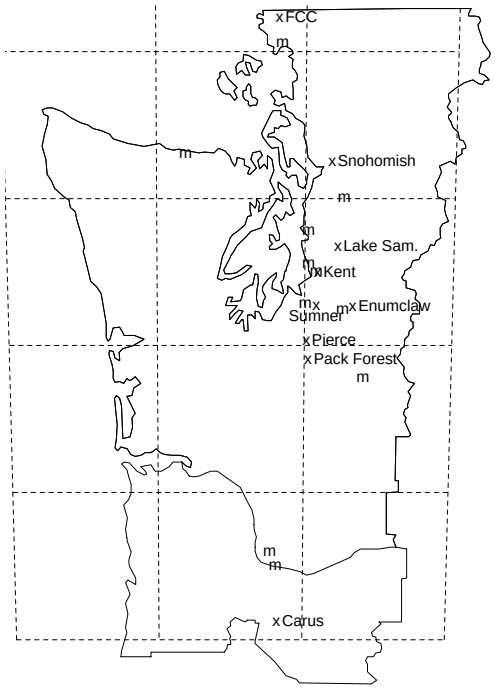

3 Method

3.1 Approach

Exploratory data analyses of the ozone monitor records and the various meteorological variables demonstrate common relationships across the ozone monitor network (e.g., Figure 1 and contents of Appendix A). This suggests it is reasonable to view the relationship between maximum daily ozone and meteorology on a regional scale, and to pursue an analysis which will reveal the dominant patterns of association between the ozone spatial field (defined by the 9 ozone monitors) and the multivariate meteorological and emissions spatial field (defined by the various grid-specific meteorological and emissions records and the surface temperature network records). Preferably, the method chosen to reveal the temporal coupling of these two spatial fields will also provide a means of deriving univariate summary measures for each field which approximate this coupling. The association between the summary measures can then be modeled with standard regression techniques to obtain a regional ozone summary which is meteorologically adjusted.

The network median daily 1 hour maximum ozone has been used as a regional ozone summary ([Bloom 96]). However, we have no reason to assume a priori that this ozone network summary will reveal the dominant patterns of association with the meteorology and emissions field, nor is there an obvious a priori regional summary of this field.

The temporal cross-correlation matrix of the ozone x {meteorology, emissions} field summarizes the association between each ozone monitor and each spatial record of the meteorological and emission variables (see Appendix A), and hence summarizes the patterns of association between these spatial fields. Canonical Covariance Analysis applies the singular value decomposition (SVD) to the cross-correlation matrix to reveal ([Breth 92], [Wall 92]):

- the number of dominant patterns of association among the ozone monitors and spatial {meteorology, emissions} variables which combine to optimally approximate the observed cross-correlations[2]; as well as
- the weight coefficients used to produce the linear combination of ozone monitors and the linear combination of spatial {meteorology, emissions} variables which best approximate, respectively, the ozone and {meteorology, emissions} components of each of these dominant patterns of association[3].

[2]See [Breth 92] for a detailed description of this use of the SVD. 'Optimality' here means maximizing the cumulative squared covariance fraction (CSCF): Let $\tilde{C}_{Napprox}$ be the rank N approximation to the cross-covariance matrix reconstructed from the first N SVD patterns, C_{obs} be the observed cross-covariance matrix. Then the

$$CSCF_N = 1 - \frac{\|\tilde{C}_{Napprox} - C_{obs}\|^2}{\|C_{obs}\|^2}$$

where

$$\|C\|^2 = \sum_i \sum_j C_{ij}^2$$

. Note that if all variables are normalized, the cross-correlation and cross-covariance matrices are identical.

[3]The weight coefficients $\{w_i\}$, $\{v_j\}$ are chosen to maximize the $\mathrm{cov}(\sum w_i Ozone_i, \sum v_j Meteorology.or.Emission_j)$ under the restriction that each field's set of weight coefficient vectors (one vector for each pattern) are orthonormal. This differs from Canonical Correlation

We can thus model the pattern of association between the fields by

1. calculating each field's weighted linear combination of variables for each of the dominant patterns[4], (i.e., one time series for each field for each dominant pattern),

2. combining these pattern summaries for the most informative N patterns to achieve a univariate approximation to this field's component of association, (i.e., one time series for each field, approximating the coupling between the two spatial fields),

3. modeling the univaraite approximation to the ozone field as a response to the univariate approximation of the meteorology field, thus producing a residual time series which represents the meteorological-adjusted ozone network summary.

This approach allows us to utilize the full spatial networks of both ozone and meteorology in deriving our daily ozone network summary and it's association with meteorology. Furthermore, it is less restrictive in devising the optimal ozone network summary than any a priori statistic selection.

In order to derive the coupling between the ozone spatial field and the other spatial fields, we conduct one SVD on the cross-correlation matrix containing both the meteorology and the emissions variables. In order to meteorologically adjust the ozone summary, we separate the summary of the dominant {meteorology, emissions} pattern, $\sum_j V_j Met.or.Emission_j$ into two components, $\sum_j V_j Meteorology_j$ and $\sum_k V_k Emissions_k$. Fitting the ozone summary to the first component provides a meteorologically adjusted network ozone summary. The presence of long term trends is measured by Spearman's rank correlation. Association between the meteorologically adjusted network ozone summary and the emissions summary is investigated by regression.

3.2 Implementation Details

The above description summarizes our usage of canonical covariance analysis but ignores important details in undertaking the proposed analysis. We identify these issues and how we've addressed them below.

3.2.1 Linearizing Transformations

As it is not reasonable to assume that the relationship between ozone and the 'raw' predictor variables is linear ([NRC 91]), transformations for each predictor variable where utilized

Analysis (CCA) in this orthonormality restriction on the weight coefficients for the patterns. The restriction to orthonormal patterns allows one to reconstruct an optimal approximation to a field's original time series from the linear combination of selected patterns (where here 'optimal' refers to the property that the residual time series, i.e. the true time series - approximate time series, is orthogonal to each of the patterns which were combined to form the approximation) ([Breth 92]).

[4]Each pattern is associated with scalar called a singular value, σ. A measure of the importance of the k^{th} pattern is obtained from

$$\frac{\sigma_k^2}{\sum_j \sigma_j^2},$$

which is equal to the fraction of the total squared covariance in the observed cross-covariance matrix explained by the approximation based on this particular pattern. See [Breth 92].

to achieve an approximately linear relationship with each ozone monitor response. Specifically, the alternating conditional expectation (ACE) algorithm ([Hastie 90]) was applied to each meteorological variable separately in association to each ozone monitor record. As employed here, the procedure derives a nonparametric transformation of the specific meteorology or emissions variable which maximizes its linear correlation with a chosen ozone monitor record. For example, this procedure allows for a potentially different linearizing nonparametric transformation of the reanalysis variable Wind Direction in the NW grid cell for each ozone monitor (Figure 7). The consistency of a given predictor variable's transformations across ozone monitors reinforced the regional perspective of surface ozone in Western Washington (Appendix B). The final transformation chosen for each predictor variable was derived by fitting a nonparametric smooth to the average transformed value, where the average is taken across ozone monitors[5] ('Final Transformation' in Figure 7). This procedure was applied independently to each meteorology and emission variable before generating the cross-correlation matrix used in the SVD. Appendix B contains graphical displays of the each predictor variable's 'ozone monitor'-specific transformations as well its final transformation.

3.3 Calculating Univariate Summaries

3.3.1 Imputation of Missing Observations

The calculation of a spatial field's univariate summary from the dominant pattern's weight coefficients requires that records are available for every site in the spatial field every day. The data obviously do not satisfy this requirement (Table 2, Figure 4).

In the case of missing predictor variables (i.e., surface temperature), there is no justification for imputing the missing records as we don't have grounds for assuming a consistent relationship amoung variables. This is especially true of the surface meteorology which is much more volatile than the reanalysis estimates. Days with incomplete meteorology network records must simply be dropped from the analysis. This was the reason the Kent surface meteorology monitor was dropped from the network.

This is not true in the case of missing response variables (ozone records). The underlying assumption of a regional-scale analysis is that ozone is a function of regional meteorology, and, therefore, on a given day there is a discernible relationship among the ozone sites. Statistically, we are assuming a temporally stationary spatial covariance matrix, $\sum_{ozone}$, across the ozone network. We can impute missing ozone monitor records for a given day from the ozone monitors observed that day by regression equations constructed from the estimated covariance matrix, $\hat{\sum}_{ozone}$.

In the presence of missing data, the covariance matrix is estimated using the Expectation-Maximization (EM) algorithm ([Little 86]). Technical details are provided in Appendix D. Note that the imputed ozone values are only used in the construction of the daily ozone network summary; the cross-correlation matrix used to generate the weight coefficients is based solely on the observed values.

[5]Specifically, a b-spline with 10 df ([Hastie 90]) was fit to averages of predictor values which had observations from five or more ozone monitors.

Figure 7: Ace-derived transformations of Wind Direction (in radians from E) in the NW grid cell. The transformation in each plot is chosen to maximize the correlation with the ozone monitor labelling the plot. The x-axis displays the untransformed variable , the y-axis the transformed value specified only to relative scale. The last plot shows the final transformation selected for Wind Direction, derived as explained in the text.

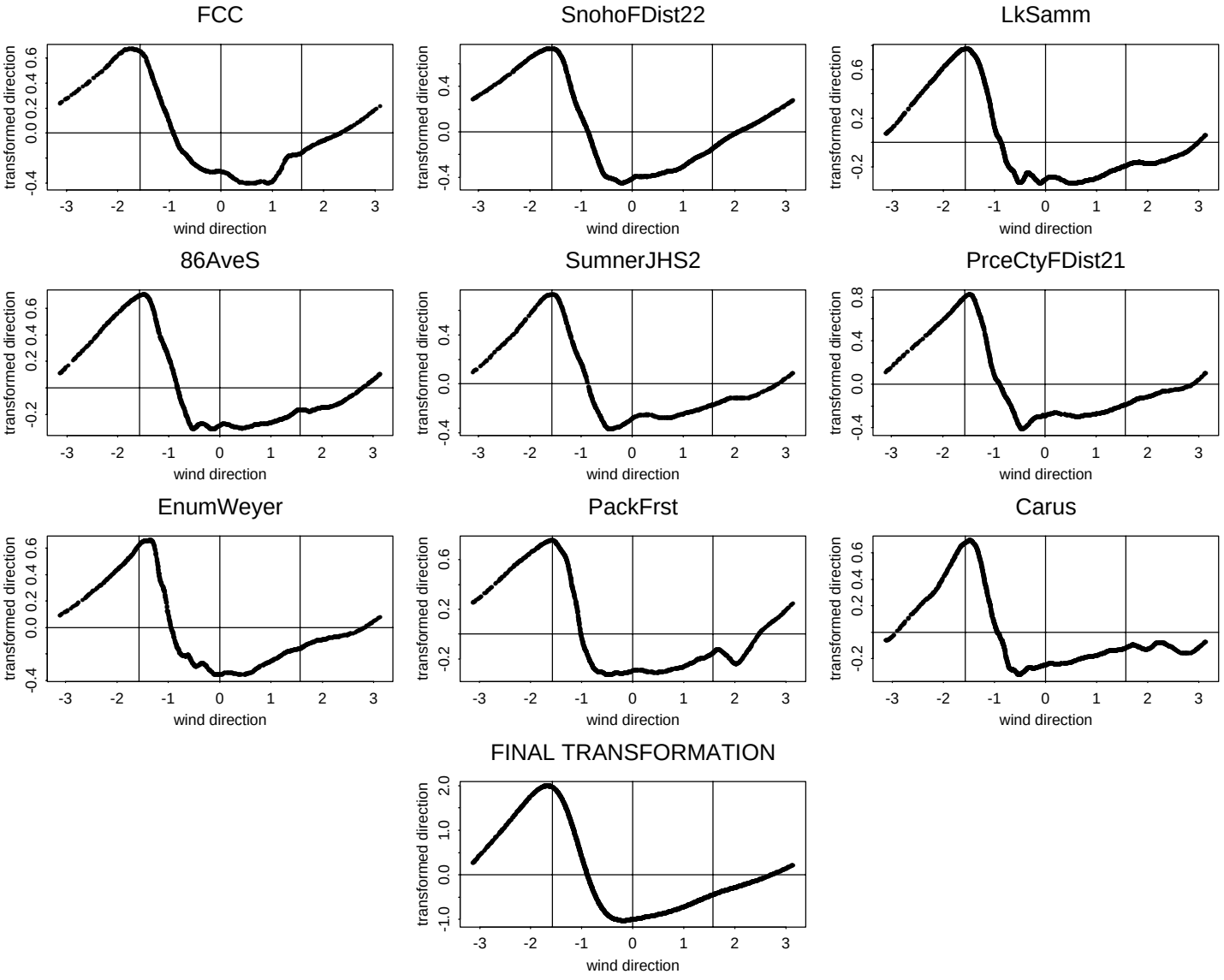

3.3.2 Composite Summary Calculations

As discussed earlier, separate univariate summaries are derived for the meteorology field and the emissions field, though the weight coefficients for each are determined from a single SVD of the cross-correlation matrix of ozone with the variables in both fields. Furthermore, as the meteorology variables are naturally partitioned as either direct surface measurements or sythesized reanalysis estimates, separate univariate composite summaries are formed for each. Thus, four composite variables are derived from the SVD:

comp.03 the univariate daily ozone network summary,

comp.RAmet the univariate daily summary of the reanalysis meteorology fields,

comp.Smet the univariate daily summary of the maximum surface temperature field,

comp.Emiss the univariate daily summary of the emission field.

The relationship between comp.03 and the other variables is the focus of the modelling analysis.

3.3.3 Modelling Issues

It is reasonable to consider interactions between the composite meteorology variables as these would not necessarily be picked up by the SVD. It is also reasonable to consider short term lag effects in the modelling (i.e., seasonal trends), if necessary. In order to maintain interpretability only lagged versions of the composite meteorology variables are considered, as opposed to composites of lagged and non-lagged meteorology variables.

3.3.4 Investigation of Long Term Trend

Spearman's rank correlation is used as a robust method of investigating long term monotonic trends in the meteorologically adjusted ozone network summary, as well as the further emissions-adjusted meteorologically adjusted ozone network summary. In each case, the rank correlation is calculated between the appropriate adjusted ozone summary and a variable recording the time index. The complete analysis sequence followed for each daily ozone summary (1 hour maximum, 8 hour maximum) is:

1. Calculate linearizing ace transformations for meteorology and emissions variables,
2. Calculate ozone x {meteorology, emissions} cross-correlation matrix,
3. Calculate SVD of cross-correlation matrix,
4. Calculate the univariate composite summaries for the dominant coupling patterns of reanalysis meteorology, surface meteorology, and emissions with ozone,
5. Regress comp.03 on comp.RA met and comp.Smet,
6. Calculate Spearman's rank correlation of meteorologically adjusted ozone summary and time index,

7. Regress meteorologically adjusted ozone summary on comp.Emiss,

8. Calculate Spearman's rank correlation of meteorology and emissions adjusted ozone summary and time index.

4 Results

4.1 Linearizing Transformations

The transformations for each predictor variable are displayed in Appendix B. The resulting cross-correlation matrices are shown in Appendix A.

4.2 Singular Value Decompositions

4.2.1 Daily 1 hour maximum ozone

The SVD of the cross-correlation matrix revealed one dominant pattern of association between the ozone field and the {meteorology, emissions} field (plot A in Figure 8). The rank one approximation to the observed cross-correlation matrix derived from this dominant pattern accounts for 99.99% of the observed matrix's cummulative squared covariance. I.e., only a single set of univariate summaries is needed to capture the association between the two fields.

The weight coefficients of this dominant pattern reveal the relative contribution of each standardized variable to the composite summaries (plots B and C in Figure 8). The variation in coefficients within a variable revals the spatial variation in the strength of association between the variable and the opposing field (and hence the weights in plot B are affected by the spatial locations of the ozone monitors). Note that the emissions coefficients contribute little to the dominant component and reveal little spatial variation.

The weight coefficients for the ozone component of the dominant pattern of association are almost uniform (plot C, Figure 8). The univariate composite summary of the ozone network is therefore approximately proportional to the mean network (standardized) ozone observation.

4.2.2 Daily 8 hour maximum ozone

The SVD results for the daily 8 hour maximum ozone statistic are approximately identical to those found for the daily 1 hour maximum (figure 9).

4.3 Imputation and Composite Calculations

Missing ozone observations were imputed, following the procedure outlined in section 3.3.1 and Appendix D, to allow calculation of the daily ozone network summary, comp.03. The imputation regressions were derived from the estimated ozone network covariance matrices (Appendix D). Though observations from 1978-1996 were used in estimating the cross-correlation matrix employed in the SVD, composite summaries were only calculated for 1978-1995 due to the unavailability of 1996 surface meteorology data.

Figure 8: SVD results for daily maximum 1 hour ozone analysis. Plot A - % of the observed cross-correlation matrix's cumulative squared covariance captured by the rank 1 approximation derived from each singular value (see footnote 4). Plots B and C - weight coefficients for the {meteorology, emissions} variables and the ozone monitors which best approximate the dominant pattern of association between the fields. The weights are listed by spatial grid or monitor, from left to right, as follows: reanalysis meteorology variables - moving east along each grid row, starting in the NW grid cell, surface temperature - moving south, following the order of monitors in Table 3, emissions - moving east along each grid row, starting in the SW grid cell.

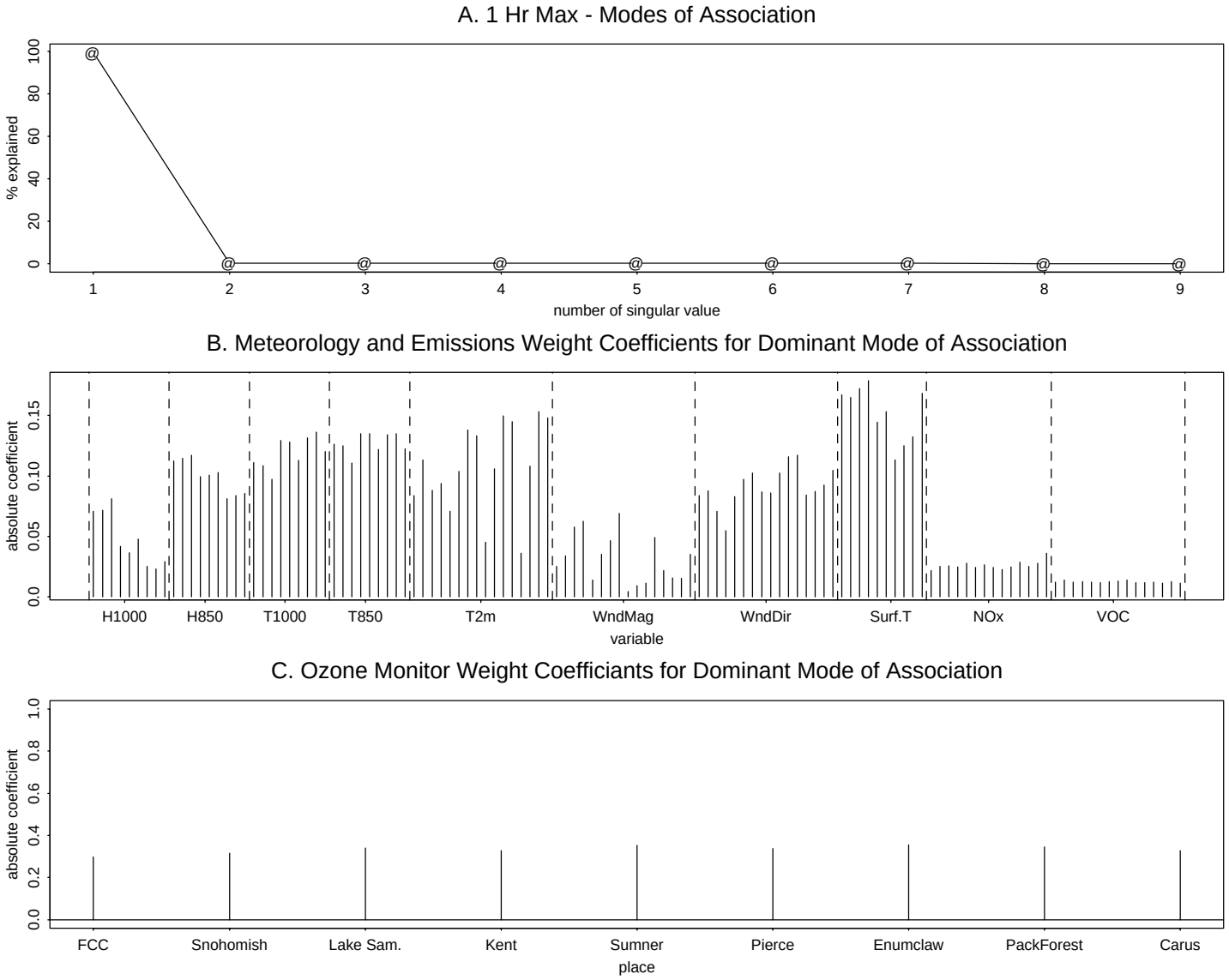

Figure 9: SVD results for daily maximum 8 hour ozone analysis. Plot A - % of the observed cross-correlation matrix's cumulative squared covariance captured by the rank 1 approximation derived from each singular value (see footnote 4). Plots B and C - weight coefficients for the {meteorology, emissions} variables and the ozone monitors which best approximate the dominant pattern of association between the fields. The weights are listed by spatial grid or monitor, from left to right, as follows: reanalysis meteorology variables - moving east along each grid row, starting in the NW grid cell, surface temperature - moving south, following the order of monitors in Table 3, emissions - moving east along each grid row, starting in the SW grid cell.

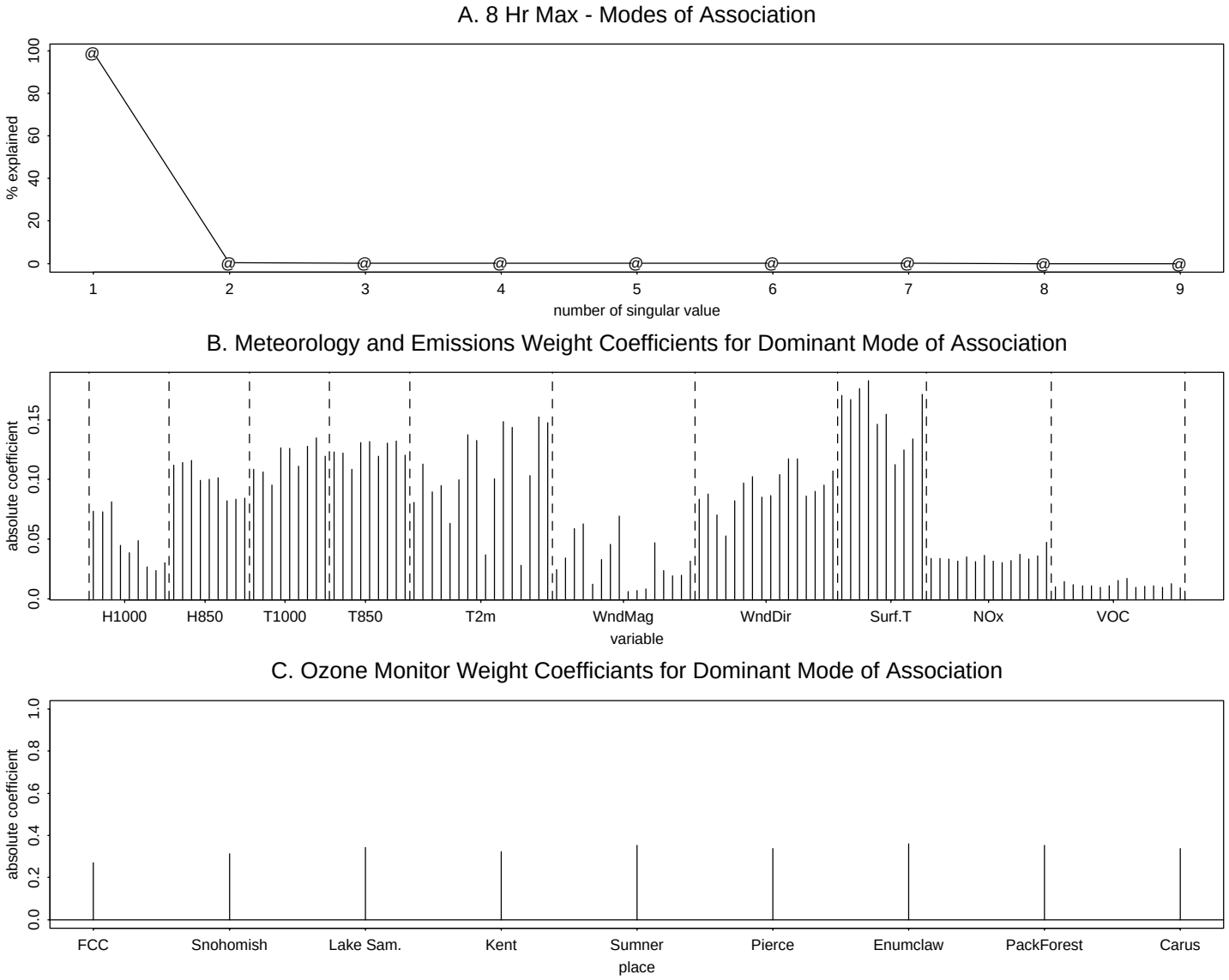

4.4 Meteorological Adjustment of Daily Ozone Composite

4.4.1 Daily 1 hour maximum

The ozone composite variable is highly correlated with the meteorology composite variables, but shows little association with the emissions composite (Table 5).

Table 5: Cross-Correlations Composites: Daily 1 hour maximum

	Comp.o3	**Comp.RAmet**	**Comp.SMet**
Comp.RAmet	0.67		
Comp.Smet	0.73	0.88	
Comp.Emiss	0.06	0.02	0.10

While the relationship between the various predictor composite variables and comp.03 is approximately linear due to the prior use of linearizing transformations, there may still be interactions between the predictor composites in their influence on comp.03. We modelled comp.03 as:

$$comp.03 = \beta_0 + \beta_1 comp.RAmet + \beta_2 comp.Smet + \beta_3 comp.RAmet * comp.Smet,$$

with the following parameter estimates:

Table 6: Coefficient Estimates, Daily 1 hour maximum

Coef	**Value**	**std.error**
β_0	0.0034	0.0009
β_1	0.0012	0.0003
β_2	0.0207	0.0013
β_3	-0.0005	0.0001
Multiple R^2	0.5414	
F-statistics	7775.8 on 3,1971 df	p-value = 0

Table 7: Coefficient Correlations, Daily 1 hour maximum

	β_0	β_1	β_2
β_1	0.00		
β_2	-0.19	-0.83	
β_3	-0.56	-0.01	0.39

The fit is good (Figure 10), though not unexpectedly the model underpredicts the most extreme events. The residuals show no trends or heteroskedasticity (Figures 11, 12), and appear approximately normal(Figure 13).

The correlation amoung meteorology composites (Table 5) results in some multicollinearity in parameter estimates (Table 7), potentially raising concern for inflated standard error estimates ([Bels 80]). However, since the goal of the analysis is to adjust comp.03 for

Figure 10: Observed versus fitted comp.03 values for daily 1 hour maximum ozone readings.

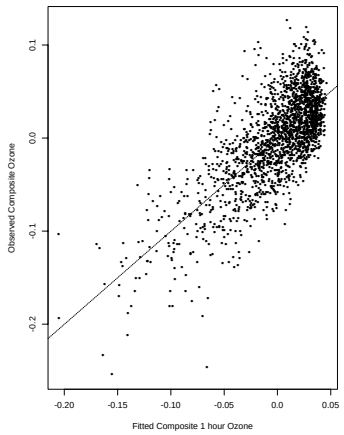

Figure 11: Residuals versus fitted comp.03 values for daily 1 hour maximum ozone readings.

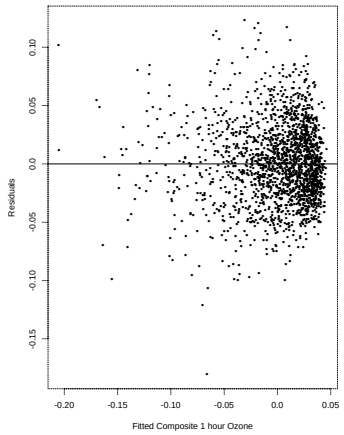

Figure 12: Square root of absolute value of residuals versus fitted comp.03 values for daily 1 hour maximum ozone readings.

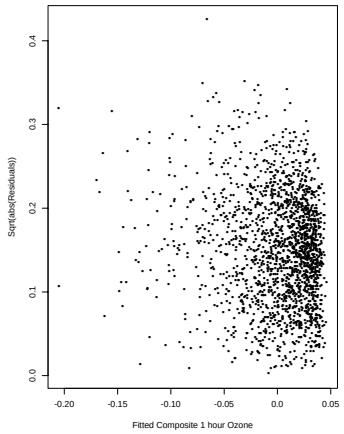

Figure 13: Normal quantile-quantile plot of residuals from meteorologically adjusting daily 1 hour maximum comp.03.

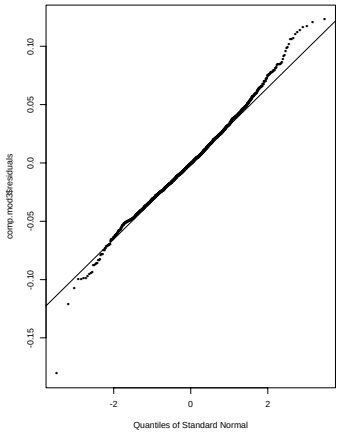

meteorology, prediction, not parameter testing, is our focus and this is unaffected by multicollinearity. For this reason no statistical tests of the coefficients are given. Note that the meteorology composites explain a substantial component of the variation in the ozone network composite.

Further issues preventing undue reliance on coefficient tests (standard errors) are

- The large sample sizes involved, which drive down the standard error estimates (making statistical significance more likely and less informative).
- The presence of positive short-term correlation in the residuals[6]. The positively correlated residuals bias the residual standard error estimates and hence any significance tests.

Short-term correlation in the residuals can be reduced by additively introducing lagged composite meteorology terms into the model[7]. However, the final conclusions are approximately identical and are therefore not given[8].

4.4.2 Daily 8 hour maximum

The 8 hour ozone composite variable is also highly correlated with the "8 hour" meteorology composite variables[9], while showing little association with the "8 hour" emission composite (Table 8).

[6]The residuals demonstrate a 1-day lag correlation of 0.42.

[7]Specifically, the change from the prior day's comp.RAmet and comp.Smet. These are less correlated with the current day composites than simply using lag 1 composities.

[8]Inclusion of the lagged composite meteorology terms increase the meteorological adjustment model R^2 to 0.59 for both the 1 and 8 hour summaries, though they fail to significantly alter the short-term correlation in the meteorologically adjusted ozone composite. The rank correlations of the resulting meteorologically adjusted ozone composites with time index are approximately identical to those found without use of lagged

Table 8: Composite Cross-Correlations: Daily 8 hour maximum

	Comp8hr.o3	**Comp8hour.RAmet**	**Comp8hr.Smet**
Comp8hr.RAmet	0.67		
Comp8hr.Smet	0.73	0.88	
Comp8hr.Emiss	0.04	0.02	0.09

Fitting the selected model

$$comp8hr.03 = \beta_0 + \beta_1 comp8hr.RAmet + \beta_2 comp8hr.Smet + \beta_3 comp8hr.RAmet * comp8hr.Smet,$$

produced the following results

Table 9: Coefficient Estimates, Daily 8 hour maximum

Coef	**Value**	**Std. Error**
β_0	0.0024	0.0007
β_1	0.0009	0.0003
β_2	0.0168	0.0010
β_3	-0.0003	0.0001
Multiple R^2	0.53	
F-statistics	752.3 on 3,1971 df	p-value = 0

Table 10: Coefficient Correlations

	β_0	$.\beta_1$	β_2
β_1	0.01		
β_2	-0.18	-0.82	
β_3	-0.56	-0.02	0.33

As with the 1 hour ozone summary, the fit is good (Figure 14). The residuals show no trends or heteroskedasticity (Figure 15, 16), and are approximately normal (Figure 17). The concerns regarding multicollinearity, auto correlated residuals, and large sample size effects on significance tests all hold as in the 1 hour analysis. The residuals have a large lag-1 correlation (0.40), as with the 1 hour data. While this can be somewhat reduced by including lagged meteorology composites in the model, the change has little influence on the final conclusions (see footnote 8).

composite terms.

[9]Recall separate ace transformations were conducted for the 1 hour and 8 hour daily maximum ozone summaries, hence the "8 hour" and "1 hour" composites will not be identical.

Figure 14: Observed versus fitted comp8hr.03 values for daily 8 hour maximum ozone readings.

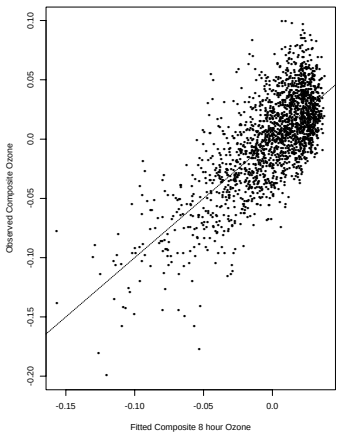

Figure 15: Residuals versus fitted comp8hr.03 values for daily 8 hour maximum ozone readings.

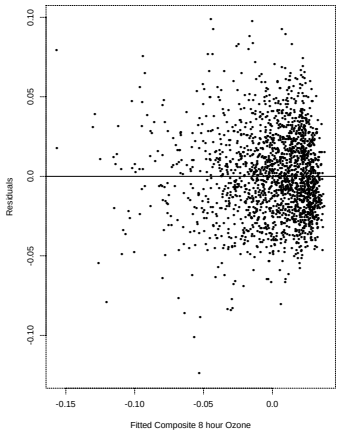

Figure 16: Square root of absolute value of residuals versus fitted comp8hr.03 values for daily 8 hour maximum ozone readings.

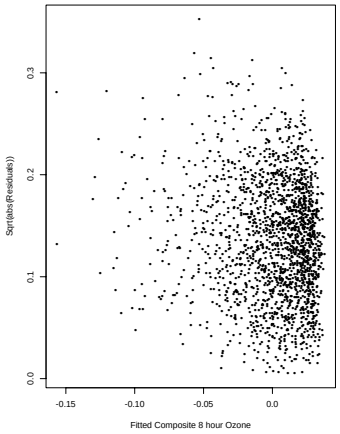

Figure 17: Normal quantile-quantile plot of residuals from meteorologically adjusting comp8hr.03.

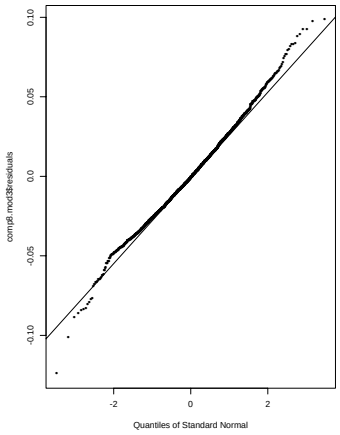

4.5 Investigation of long term trend in the meteorologically adjusted composite ozone summary

4.5.1 Daily 1 hour maximum

There appears to be a slight long term increase in the seasonal distribution of meteorologically adjusted composite ozone (Figure 18). The Spearman's rank correlation of the meteorologically adjusted composite ozone summary and the time index is rho=0.118[10].

Figure 18: Seasonal distribution of meteorologically adjusted daily 1 hour maximum ozone composite. Note the slight increasing long term trend in seasonal median.

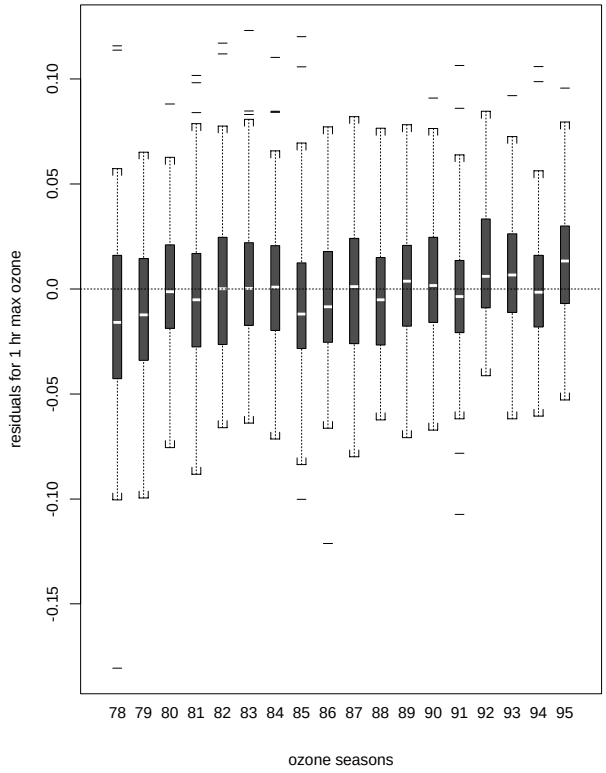

4.5.2 Daily 8 hour maximum

There appears to be a slight long term increase in the seasonal distribution of meteorologically adjusted composite ozone (Figure 19), though it appears weaker than in the 1 hour analysis. The Spearman's rank correlation is rho=0.068[11]

[10] A two-sided test of zero correlation is rejected with a p-value of zero (normal approximation, z=5.2).
[11] A two-sided test is rejected with a p-value of 0.0025, (z=3.03).

Figure 19: Seasonal distribution of meteorologically adjusted daily 8 hour maximum ozone composite. Note the slight increasing long term trend in seasonal median.

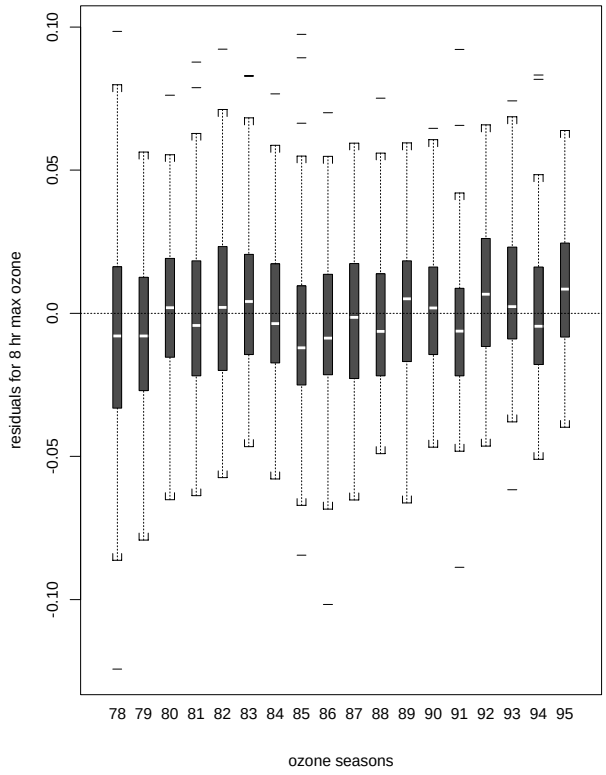

4.6 Association of the meteorologically adjusted ozone composite and the emissions composite

4.6.1 Daily 1 hour maximum

The meteorologically adjusted ozone composite derived above (without lags) showed no association with the emissons composite (Figure 20).

$$met.adjustedcomp.03 = \beta_0 + \beta_1 Comp.Emiss$$

Coef	Value	Std. Error
β_0	0.000	0.0008
β_1	-0.00013	0.0020
Multiple R^2	0.0002	
F-statistic	0.412 on 1, 1971 df	p-value=0.52

Figure 20: Observed versus fitted (from comp.Emiss) meteorologically adjusted comp.03 values.

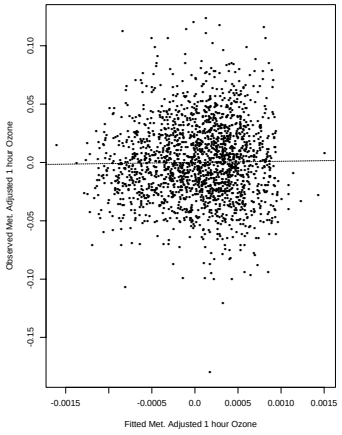

4.6.2 Daily 8 hour maximum

The meterologically adjusted ozone composite derived above (without lags) showed no association with the emissions composite (Figure 21).

$$met.adjustedcomp8hr.03 = \beta_0 + \beta_1 comp8hr.Emiss$$

Coef	Value	Std. Error
β_0	0.0000	0.0006
β_1	-0.0021	0.0013
Multiple R^2	0.0012	
F-statistics	2.5 on 1, 1971 df	p-value = 0.11

4.7 Investigation of long term trends in emission- and meteorologically-adjusted composite ozone

As neither analysis showed a significant association of meteorologically adjusted ozone composite with the respective emissions composite, the long term trend results given above need not be amended.

5 Discussion

5.1 Regional Signal

The analysis reveals a strong regional-scale response in ozone, both in the uniformity across ozone monitors of a predictor variable's linearizing transformation (Appendix B) and in the uniformity across ozone monitors of the dominant coupling pattern's weight coefficients

Figure 21: Observed versus fitted (from comp8hr.Emiss) meteorologically adjusted comp8hr.03 values.

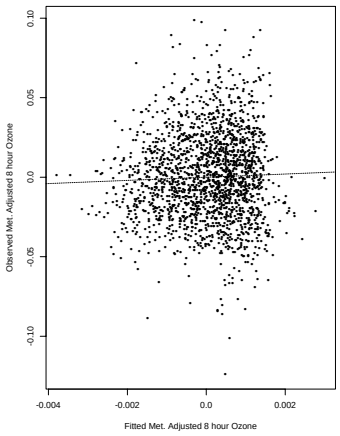

(Section 4.2). This regional-scale response was hinted at by the large number of high ozone days Puget Sound and Portland share in common ([Recker 97]), but has not otherwise been previously addressed.

5.2 Meteorological Adjustment

The analysis reveals a relatively simple coupling between the ozone network and the {meteorology, emissions} field: a single pattern of association linking comp.03, which is approximately proportional to the regional average standardized deviation from each ozone monitor's long-term mean (Figure 8, plot C), with a predominately meteorological composite driven by temperature, with contributions from wind direction and geopotential height (Figure 8, plot B). Comp.O3, being approximately a regional average, is akin to the network average Harrison used in investigating ozone trends[12]([Harris 94]). However, as comp.O3 is an average of locally standardized observations, it is not subject to variability from differences in mean ozone level across monitors as a straight network average would be. It is thus a more precise and sensitive summary for trend investigation.

The previous attempt at deriving meteorologically adjusted ozone for any of the records analyzed here was a to develop monitor-specific models adjusting daily maximum 1 hour ozone for maximum daily temperature at SeaTac airport ([Harris 97]). The model for Enumclaw produced an R^2 of 0.82, though interpretation is limited as the details of the observation period used are not reported. It is clear, however, that a local, monitor-specific model *should* provide a better fit (i.e., higher R^2) than a model of regional composite response given the spatial averaging of the signal. Given the spatial scale of the analysis, the observed R^2s from the meteorological adjustment models are quite good.

One might consider using the composite meteorology predictors to develop monitor-specific ozone models. While the correlation of each monitor with the full {meteorology, emissions} composite ranges from 0.55 to 0.67 (for the daily maximum 1 hour comp.O3), it

[12]Though he looked at network average 1 hour maximums averaged across each month, rather than daily.

is still less than observed in relation to just maximum daily surface temperature at SeaTac airport (0.7 - 0.8). The composite predictors are good regional predictors but poor local predictors. This is partially due to the fact that the weight coefficients from the SVD must be nonzero, hence uniformative predictors can only be downweighted but never dropped completely.

An alternative approach to combining a common regional structure with the specificity of a site-specific model would be to use ridge regression ([Ryan 97]) with each grid-specific meteorology or emissions variable entered as a separate predictor, along with a categorical variable to distinguish ozone monitors (and interaction terms) . One could then force a common 'regional' model structure to be shared across monitors, but with monitor-specific coefficients.

5.3 Prediction

The models fit for meteorological adjustment do not lend themselves to use for prediction. Firstly, predicting a regional-scale composite response is of rather limited interest. Secondly, prediction would require specification of both the short-term and long-term temporal structure in the residuals so that these could be accounted for and the prediction error reduced. Most fundamentally, the models developed for trend investigation try to capture mean associations between ozone and meteorology, while the goal of prediction would presumably be to forecast *extreme* ozone events. The models presented here were not developed to capture the association between extreme ozone events and meteorology. Note, further, that incorporation of new observations or changes to either the ozone or the surface meteorology networks would require repeating the full analysis as the underlying cross-correlation matrix would change.

5.4 Association of Meteorologically Adjusted Ozone and Emissions

No association was found between the emissions composite and the meteorologically adjusted ozone composite. To a large degree, this is probably due to differences in the temporal and spatial scales of the emissions estimation process in comparison to that found in the ozone network. For example, the large point source emissions estimates are based on annual total emissions: each day of the season for a given year is assigned 1/365 of the annual total emissions (Appendix E). The use of total VOC and NO_x also caused a loss of species-specific signals ([West 96], [Harris 96]), but a more detailed emissions analysis was beyond the scope of the analysis. A portion of the short-term time structure in the meteorologically adjusted ozone composites may be associated with seasonal trends in regional biogenic emissions ([Guenth 97]), but this could not be explored further with the current data.

5.5 Trend Investigation

A previous analysis for trends ([Harris 94]), using a selection of ozone monitors overlapping but not identical to that used here, failed to detect trends in either spatially averaged

monthly averages[13] or in the 8 hour averages (exceeding 0.040 ppm) in just the summer months of the analysis period. This contrasts with our own results of positive trends in both meteorologically adjusted daily maximum 1 hour and 8 hour regional ozone composites, which reveal increasing regional-average, locally-standardized ozone levels. The contrasting results can be explained by differences in time scale and handling of spatial variation, as well as fundamental differences in analytical approaches.

1. The previous analysis used the full annual time record, which introduces variation due to changing regional sources of ozone (e.g., stratospheric intrusion). Our analysis is restricted to the peak anthropogenic-influences ozone season, June through September.

2. The previous analysis used monthly averages, while we focus on daily maximum 1 or 8 hour composites. Using daily summaries increases sample sizes and reduces signal loss due to temporal averaging. The resulting increase in short-term correlation among the meteorologically adjusted ozone composite presented little formal difficulties in the trend analysis, though it would need to be addressed in development of a predictive model.

3. The previous analysis used the average observation across the network, while we analyze the (approximate) average locally-standardized exceedance across the network. The latter summary is not affected by spatial variation in long-term mean ozone levels, and therefore more precisely reveals temporal patterns in regional exceedances from long-term means.

4. The previous analysis' selection of network average as univariate ozone composite was a priori, while we arrived at the (approximate) network average because the canonical covariance analysis showed it to be the linear combination of ozone monitor records which maximally captured the coupling of the ozone and {meteorology, emissions} fields. It was thus chosen on the grounds that it would best lend itself to meteorological adjustment with respect to the current selection of meteorology and emissions variables.

5.6 Daily maximum 1 and 8 hour summaries

It is interesting to note that both daily ozone statistics produced almost identical svd results (Section 4.2) and meteorological adjustments (model fits in Section 4.4), though differing strengths of association with time (i.e., rank correlations). The results are somewhat counter to the view of the 8 hour maximum as the more robust summary statistic, and hence better able to reveal underlying trends. This view would suggest that the strongest trend should be found in the 8 hour summary. While this argument ignores differences in sensitivities of the summaries to the meteorological variables used in this analysis, the model fits suggest that the sensitivities are fairly comparable.

[13] 14 ozone stations, with records available in the period 1983 - 1993 but not necessarily for the full period for any site, had their site-specific monthly averages further averaged across the active sites. See [Harris 94].

6 Conclusion

The canonical covariance analysis revealed positive long-term trends in both the daily maximum 1 and 8 hour ozone regional composites after meteorological adjustement, a result previously not detected for this region. No association was detected between either meteorologically adjusted ozone composite and the regional emissions composites. This is likely due to differences in the temporal and spatial scales of the component estimates incorporated into the emissions estimation procedure, in comparison to the daily ozone observations. The composite variables, raw data, and S-plus functions used in the analysis are available from the authors and on-line (NRCSE website http://www.stat.washington.edu/NRCSE/).

References

[Bels 80] Belsley, D. A., E. Kuh, R. E. Welsch. 1980. *Regression Diagnostics: Identifying Influential Data and Sources of Collinearity.* Wiley and Sons, New York.

[Bloom 96] Bloomfield, P., J. A. Royle, L. J. Steinberg, Q. Yang. 1996. Accounting for meteorological effects in measuring urban ozone levels and trends. Atmospheric Environment 30(17): 3067 - 3077.

[Breth 92] Bretherton, C. S., C. Smith, J. M. Wallace. 1992. An intercomparison of methods for finding coupled patterns in climate data. Journal of Climate, 5: 541 - 560.

[EPA 95] Environmental Protection Agency. 1995. Review of the National Ambient Air Quality Standards for Ozone: Assessment of Scientific and Technical Information. OAPQS Staff Paper, EPA - 452/R.

[Fig 95] Figueroa, C. M., S. A. Otterson, C. R. Bowman, R. W. Miller. 1995. Preliminary analysis and results of the 1995 passive ozone sampler survy in Western Washington. Report C9500239 to Washington Department of Ecology.

[Guenth 97] Guenther, X. 1997. Seasonal and spatial variations in natural volatile organic compound emissions. Ecological Applications 7(1): 34 - 45.

[Harris 94] Harrison, H. 1994. Analysis of air-quality data in the Puget Sound Airshed. Report to Washington Department of Ecology.

[Harris 96] Harrison, H. 1996. On the contribution of biogenic terpenes to the synthesis of ozone in the downwind plume of the urban corridor of Central Puget Sound. Report to the Southwest Air Pollution Control Authority, 1308 NE 134th St., Vancouver, WA, 98685-2747.

[Harris 97] Harrison, H. 1997. Ozone in Western Washington: measurements and models. Talk presented at the Cascadia Tropospheric Ozone Peer Review, September 9, 10, 1997, University of Washington.

[Hastie 90] Hastie, T. J., R. J. Tibshirani. 1990. *Generalized Additive Models*. London: Chapman and Hall.

[Hydro 95] Hydrosphere Environmental Databases: NCDC Summary of the Day. 1995. Hydrosphere Data Products, Inc. 1002 Walnut, Suite 200, Boulder, CO. 80302.

[Kalnay 96] Kalnay, E., M. Kanamitsu, R. Kistler, W. Collins, D. Deaven, L. Gandin, M. Iredell, S. Saha, G. White, J. Woollen, Y. Zhu, A. Leetmaa, R. Reynolds, M. Chelliah, W. Ebisuzaki, W. Higgins, J. Janowiak, K. Mo, C. Ropelewski, J. Wang, R. Jenne, D. Joseph. 1996. The NCEP/NCAR 40-year Reanalysis Project. Bull. American Meteorological Society, 77(3): 437-471.

[Little 86] Little, R. J. A., D. B. Rubin. 1986. *Statistical Analysis with Missing Data*. Wiley and Sons, New York.

[Logan 85] Logan, J. A. 1985. Tropospheric ozone: seasonal behavior, trends, and anthropogenic influence. Journal of Geophysical Research, 90: 10463 - 10482.

[Mass 97] Mass, C. 1997. Application of high resolution mesoscale modeling for air quality applications over the Pacific Northwest. Talk presented at the Cascadia Tropospheric Ozone Peer Review, September 9, 10, 1997, University of Washington.

[NRCSE 98] National Research Center for Statistics and the Environment. Review of statistical methods for meteorologically adjusting surface ozone observations. Draft technical report.

[NRC 91] National Research Council. 1991. *Rethinking the ozone problem in urban and regional air pollution*. National Academy Press, Washington, D. C.

[Recker 97] Recker, E. 1997. Synoptic conditions accompanying high ozone events in Northwestern Oregon and Western Washington. Report to the Southwest Air Pollution Control Authority, Vancouver, Washington, August 20, 1997.

[Ryan 97] Ryan, T. P. 1997. *Modern Regression Methods*. Wiley and Sons, New York.

[Wall 92] Wallace, J. M., C. Smith, C. Bretherton. 1992. Singular value decomposition of wintertime sea surface temperature and 500-mb height anomalies. Journal of Climate, 5:561-576.

[Wax 91] Waxman, H., G. Wetstone, P. Barnett. 1991. Roadmap to Title I of the Clean Air Act Amendments of 1990: bringing blue skies back to America's cities. Environmental Law, 21(4): 1843 - 1946.

[West 96] Westberg, H., B. Hopkins, E. Allwine. 1996. Speciated VOC measurements in the Seattle-Central Pierce County corridor during the summer of 1995. Report C9500239, Washington Department of Ecology.

[Wool 97] Wooldridge, G., K. Zeller, R. Musselman. 1997. Ozone concentration characteristics at a high-elevation forest site. Theoretical and Applied Climatology 56: 153 - 164.

A Exploratory Analysis of Regional Ozone Signal

Pairwise scatterplots of the ozone monitor records display common regional ozone patterns (Figures 1, 22). Similarly, cross-correlations between each ozone monitor and each transformed[14] {meteorology, emissions} variable display common associations across the region (Figures 23, 24, Tables 11, 14).

Figure 22: Relationship of co-occurring daily maximum 8 hour ozone readings among pairs of network monitors.

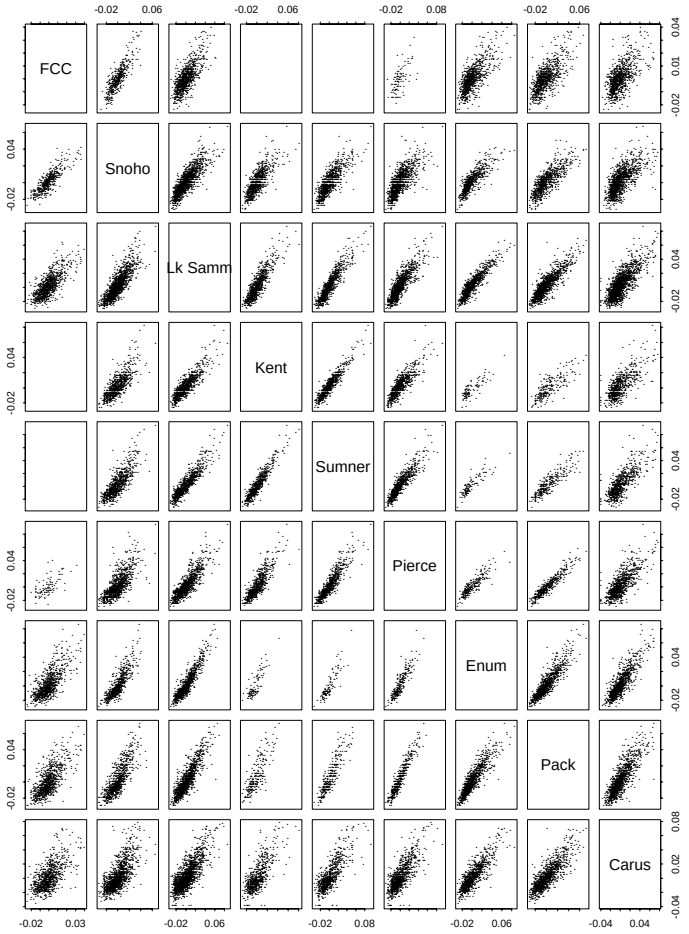

[14]See Appendix B.

Table 11: Cross-correlations for daily 1 hour maximum ozone.

Variable	FCC	Snoho	Lk Samm	Kent	Sumner	Pierce	Enumclaw	Pack Forest	Carus
H1000 Grid1	-0.238	-0.297	-0.334	-0.282	-0.322	-0.345	-0.291	-0.381	-0.299
H1000 Grid2	-0.254	-0.311	-0.332	-0.279	-0.322	-0.342	-0.295	-0.390	-0.298
H1000 Grid3	-0.314	-0.357	-0.368	-0.311	-0.360	-0.377	-0.343	-0.434	-0.336
H1000 Grid4	-0.133	-0.158	-0.202	-0.165	-0.200	-0.200	-0.168	-0.224	-0.190
H1000 Grid5	-0.118	-0.147	-0.173	-0.145	-0.180	-0.175	-0.145	-0.199	-0.156
H1000 Grid6	-0.171	-0.204	-0.215	-0.180	-0.230	-0.229	-0.197	-0.255	-0.195
H1000 Grid7	-0.109	-0.079	-0.124	-0.106	-0.130	-0.091	-0.123	-0.111	-0.128
H1000 Grid8	-0.104	-0.076	-0.105	-0.105	-0.126	-0.075	-0.126	-0.096	-0.102
H1000 Grid9	-0.108	-0.114	-0.124	-0.113	-0.144	-0.120	-0.148	-0.152	-0.121
H850 Grid1	-0.407	-0.468	-0.513	-0.465	-0.507	-0.517	-0.491	-0.564	-0.478
H850 Grid2	-0.421	-0.485	-0.519	-0.462	-0.519	-0.524	-0.508	-0.581	-0.493
H850 Grid3	-0.435	-0.499	-0.522	-0.458	-0.530	-0.533	-0.525	-0.594	-0.504
H850 Grid4	-0.355	-0.397	-0.455	-0.403	-0.439	-0.453	-0.447	-0.506	-0.445
H850 Grid5	-0.366	-0.411	-0.455	-0.396	-0.448	-0.455	-0.457	-0.518	-0.453
H850 Grid6	-0.382	-0.427	-0.457	-0.391	-0.457	-0.463	-0.470	-0.531	-0.459
H850 Grid7	-0.286	-0.306	-0.371	-0.318	-0.348	-0.360	-0.390	-0.424	-0.393
H850 Grid8	-0.303	-0.325	-0.373	-0.318	-0.360	-0.365	-0.401	-0.441	-0.401
H850 Grid9	-0.318	-0.341	-0.375	-0.311	-0.367	-0.374	-0.410	-0.456	-0.402
T1000 Grid1	0.498	0.452	0.494	0.510	0.535	0.454	0.525	0.426	0.482
T1000 Grid2	0.471	0.429	0.485	0.480	0.515	0.439	0.543	0.422	0.492
T1000 Grid3	0.398	0.377	0.437	0.422	0.464	0.386	0.504	0.378	0.462
T1000 Grid4	0.541	0.536	0.557	0.584	0.609	0.550	0.612	0.548	0.550
T1000 Grid5	0.531	0.512	0.559	0.563	0.587	0.529	0.642	0.540	0.574
T1000 Grid6	0.452	0.441	0.498	0.490	0.515	0.450	0.587	0.465	0.536
T1000 Grid7	0.512	0.542	0.565	0.578	0.602	0.580	0.623	0.595	0.568
T1000 Grid8	0.529	0.540	0.596	0.590	0.616	0.581	0.681	0.603	0.619
T1000 Grid9	0.458	0.463	0.534	0.519	0.541	0.489	0.621	0.514	0.579
T850 Grid1	0.561	0.513	0.551	0.573	0.589	0.525	0.594	0.523	0.556
T850 Grid2	0.543	0.497	0.547	0.554	0.577	0.515	0.610	0.516	0.563
T850 Grid3	0.458	0.436	0.490	0.483	0.520	0.450	0.559	0.450	0.518
T850 Grid4	0.548	0.541	0.584	0.603	0.614	0.581	0.640	0.594	0.606
T850 Grid5	0.543	0.532	0.584	0.590	0.609	0.573	0.663	0.591	0.618
T850 Grid6	0.480	0.475	0.533	0.524	0.554	0.506	0.620	0.524	0.577
T850 Grid7	0.504	0.523	0.587	0.589	0.599	0.595	0.645	0.615	0.620
T850 Grid8	0.504	0.522	0.589	0.584	0.603	0.588	0.668	0.613	0.634
T850 Grid9	0.452	0.470	0.537	0.522	0.551	0.515	0.622	0.541	0.593

Table 12: Cross-correlations for daily 1 hour maximum ozone.*cont.*

Variable	FCC	Snoho	Lk Samm	Kent	Sumner	Pierce	Enumclaw	Pack Forest	Carus
T2m Grid1	-0.247	-0.192	-0.194	-0.225	-0.190	-0.188	-0.139	-0.173	-0.165
T2m Grid2	-0.309	-0.278	-0.290	-0.296	-0.275	-0.271	-0.234	-0.271	-0.254
T2m Grid3	-0.316	-0.314	-0.324	-0.303	-0.302	-0.297	-0.270	-0.306	-0.281
T2m Grid4	-0.322	-0.348	-0.349	-0.311	-0.323	-0.324	-0.313	-0.351	-0.316
T2m Grid5	-0.236	-0.235	-0.262	-0.271	-0.257	-0.245	-0.199	-0.226	-0.224
T2m Grid6	-0.271	-0.278	-0.297	-0.281	-0.282	-0.268	-0.250	-0.272	-0.259
T2m Grid7	-0.310	-0.330	-0.351	-0.307	-0.330	-0.311	-0.335	-0.347	-0.332
T2m Grid8	-0.324	-0.335	-0.358	-0.298	-0.317	-0.314	-0.360	-0.366	-0.351
T2m Grid9	-0.217	-0.236	-0.255	-0.237	-0.241	-0.231	-0.232	-0.234	-0.248
T2m Grid10	-0.244	-0.265	-0.289	-0.256	-0.279	-0.257	-0.269	-0.258	-0.278
T2m Grid11	-0.263	-0.277	-0.304	-0.259	-0.292	-0.276	-0.318	-0.299	-0.311
T2m Grid12	-0.265	-0.269	-0.288	-0.247	-0.266	-0.261	-0.315	-0.306	-0.310
T2m Grid13	-0.179	-0.203	-0.234	-0.214	-0.218	-0.204	-0.231	-0.218	-0.240
T2m Grid14	-0.214	-0.220	-0.260	-0.223	-0.248	-0.221	-0.269	-0.240	-0.270
T2m Grid15	-0.222	-0.213	-0.253	-0.212	-0.228	-0.217	-0.286	-0.257	-0.271
T2m Grid16	-0.208	-0.193	-0.217	-0.204	-0.205	-0.186	-0.257	-0.257	-0.239
Wind Magnitude Grid1	0.359	0.338	0.352	0.434	0.459	0.368	0.371	0.288	0.327
Wind Magnitude Grid2	0.479	0.467	0.508	0.511	0.558	0.463	0.540	0.448	0.482
Wind Magnitude Grid3	0.393	0.360	0.392	0.370	0.438	0.334	0.466	0.365	0.359
Wind Magnitude Grid4	0.430	0.379	0.412	0.372	0.429	0.355	0.505	0.409	0.401
Wind Magnitude Grid5	0.276	0.303	0.289	0.387	0.362	0.347	0.272	0.265	0.282
Wind Magnitude Grid6	0.414	0.423	0.442	0.527	0.534	0.484	0.455	0.392	0.422
Wind Magnitude Grid7	0.552	0.561	0.609	0.600	0.650	0.589	0.672	0.600	0.586
Wind Magnitude Grid8	0.537	0.532	0.588	0.568	0.615	0.563	0.668	0.583	0.586
Wind Magnitude Grid9	0.159	0.200	0.174	0.286	0.224	0.250	0.145	0.180	0.166
Wind Magnitude Grid10	0.401	0.445	0.450	0.523	0.527	0.515	0.440	0.442	0.427
Wind Magnitude Grid11	0.587	0.611	0.660	0.654	0.704	0.669	0.714	0.661	0.634
Wind Magnitude Grid12	0.566	0.583	0.639	0.611	0.661	0.631	0.729	0.647	0.638
Wind Magnitude Grid13	0.123	0.156	0.134	0.234	0.171	0.202	0.116	0.166	0.130
Wind Magnitude Grid14	0.382	0.442	0.458	0.527	0.531	0.535	0.450	0.475	0.446
Wind Magnitude Grid15	0.570	0.615	0.678	0.655	0.709	0.693	0.735	0.695	0.664
Wind Magnitude Grid16	0.553	0.584	0.657	0.621	0.670	0.650	0.740	0.669	0.662

Table 13: Cross-correlations for daily 1 hour maximum ozone. *cont.*

Variable	FCC	Snoho	Lk Samm	Kent	Sumner	Pierce	Enumclaw	Pack Forest	Carus
Wind Direction Grid1	-0.194	-0.098	-0.122	-0.134	-0.109	-0.113	-0.041	-0.108	-0.090
Wind Direction Grid2	-0.266	-0.132	-0.156	-0.157	-0.142	-0.146	-0.101	-0.144	-0.117
Wind Direction Grid3	-0.343	-0.241	-0.257	-0.244	-0.255	-0.258	-0.222	-0.249	-0.225
Wind Direction Grid4	-0.311	-0.270	-0.275	-0.269	-0.279	-0.283	-0.252	-0.283	-0.246
Wind Direction Grid5	-0.119	-0.071	-0.065	-0.090	-0.081	-0.070	0.027	-0.046	-0.048
Wind Direction Grid6	-0.242	-0.161	-0.159	-0.166	-0.157	-0.140	-0.099	-0.134	-0.141
Wind Direction Grid7	-0.310	-0.227	-0.206	-0.180	-0.189	-0.179	-0.184	-0.200	-0.179
Wind Direction Grid8	-0.365	-0.321	-0.299	-0.248	-0.288	-0.286	-0.315	-0.326	-0.280
Wind Direction Grid9	-0.026	0.000	0.021	-0.013	-0.016	0.027	0.097	0.048	0.028
Wind Direction Grid10	-0.107	-0.082	-0.041	-0.059	-0.072	-0.015	0.016	-0.003	-0.025
Wind Direction Grid11	-0.134	-0.118	-0.046	-0.030	-0.056	-0.016	-0.012	-0.030	-0.024
Wind Direction Grid12	-0.244	-0.262	-0.211	-0.157	-0.216	-0.204	-0.204	-0.241	-0.207
Wind Direction Grid13	0.039	0.073	0.112	0.048	0.055	0.137	0.150	0.154	0.078
Wind Direction Grid14	-0.021	0.030	0.091	0.049	0.049	0.127	0.102	0.124	0.056
Wind Direction Grid15	-0.042	0.017	0.095	0.082	0.074	0.115	0.094	0.089	0.061
Wind Direction Grid16	-0.186	-0.178	-0.137	-0.090	-0.133	-0.150	-0.156	-0.190	-0.169
Bellingham T	0.339	0.408	0.381	0.366	0.381	0.376	0.341	0.392	0.315
Monroe T	0.353	0.409	0.394	0.365	0.388	0.411	0.366	0.431	0.341
State EMSU T	0.274	0.339	0.318	0.301	0.302	0.346	0.276	0.355	0.277
SeaTac Airport T	0.222	0.270	0.244	0.225	0.217	0.255	0.214	0.294	0.217
Puyallup T	0.367	0.412	0.375	0.345	0.349	0.368	0.357	0.405	0.292
Buckley T	0.392	0.451	0.442	0.395	0.415	0.475	0.404	0.491	0.370
Longmire T	0.392	0.443	0.466	0.418	0.454	0.520	0.414	0.524	0.406
Vancouver T	0.344	0.400	0.398	0.364	0.390	0.430	0.335	0.440	0.325
Portland Airport T	0.328	0.396	0.404	0.357	0.362	0.410	0.371	0.439	0.315

Table 14: Cross-correlations for daily 8 hour maximum ozone.

Variable	FCC	Snoho	Lk Samm	Kent	Sumner	Pierce	Enumclaw	Pack Forest	Carus
H1000 Grid1	-0.210	-0.292	-0.356	-0.264	-0.325	-0.341	-0.284	-0.376	-0.311
H1000 Grid2	-0.221	-0.303	-0.346	-0.252	-0.318	-0.334	-0.286	-0.382	-0.311
H1000 Grid3	-0.267	-0.345	-0.372	-0.275	-0.346	-0.366	-0.331	-0.424	-0.347
H1000 Grid4	-0.121	-0.158	-0.231	-0.161	-0.215	-0.206	-0.163	-0.223	-0.198
H1000 Grid5	-0.103	-0.147	-0.194	-0.133	-0.191	-0.178	-0.138	-0.197	-0.165
H1000 Grid6	-0.144	-0.198	-0.229	-0.156	-0.232	-0.226	-0.189	-0.252	-0.206
H1000 Grid7	-0.090	-0.078	-0.139	-0.111	-0.144	-0.100	-0.110	-0.113	-0.124
H1000 Grid8	-0.087	-0.075	-0.105	-0.104	-0.131	-0.079	-0.111	-0.100	-0.094
H1000 Grid9	-0.091	-0.112	-0.132	-0.106	-0.156	-0.123	-0.142	-0.154	-0.126
H850 Grid1	-0.342	-0.444	-0.515	-0.428	-0.492	-0.499	-0.472	-0.548	-0.490
H850 Grid2	-0.354	-0.458	-0.515	-0.423	-0.499	-0.504	-0.488	-0.563	-0.502
H850 Grid3	-0.366	-0.468	-0.512	-0.417	-0.504	-0.512	-0.503	-0.576	-0.511
H850 Grid4	-0.298	-0.377	-0.461	-0.370	-0.430	-0.435	-0.431	-0.492	-0.453
H850 Grid5	-0.306	-0.388	-0.455	-0.360	-0.435	-0.434	-0.438	-0.501	-0.459
H850 Grid6	-0.317	-0.400	-0.451	-0.351	-0.438	-0.439	-0.449	-0.513	-0.464
H850 Grid7	-0.244	-0.291	-0.382	-0.293	-0.350	-0.346	-0.378	-0.412	-0.396
H850 Grid8	-0.255	-0.307	-0.376	-0.287	-0.357	-0.346	-0.386	-0.426	-0.404
H850 Grid9	-0.263	-0.320	-0.369	-0.274	-0.357	-0.350	-0.392	-0.439	-0.405
T1000 Grid1	0.447	0.416	0.454	0.480	0.498	0.429	0.506	0.417	0.464
T1000 Grid2	0.426	0.393	0.450	0.458	0.482	0.414	0.525	0.414	0.467
T1000 Grid3	0.362	0.345	0.408	0.407	0.438	0.362	0.487	0.370	0.433
T1000 Grid4	0.474	0.500	0.504	0.547	0.569	0.524	0.590	0.541	0.537
T1000 Grid5	0.474	0.477	0.515	0.534	0.554	0.504	0.624	0.535	0.552
T1000 Grid6	0.411	0.408	0.462	0.469	0.489	0.425	0.570	0.461	0.506
T1000 Grid7	0.435	0.505	0.508	0.534	0.558	0.549	0.598	0.587	0.559
T1000 Grid8	0.469	0.506	0.553	0.559	0.586	0.554	0.664	0.599	0.600
T1000 Grid9	0.419	0.432	0.501	0.499	0.521	0.465	0.607	0.512	0.551
T850 Grid1	0.490	0.471	0.497	0.532	0.542	0.505	0.567	0.514	0.544
T850 Grid2	0.479	0.456	0.499	0.520	0.533	0.494	0.587	0.509	0.545
T850 Grid3	0.408	0.398	0.450	0.459	0.483	0.428	0.538	0.444	0.493
T850 Grid4	0.461	0.501	0.528	0.554	0.567	0.558	0.608	0.584	0.595
T850 Grid5	0.467	0.492	0.534	0.552	0.566	0.551	0.637	0.584	0.599
T850 Grid6	0.421	0.438	0.489	0.496	0.518	0.482	0.597	0.520	0.552
T850 Grid7	0.418	0.486	0.536	0.537	0.554	0.565	0.614	0.602	0.609
T850 Grid8	0.429	0.485	0.543	0.543	0.564	0.560	0.641	0.603	0.615
T850 Grid9	0.399	0.435	0.499	0.494	0.521	0.489	0.601	0.535	0.566

Table 15: Cross-correlations for daily 8 hour maximum ozone.*cont.*

Variable	FCC	Snoho	Lk Samm	Kent	Sumner	Pierce	Enumclaw	Pack Forest	Carus
T2m Grid1	-0.231	-0.181	-0.198	-0.229	-0.199	-0.192	-0.142	-0.171	-0.169
T2m Grid2	-0.287	-0.268	-0.288	-0.297	-0.276	-0.272	-0.229	-0.270	-0.259
T2m Grid3	-0.299	-0.307	-0.319	-0.304	-0.307	-0.295	-0.260	-0.302	-0.287
T2m Grid4	-0.302	-0.343	-0.342	-0.306	-0.321	-0.318	-0.299	-0.346	-0.317
T2m Grid5	-0.210	-0.221	-0.260	-0.272	-0.261	-0.246	-0.192	-0.221	-0.224
T2m Grid6	-0.249	-0.265	-0.292	-0.283	-0.283	-0.269	-0.238	-0.266	-0.261
T2m Grid7	-0.288	-0.320	-0.344	-0.303	-0.325	-0.307	-0.317	-0.340	-0.333
T2m Grid8	-0.292	-0.324	-0.348	-0.285	-0.307	-0.301	-0.341	-0.360	-0.347
T2m Grid9	-0.199	-0.228	-0.264	-0.236	-0.251	-0.238	-0.223	-0.232	-0.251
T2m Grid10	-0.226	-0.256	-0.292	-0.250	-0.277	-0.255	-0.254	-0.254	-0.277
T2m Grid11	-0.246	-0.266	-0.307	-0.247	-0.287	-0.267	-0.299	-0.295	-0.308
T2m Grid12	-0.232	-0.256	-0.287	-0.230	-0.253	-0.247	-0.297	-0.304	-0.302
T2m Grid13	-0.159	-0.204	-0.248	-0.215	-0.233	-0.214	-0.228	-0.223	-0.244
T2m Grid14	-0.194	-0.217	-0.268	-0.214	-0.252	-0.221	-0.256	-0.240	-0.267
T2m Grid15	-0.201	-0.208	-0.261	-0.199	-0.225	-0.211	-0.267	-0.257	-0.268
T2m Grid16	-0.178	-0.183	-0.218	-0.188	-0.200	-0.186	-0.242	-0.265	-0.234
Wind Magnitude Grid1	0.304	0.318	0.325	0.411	0.430	0.334	0.346	0.272	0.319
Wind Magnitude Grid2	0.440	0.442	0.485	0.491	0.535	0.441	0.529	0.438	0.470
Wind Magnitude Grid3	0.364	0.343	0.387	0.377	0.434	0.323	0.460	0.357	0.356
Wind Magnitude Grid4	0.402	0.360	0.410	0.371	0.417	0.343	0.502	0.403	0.386
Wind Magnitude Grid5	0.198	0.266	0.225	0.343	0.305	0.301	0.235	0.248	0.279
Wind Magnitude Grid6	0.342	0.387	0.399	0.493	0.494	0.448	0.426	0.374	0.418
Wind Magnitude Grid7	0.497	0.534	0.579	0.575	0.621	0.567	0.657	0.590	0.577
Wind Magnitude Grid8	0.490	0.501	0.561	0.545	0.583	0.541	0.652	0.573	0.573
Wind Magnitude Grid9	0.077	0.163	0.101	0.242	0.167	0.207	0.100	0.163	0.168
Wind Magnitude Grid10	0.312	0.406	0.391	0.479	0.473	0.476	0.405	0.429	0.432
Wind Magnitude Grid11	0.520	0.580	0.620	0.618	0.663	0.646	0.691	0.650	0.629
Wind Magnitude Grid12	0.510	0.549	0.604	0.577	0.621	0.605	0.707	0.638	0.625
Wind Magnitude Grid13	0.035	0.124	0.064	0.197	0.118	0.161	0.069	0.147	0.134
Wind Magnitude Grid14	0.288	0.406	0.408	0.486	0.484	0.497	0.414	0.461	0.452
Wind Magnitude Grid15	0.498	0.588	0.646	0.616	0.673	0.669	0.713	0.688	0.662
Wind Magnitude Grid16	0.498	0.555	0.630	0.585	0.639	0.625	0.720	0.663	0.651

Table 16: Cross-correlations for daily 8 hour maximum ozone.*cont.*

Variable	FCC	Snoho	Lk Samm	Kent	Sumner	Pierce	Enumclaw	Pack Forest	Carus
Wind Direction Grid1	-0.174	-0.087	-0.117	-0.129	-0.115	-0.117	-0.028	-0.093	-0.087
Wind Direction Grid2	-0.245	-0.125	-0.154	-0.159	-0.156	-0.152	-0.086	-0.132	-0.117
Wind Direction Grid3	-0.310	-0.234	-0.254	-0.244	-0.261	-0.262	-0.210	-0.245	-0.222
Wind Direction Grid4	-0.268	-0.263	-0.271	-0.269	-0.272	-0.288	-0.238	-0.278	-0.246
Wind Direction Grid5	-0.117	-0.064	-0.053	-0.078	-0.079	-0.068	0.040	-0.028	-0.045
Wind Direction Grid6	-0.224	-0.144	-0.135	-0.152	-0.152	-0.134	-0.081	-0.118	-0.136
Wind Direction Grid7	-0.278	-0.213	-0.183	-0.178	-0.191	-0.180	-0.169	-0.190	-0.175
Wind Direction Grid8	-0.318	-0.315	-0.287	-0.246	-0.285	-0.293	-0.303	-0.322	-0.276
Wind Direction Grid9	-0.053	0.001	0.037	0.000	-0.012	0.030	0.105	0.063	0.031
Wind Direction Grid10	-0.117	-0.069	-0.005	-0.041	-0.058	-0.009	0.030	0.011	-0.022
Wind Direction Grid11	-0.121	-0.100	-0.006	-0.018	-0.044	-0.012	0.006	-0.018	-0.024
Wind Direction Grid12	-0.191	-0.250	-0.185	-0.137	-0.200	-0.196	-0.188	-0.229	-0.204
Wind Direction Grid13	0.001	0.076	0.142	0.058	0.060	0.133	0.156	0.160	0.087
Wind Direction Grid14	-0.040	0.044	0.137	0.060	0.061	0.126	0.114	0.129	0.061
Wind Direction Grid15	-0.036	0.036	0.145	0.093	0.087	0.115	0.115	0.098	0.059
Wind Direction Grid16	-0.133	-0.162	-0.099	-0.066	-0.114	-0.143	-0.130	-0.177	-0.170
Bellingham T	0.283	0.396	0.358	0.344	0.364	0.370	0.329	0.390	0.329
Monroe T	0.292	0.393	0.379	0.344	0.372	0.400	0.359	0.431	0.353
State EMSU T	0.215	0.322	0.308	0.278	0.278	0.340	0.270	0.349	0.288
SeaTac Airport T	0.164	0.257	0.226	0.200	0.187	0.253	0.200	0.280	0.223
Puyallup T	0.293	0.396	0.359	0.325	0.331	0.357	0.344	0.400	0.313
Buckley T	0.309	0.433	0.433	0.372	0.395	0.465	0.393	0.485	0.387
Longmire T	0.310	0.431	0.464	0.388	0.431	0.503	0.402	0.516	0.421
Vancouver T	0.274	0.385	0.389	0.329	0.354	0.412	0.315	0.428	0.338
Portland Airport T	0.261	0.390	0.410	0.337	0.351	0.394	0.360	0.433	0.334

Figure 23: Absolute cross-correlations between daily maximum 1 hour ozone from each monitor and each transformed meteorology variable's grid or site record. Predictor grids or monitors are ordered, from bottom to top, as follows: reanalysis meteorology variables - moving east along each grid row, starting in the NW grid cell, surface temperature - moving south, following the order of monitors in Table 3, emissions - moving east along each grid row, starting in the SW grid cell. Note the common pattern of cross-correlation demonstrated by the dominant horizontal striations.

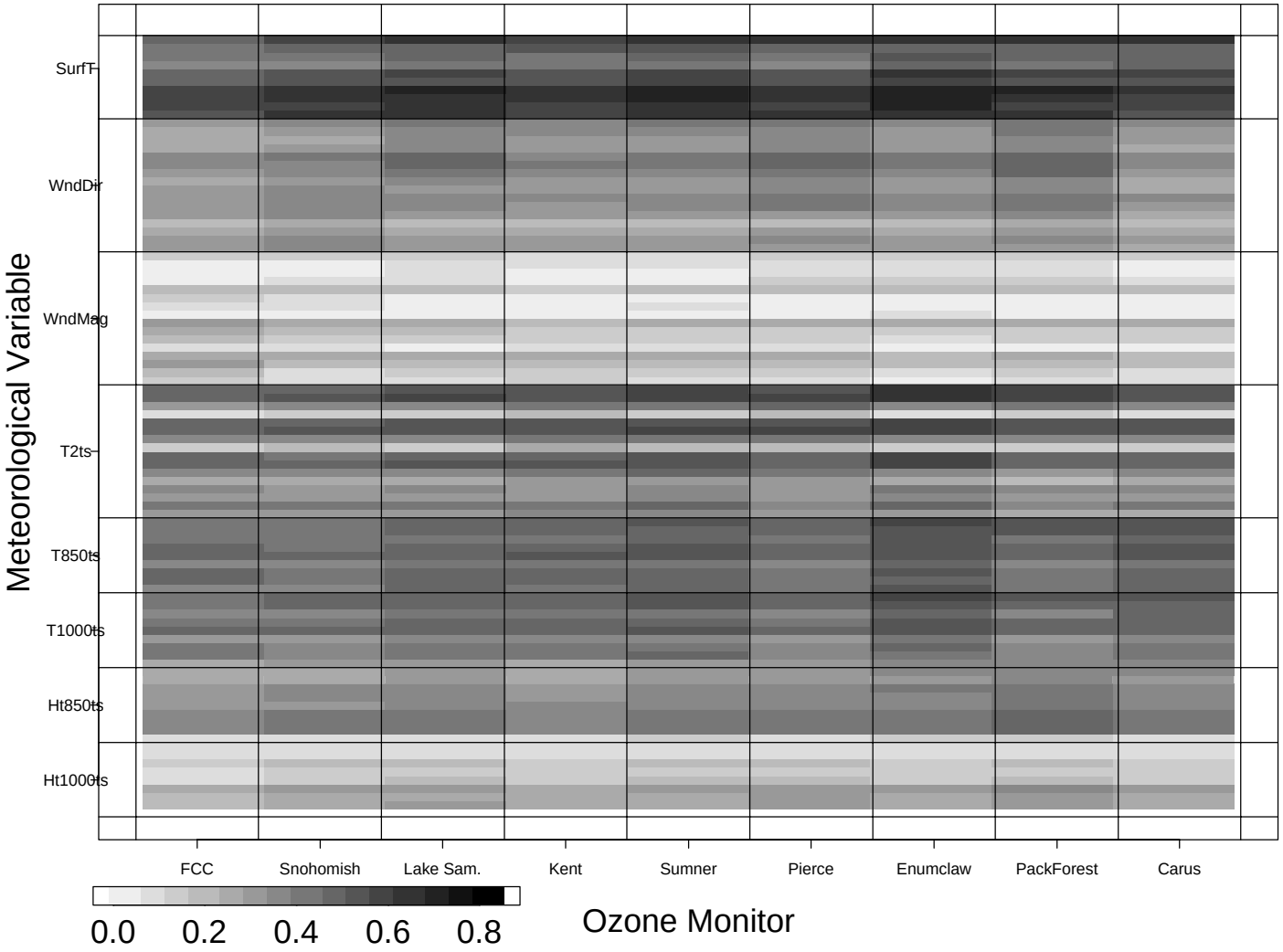

Figure 24: Absolute cross-correlations between daily maximum 8 hour ozone from each monitor and each transformed meteorology variable's grid or site record. Predictor grids or monitors are ordered, from bottom to top, as follows: reanalysis meteorology variables - moving east along each grid row, starting in the NW grid cell, surface temperature - moving south, following the order of monitors in Table 3, emissions - moving east along each grid row, starting in the SW grid cell. Note the common pattern of cross-correlation demonstrated by the dominant horizontal striations.

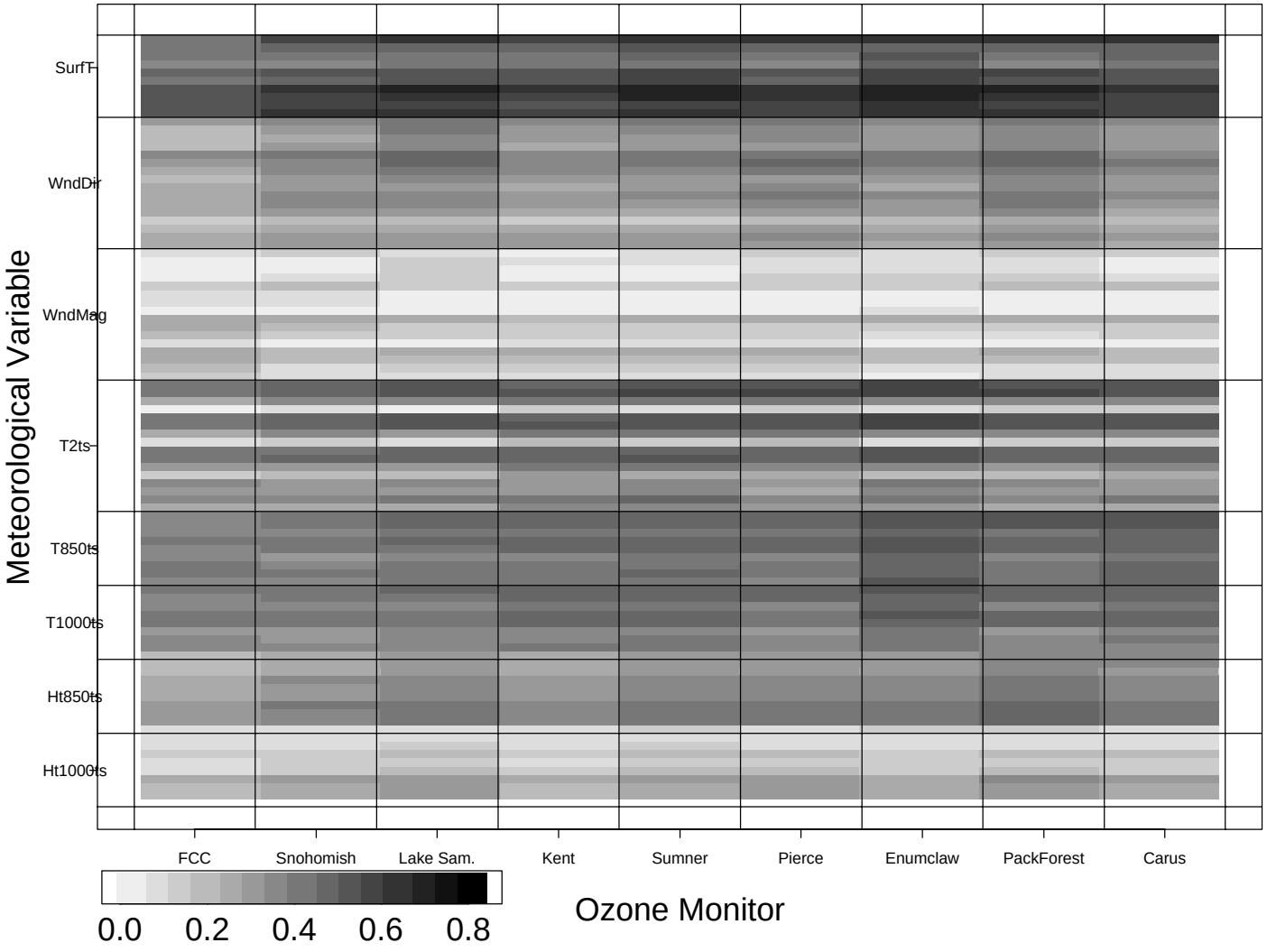

B Transformations

Following are the linearizing ace transformations for each meteorological and emission variable with each ozone monitor (dashed lines), overlaid with the final transformation (solid line). The constancy of predictor transformations across the ozone monitors led to the derivation of a final transformation for each predictor variable, which was calculated by

1. Calculating the average transformed value across ozone monitors for each value of the predictor variable observed at 5 or more ozone monitors, and

2. fitting a nonparametric smooth[15] through these average values.

The values of the predictor from this final transformation were used in place of the raw predictor values in the calculation of the cross-correlations used in the SVD analysis (see Section 3). Note that while ACE allows for transformations of both the predictor and response (ozone monitor i) variables, we restrict to linear transformations of the ozone response which, as regards correlation, is equivalent to no transformation of ozone.

[15]Specifically, a b-spline with 10 df.

B.1 Daily 1 hour maximum

Figure 25: ACE transformations of 1000-mb geopotential height. The x-axis displays the untransformed variable, the y-axis the transformed value specified only to relative scale. Dashed curves represent ozone monitor-specific transformations of the given grid cell of 1000-mb height, the solid curve is the final transformation for that grid cell's 1000-mb height. See Section 3.2.1 for details. Grid cell display corresponds to map in Figure 5, i.e., grid 1 is NW corner.

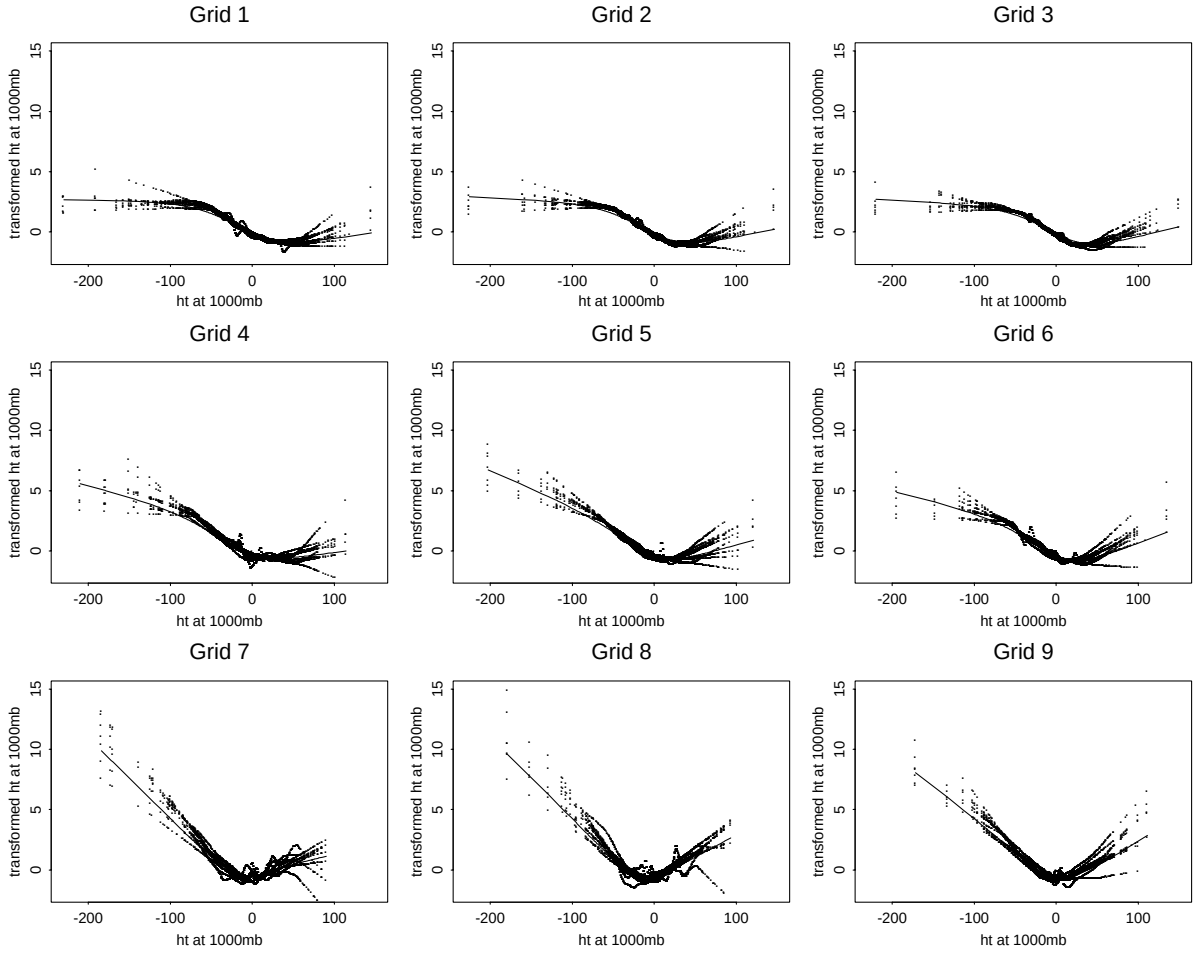

Figure 26: ACE transformations of 850-mb geopotential height. See Figure 25 for details.

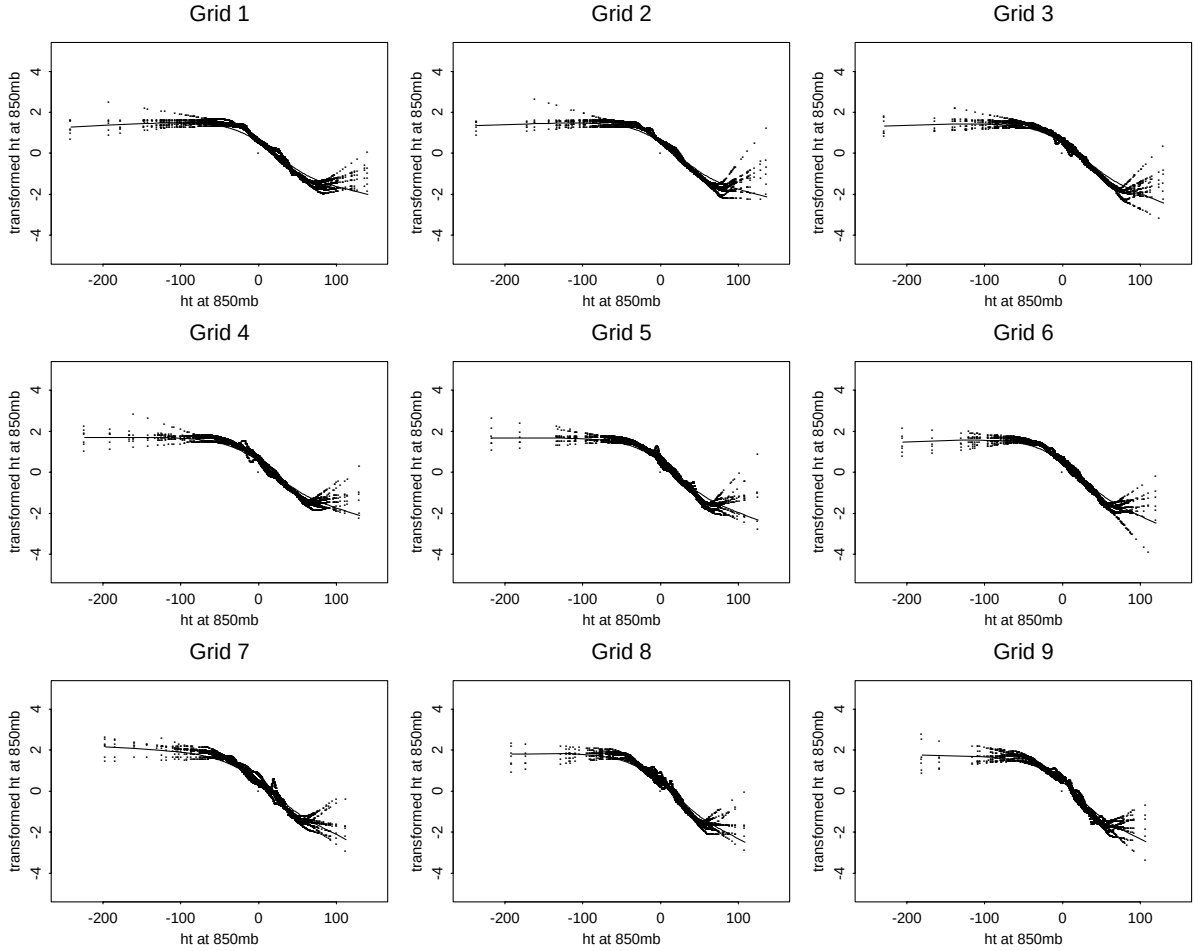

Figure 27: ACE transformations of 1000-mb mean temperature. See Figure 25 for details.

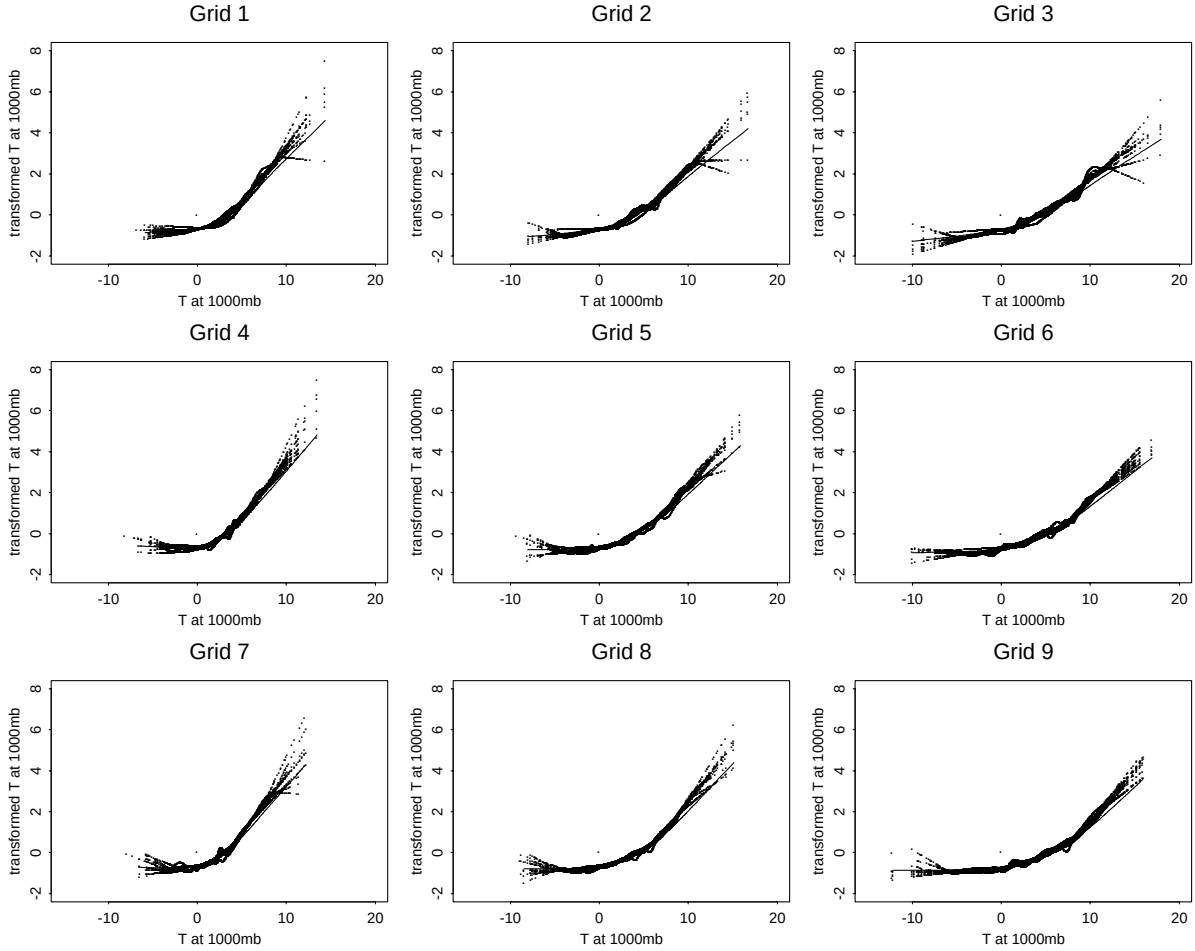

Figure 28: ACE transformations of 850-mb mean temperature. See Figure 25 for details.

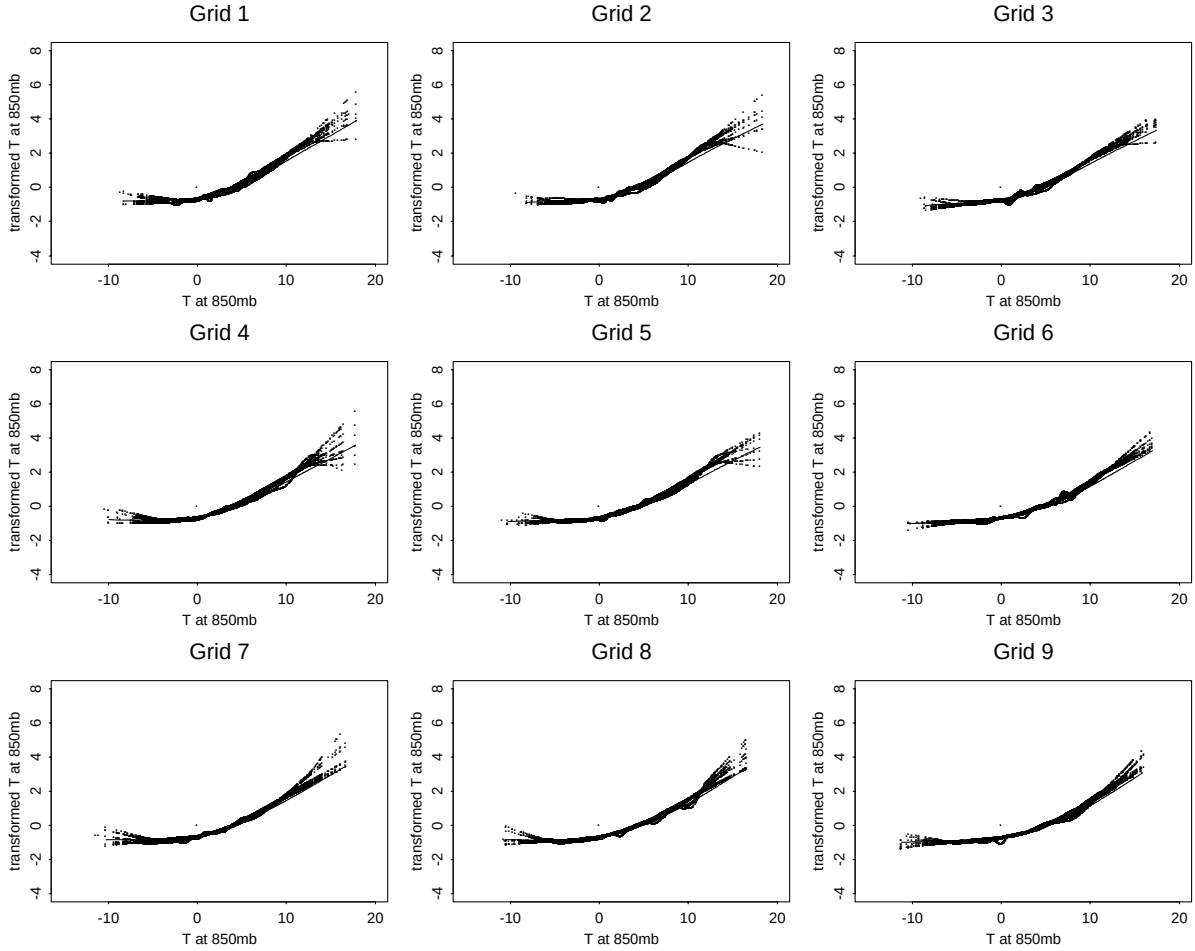

Figure 29: ACE transformations of 2 m mean temperature. See Figure 25 for details.

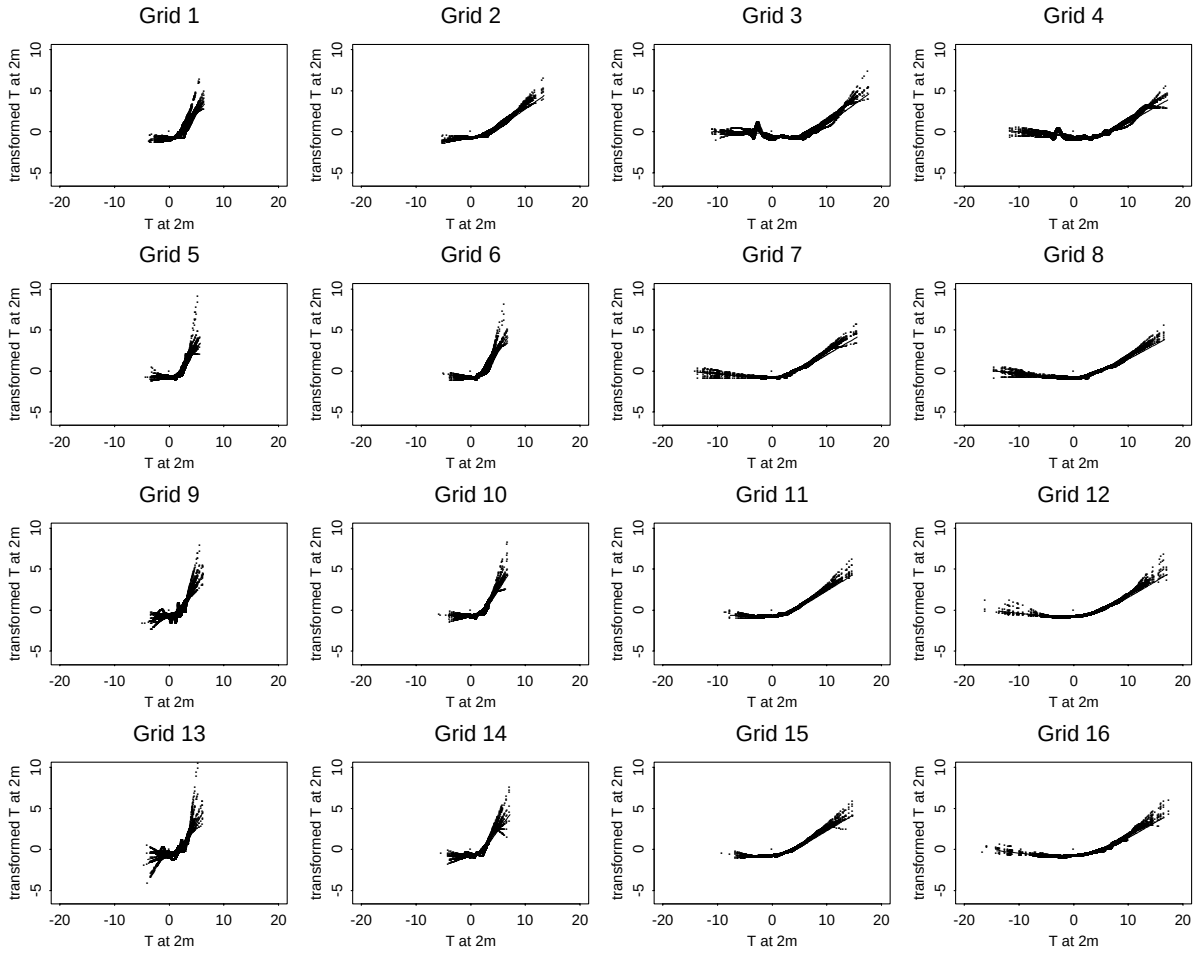

Figure 30: ACE transformations of wind direction. See Figure 25 for details.

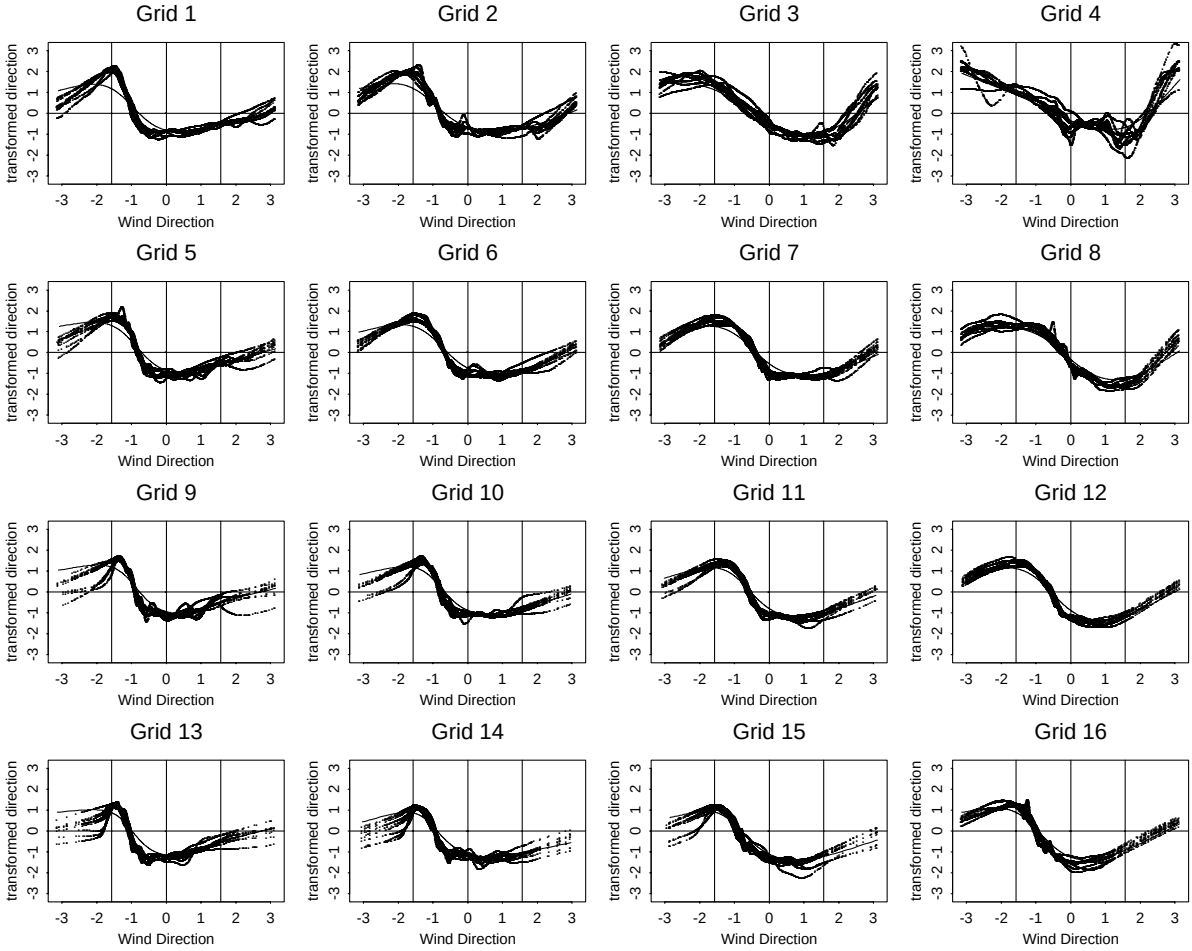

Figure 31: ACE transformations of maximum surface temperature, by meteorology monitor. See Figure 25 for details.

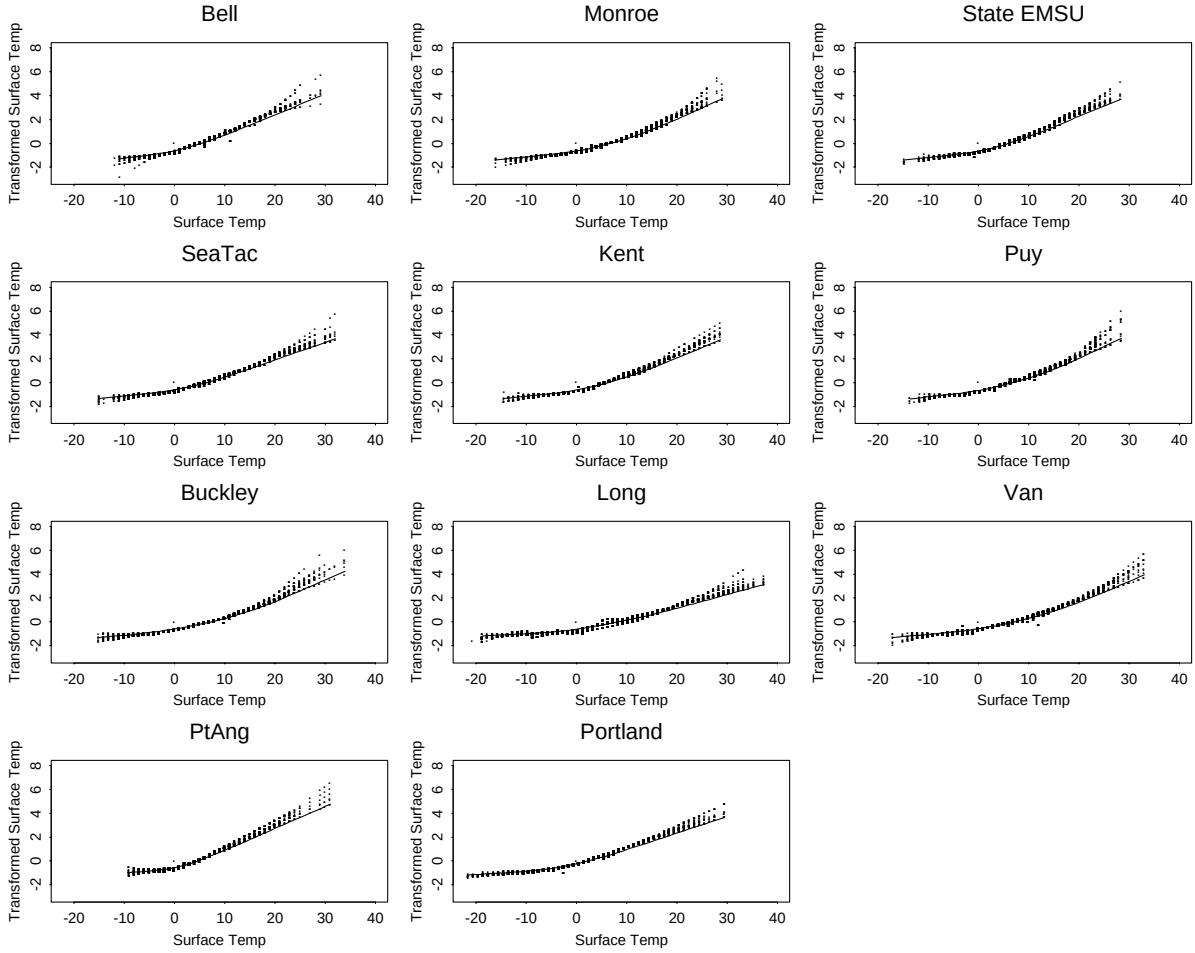

Figure 32: ACE transformations of total NO_x. See Figure 25 for details. Grid 1 corresponds to SW corner, grid 2 to the cell directly east, grid 4 to the cell directly north of cell 1, etc.

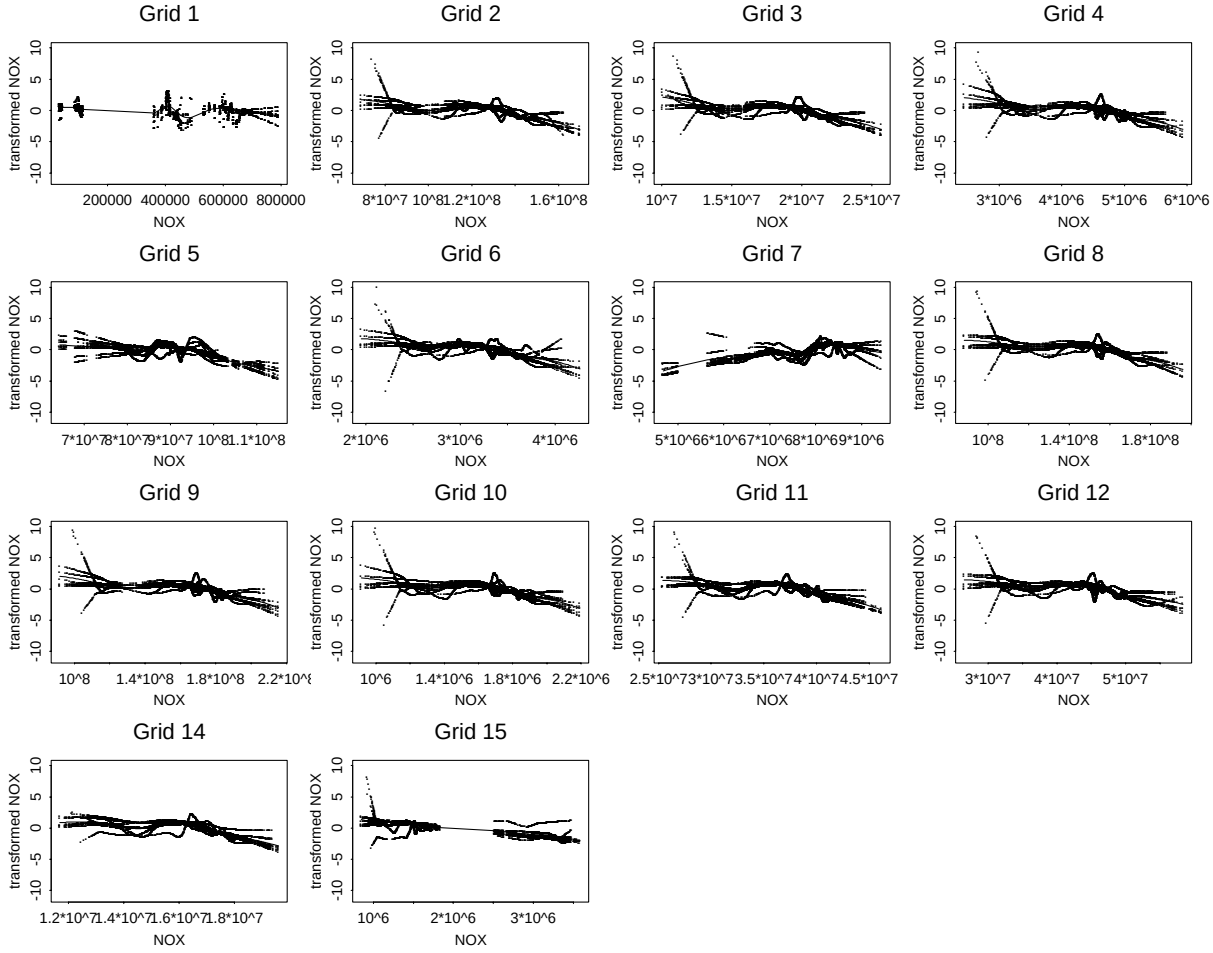

Figure 33: ACE transformations of total VOC. See Figure 25 for details.Grid 1 corresponds to SW corner, grid 2 to the cell directly east, grid 4 to the cell directly north of cell 1, etc.

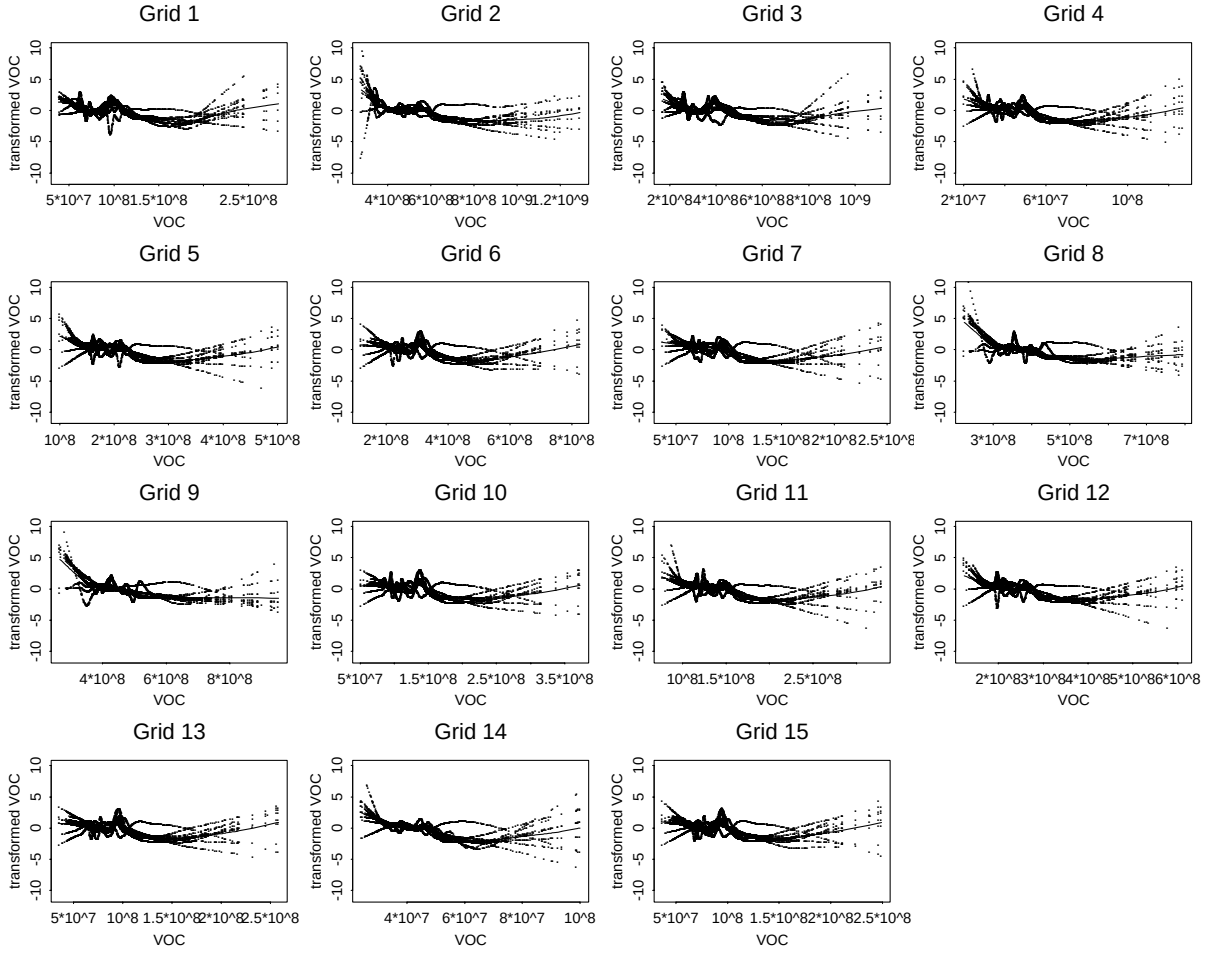

B.2 Daily 8 hour maximum

Figure 34: ACE transformations of 1000-mb geopotential height. See Figure ?? for details.

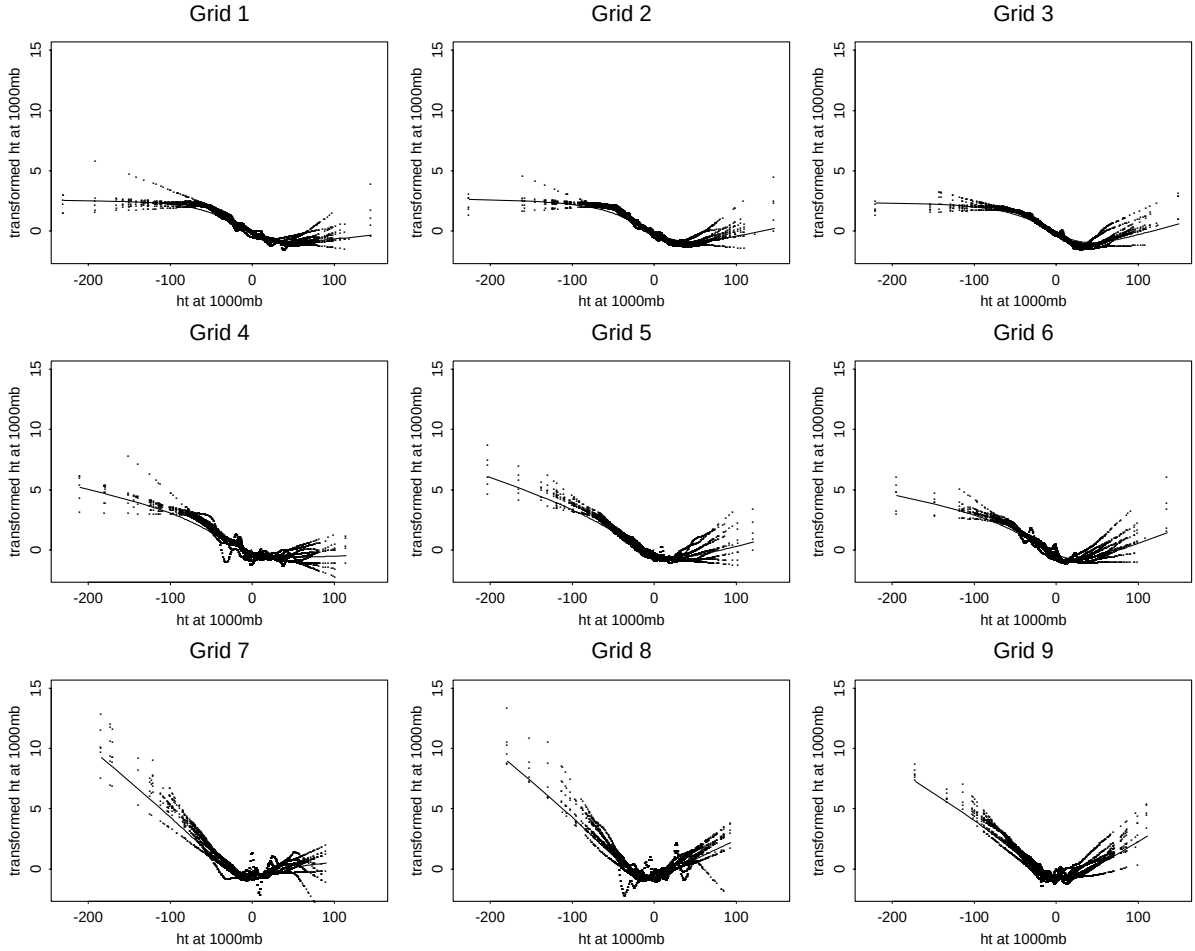

Figure 35: ACE transformations of 850-mb geopotential height. See Figure 25 for details.

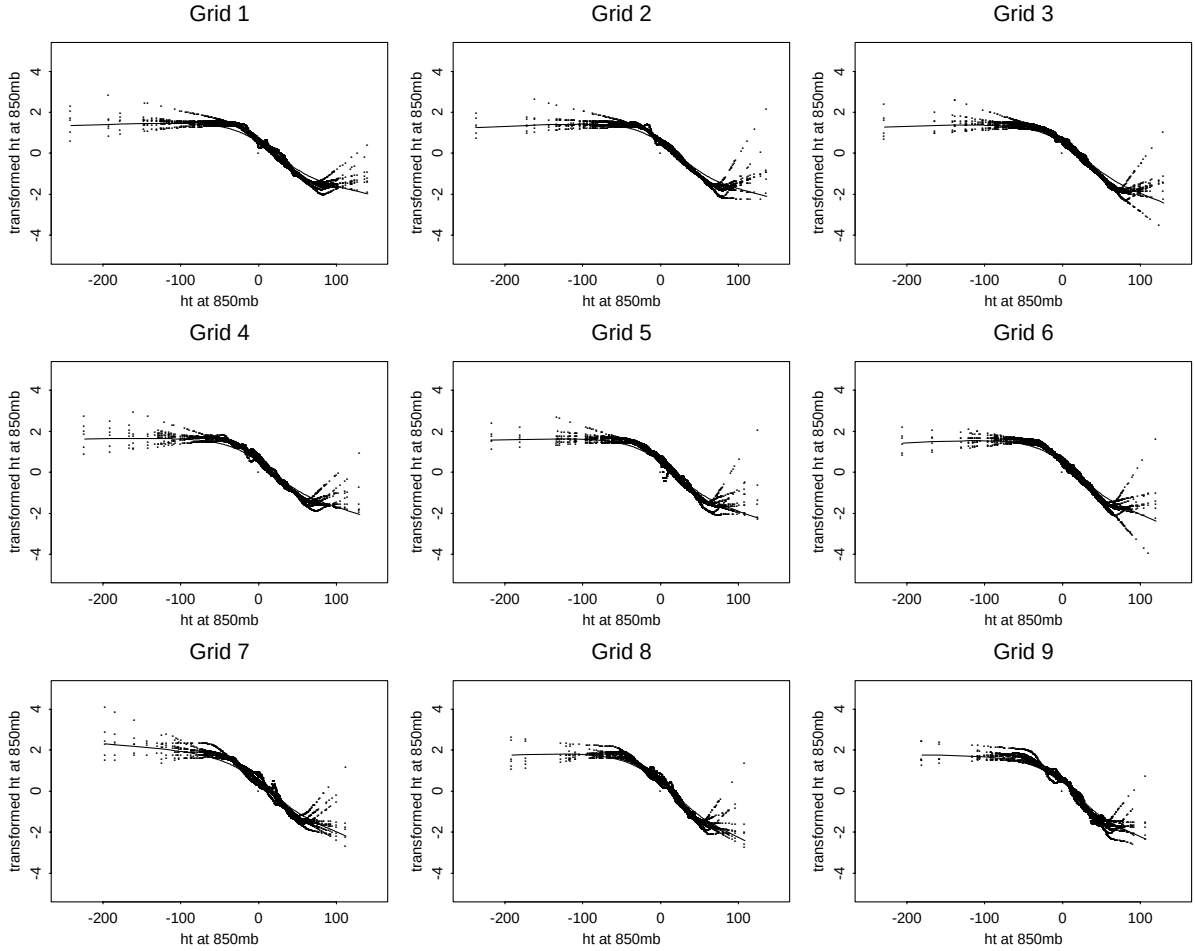

Figure 36: ACE transformations of 1000-mb mean temperature. See Figure 25 for details.

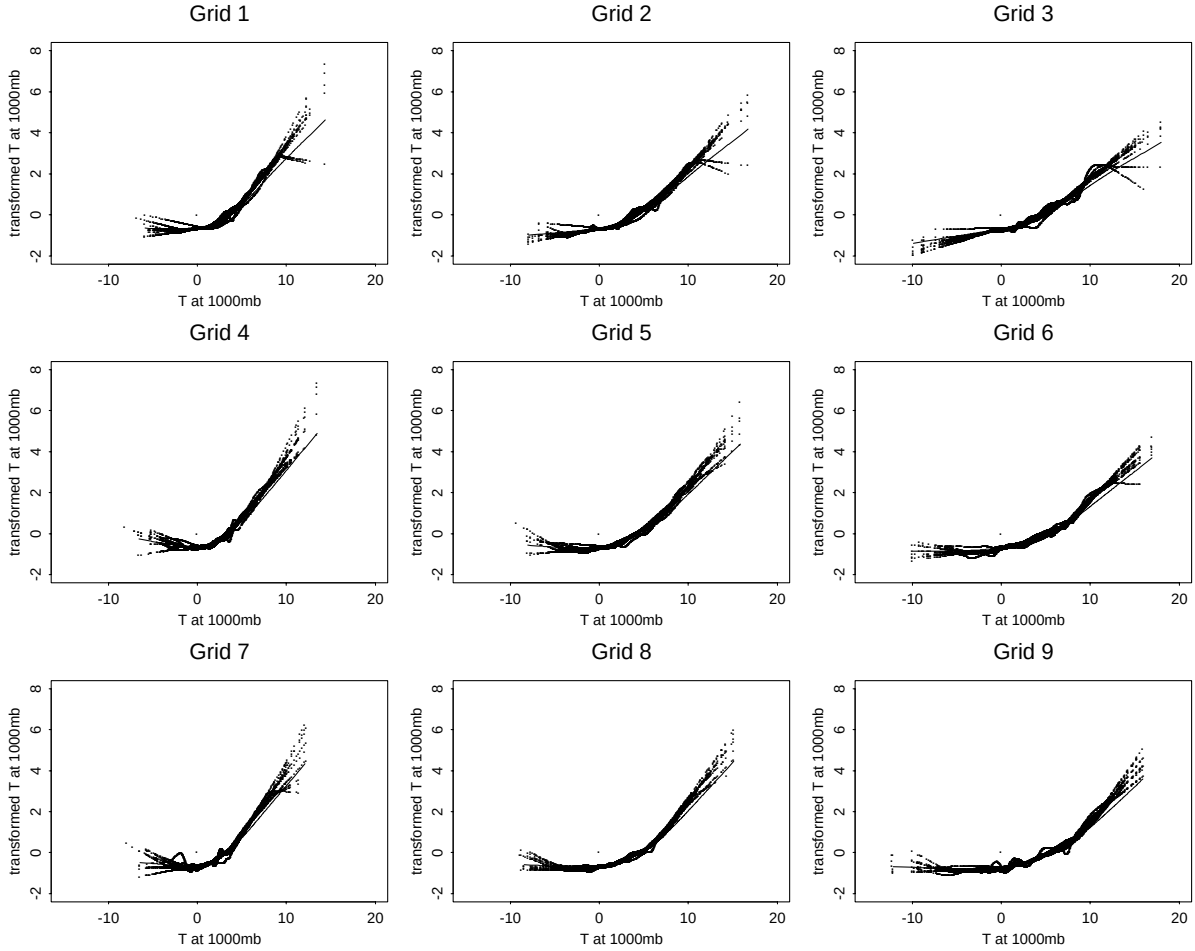

Figure 37: ACE transformations of 850-mb mean temperature. See Figure 25 for details.

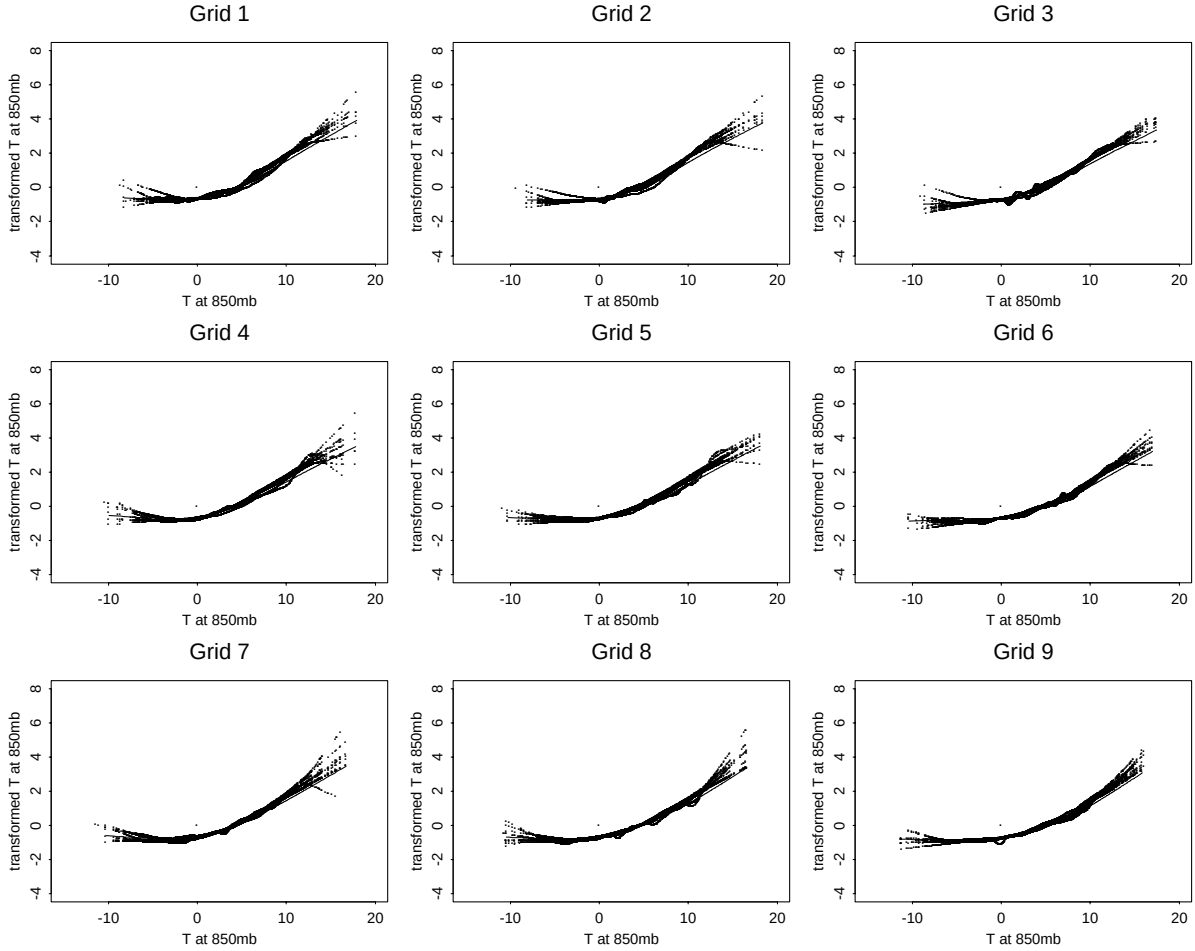

Figure 38: ACE transformations of 2 m mean temperature. See Figure 25 for details.

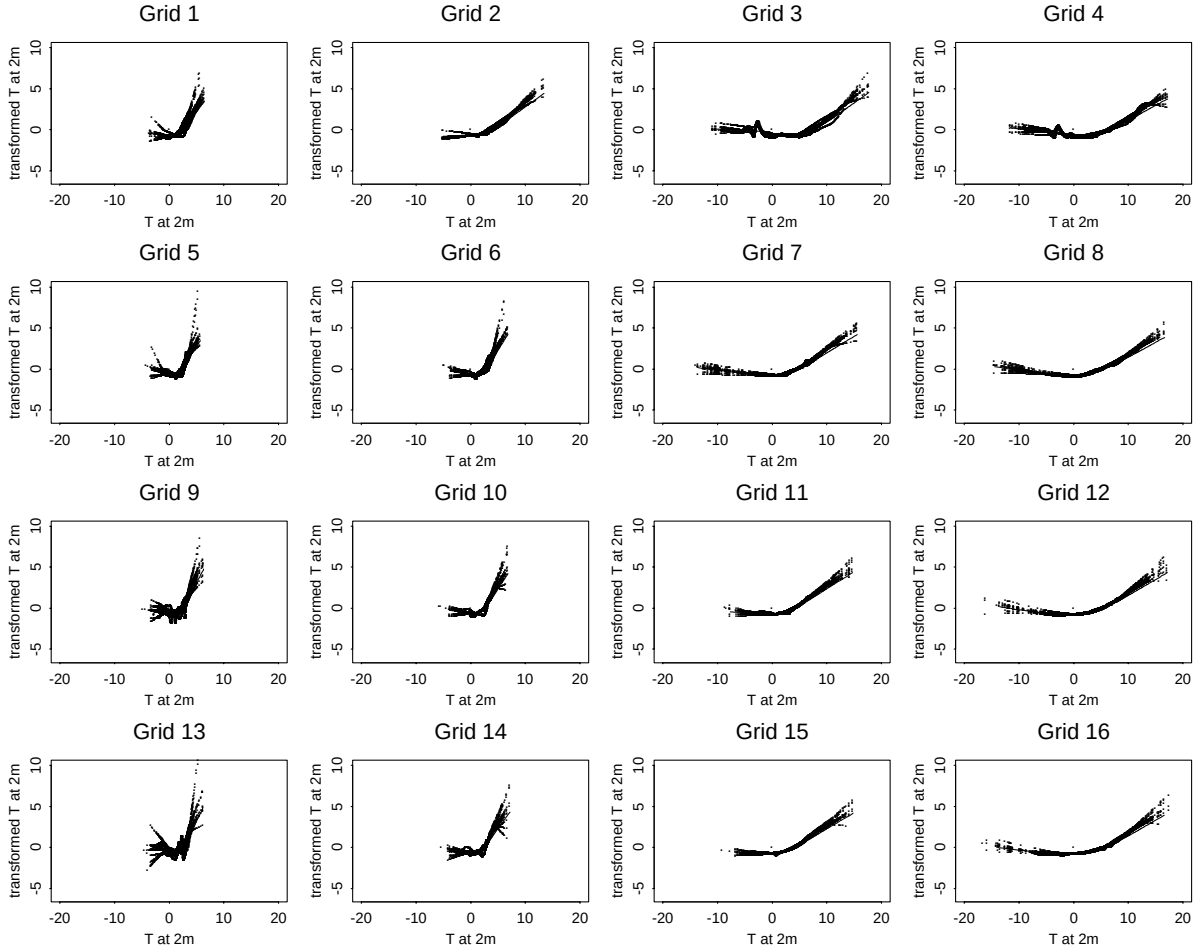

Figure 39: ACE transformations of wind direction. See Figure 25 for details.

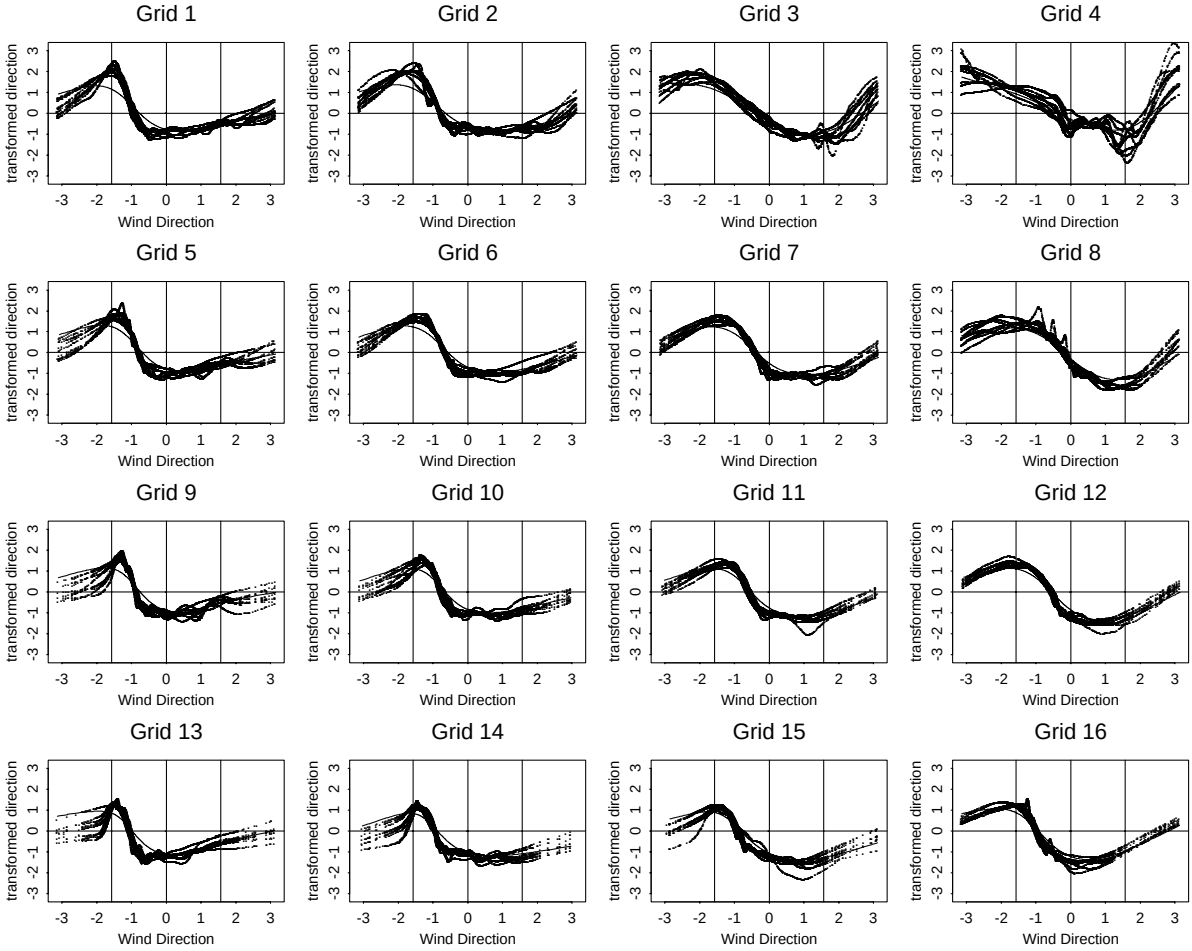

Figure 40: ACE transformations of maximum surface temperature, by meteorology monitor. See Figure 25 for details.

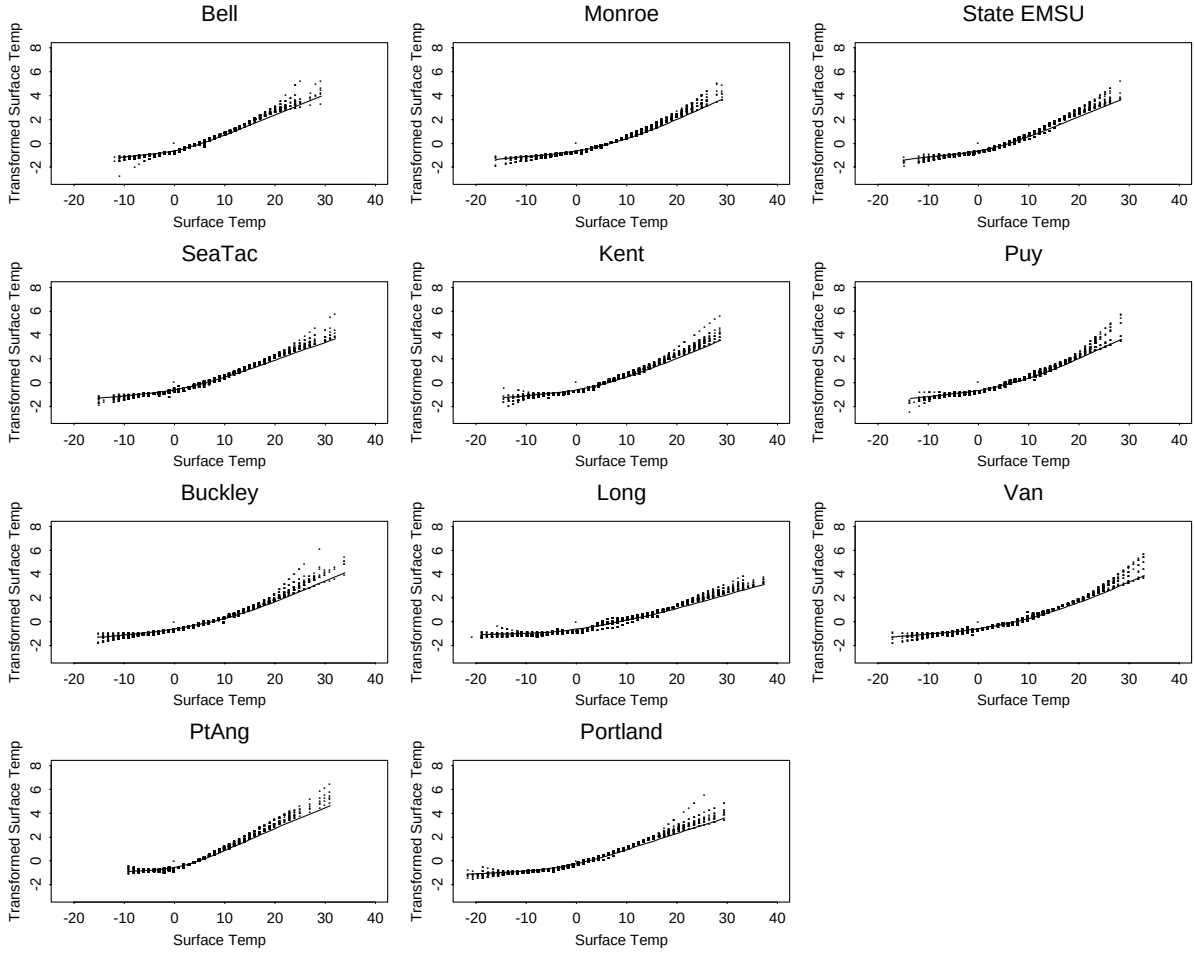

Figure 41: ACE transformations of total NO_x. See Figure 25 for details. Grid 1 corresponds to SW corner, grid 2 to the cell directly east, grid 4 to the cell directly north of cell 1, etc.

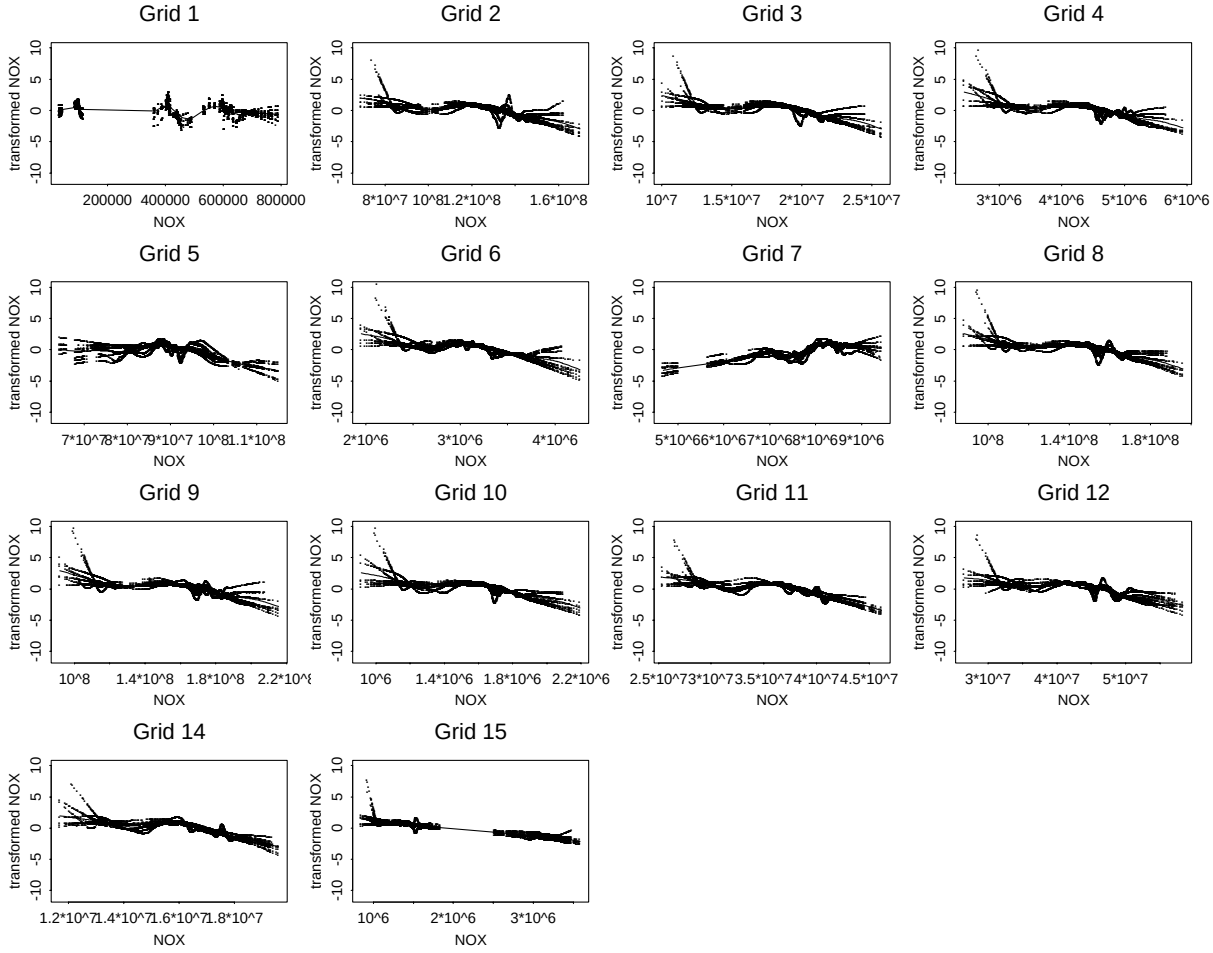

Figure 42: ACE transformations of total VOC. See Figure 25 for details.Grid 1 corresponds to SW corner, grid 2 to the cell directly east, grid 4 to the cell directly north of cell 1, etc.

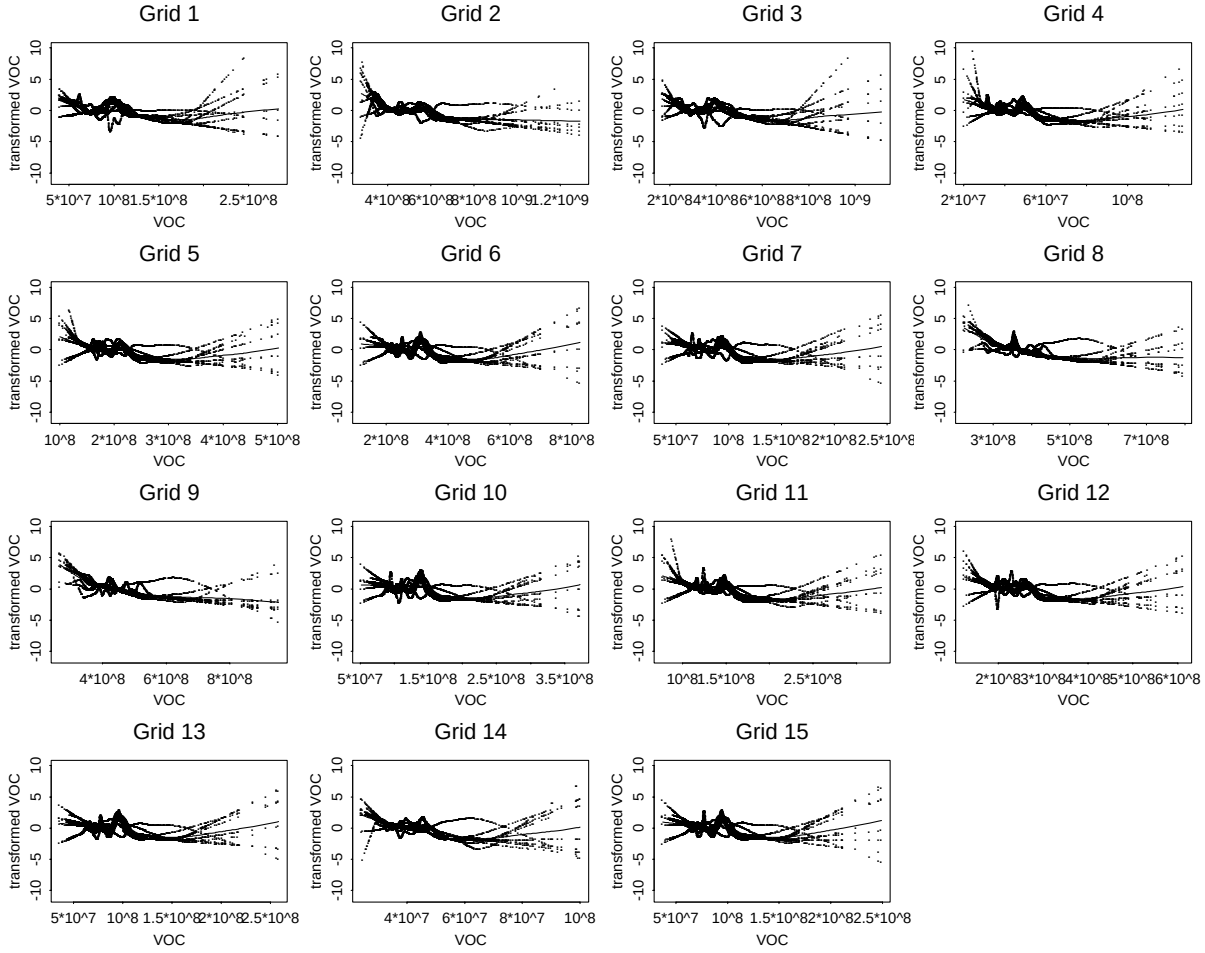

C Singular Value Decompositions

The weight coefficients for the dominant coupling patterns are given below. The linear combination of the product of the weight coefficients and the standardized variables form the composite regional summaries used in the analysis.

Table 17: SVD Weight Coefficients

Variable	**1 Hour SVD**	**8 Hour SVD**
H1000 Grid1	0.071	0.073
H1000 Grid2	0.072	0.073
H1000 Grid3	0.081	0.081
H1000 Grid4	0.042	0.045
H1000 Grid5	0.037	0.039
H1000 Grid6	0.048	0.049
H1000 Grid7	0.025	0.027
H1000 Grid8	0.023	0.023
H1000 Grid9	0.029	0.030
H850 Grid1	0.112	0.112
H850 Grid2	0.115	0.114
H850 Grid3	0.117	0.116
H850 Grid4	0.099	0.100
H850 Grid5	0.101	0.100
H850 Grid6	0.103	0.101
H850 Grid7	0.081	0.082
H850 Grid8	0.084	0.084
H850 Grid9	0.085	0.084
T1000 Grid1	-0.111	-0.108
T1000 Grid2	-0.108	-0.106
T1000 Grid3	-0.097	-0.096
T1000 Grid4	-0.129	-0.126
T1000 Grid5	-0.128	-0.126
T1000 Grid6	-0.113	-0.111
T1000 Grid7	-0.131	-0.128
T1000 Grid8	-0.136	-0.135
T1000 Grid9	-0.120	-0.119
T850 Grid1	-0.126	-0.123
T850 Grid2	-0.125	-0.122
T850 Grid3	-0.111	-0.108
T850 Grid4	-0.135	-0.131
T850 Grid5	-0.135	-0.132
T850 Grid6	-0.122	-0.120
T850 Grid7	-0.134	-0.131
T850 Grid8	-0.135	-0.132
T850 Grid9	-0.122	-0.120

Table 18: SVD Weight Coefficients *cont.*

Variable	**1 Hour SVD**	**8 Hour SVD**
T2m Grid1	-0.084	-0.081
T2m Grid2	-0.113	-0.113
T2m Grid3	-0.088	-0.090
T2m Grid4	-0.094	-0.095
T2m Grid5	-0.071	-0.063
T2m Grid6	-0.104	-0.100
T2m Grid7	-0.138	-0.137
T2m Grid8	-0.133	-0.133
T2m Grid9	-0.045	-0.037
T2m Grid10	-0.106	-0.101
T2m Grid11	-0.150	-0.149
T2m Grid12	-0.145	-0.144
T2m Grid13	-0.036	-0.028
T2m Grid14	-0.108	-0.103
T2m Grid15	-0.153	-0.153
T2m Grid16	-0.148	-0.148
Wind Magnitude Grid1	0.025	0.024
Wind Magnitude Grid2	0.034	0.034
Wind Magnitude Grid3	0.058	0.059
Wind Magnitude Grid4	0.062	0.063
Wind Magnitude Grid5	0.014	0.012
Wind Magnitude Grid6	0.035	0.033
Wind Magnitude Grid7	0.047	0.046
Wind Magnitude Grid8	0.069	0.070
Wind Magnitude Grid9	-0.004	-0.006
Wind Magnitude Grid10	0.009	0.007
Wind Magnitude Grid11	0.011	0.008
Wind Magnitude Grid12	0.049	0.047
Wind Magnitude Grid13	-0.022	-0.024
Wind Magnitude Grid14	-0.016	-0.019
Wind Magnitude Grid15	-0.015	-0.020
Wind Magnitude Grid16	0.035	0.031
Wind Direction Grid1	-0.084	-0.084
Wind Direction Grid2	-0.088	-0.088
Wind Direction Grid3	-0.071	-0.070
Wind Direction Grid4	-0.055	-0.053
Wind Direction Grid5	-0.083	-0.082
Wind Direction Grid6	-0.097	-0.097
Wind Direction Grid7	-0.103	-0.102
Wind Direction Grid8	-0.087	-0.085
Wind Direction Grid9	-0.086	-0.087

Table 19: SVD Weight Coefficients *cont.*

Variable	**1 Hour SVD**	**8 Hour SVD**
Wind Direction Grid10	-0.102	-0.104
Wind Direction Grid11	-0.116	-0.117
Wind Direction Grid12	-0.117	-0.118
Wind Direction Grid13	-0.084	-0.086
Wind Direction Grid14	-0.087	-0.090
Wind Direction Grid15	-0.092	-0.095
Wind Direction Grid16	-0.105	-0.107
Bellingham T	-0.167	-0.171
Monroe T	-0.165	-0.167
State EMSU T	-0.172	-0.176
SeaTac Airport T	-0.179	-0.183
Puyallup T	-0.144	-0.146
Buckley T	-0.153	-0.155
Longmire T	-0.113	-0.113
Vancouver T	-0.125	-0.125
Portland Airport T	-0.133	-0.134
NOx Grid1	-0.168	-0.172
NOx Grid2	-0.022	-0.034
NOx Grid3	-0.025	-0.034
NOx Grid4	-0.026	-0.033
NOx Grid5	-0.025	-0.032
NOx Grid6	-0.028	-0.035
NOx Grid7	-0.025	-0.031
NOx Grid8	-0.027	-0.036
NOx Grid9	-0.024	-0.032
NOx Grid10	-0.023	-0.030
NOx Grid11	-0.025	-0.032
NOx Grid12	-0.029	-0.037
NOx Grid13	-0.026	-0.033
NOx Grid14	-0.028	-0.036
NOx Grid15	-0.036	-0.047
VOC Grid1	0.012	0.010
VOC Grid2	0.014	0.014
VOC Grid3	0.012	0.012
VOC Grid4	0.013	0.011
VOC Grid5	0.012	0.011
VOC Grid6	0.012	0.009
VOC Grid7	0.013	0.011
VOC Grid8	0.013	0.015
VOC Grid9	0.014	0.017

Table 20: SVD Weight Coefficients *cont.*

Variable	**1 Hour SVD**	**8 Hour SVD**
VOC Grid10	0.012	0.010
VOC Grid11	0.012	0.010
VOC Grid12	0.012	0.011
VOC Grid13	0.012	0.009
VOC Grid14	0.013	0.013
VOC Grid15	0.012	0.009
FCC	-0.297	-0.272
Snoho	-0.315	-0.313
Lk Samm	-0.341	-0.342
Kent	-0.327	-0.324
Sumner	-0.352	-0.352
Pierce	-0.337	-0.339
Enumclaw	-0.356	-0.360
Pack Forest	-0.344	-0.353
Carus	-0.327	-0.338

D Imputation of Missing Ozone Records

See [Little 86] for a thorough discussion of imputation using the EM algorithm. Here we assume that the ozone monitor records for the network follow a multivariate normal distribution,

$$\begin{pmatrix} O_{3,FCC} \\ O_{3,Snoho} \\ . \\ . \\ . \\ O_{3,Carus} \end{pmatrix} \sim N(\mu_{dayofseason}, \sum_{Ozone}).$$

The procedure follows five steps:

1. Estimate the seasonal mean trend at each ozone site, e.g.

$$\hat{\mu}_{FCC,June1} = \sum_{years} O_{FCC,June1,yeari}/n$$

   .

2. Remove the seasonal mean trend at each sie, centering the network distribution around the zero-vector.

3. Use the EM algorithm to calculate $\hat{\sum}_{Ozone}$, (Tables 21, 22).

4. For each monitor with missing observations, and each combination of monitors with observations available on those days that the monitor of interest was unobserved, calculate the linear regression equation

$$O_{3missing,dayi} = \beta_{0,missing} + \sum_{observedj} \beta_{j,missing} O_{3observed,dayi}$$

   from $\hat{\sum}_{ozone}$.

5. Use equations from the previous step to impute the unobserved records.

The estimated covariance matrices for the locally-standardized ozone monitors are given below.

Table 21: 1 Hour Ozone Covariance Matrix, estimated using EM algorithm.

Monitor	FCC	Snoho	Lk Samm	Kent	Sumner	Pierce	Enumclaw	Pack Forest	Carus
FCC	0.000138	0.000145	0.000175	0.000149	0.000139	0.000152	0.000190	0.000175	0.000149
Snoho	0.000145	0.000245	0.000248	0.000181	0.000221	0.000214	0.000251	0.000239	0.000209
Lk Samm	0.000175	0.000248	0.000400	0.000257	0.000323	0.000322	0.000381	0.000352	0.000312
Kent	0.000149	0.000181	0.000257	0.000246	0.000258	0.000250	0.000281	0.000229	0.000221
Sumner	0.000139	0.000221	0.000323	0.000258	0.000363	0.000326	0.000344	0.000314	0.000286
Pierce	0.000152	0.000214	0.000322	0.000250	0.000326	0.000387	0.000343	0.000346	0.000296
Enumclaw	0.000190	0.000251	0.000381	0.000281	0.000344	0.000343	0.000459	0.000392	0.000355
Pack Forest	0.000175	0.000239	0.000352	0.000229	0.000314	0.000346	0.000392	0.000428	0.000333
Carus	0.000149	0.000209	0.000312	0.000221	0.000286	0.000296	0.000355	0.000333	0.000428

Table 22: 8 Hour Ozone Covariance Matrix, estimated using EM algorithm.

Monitor	FCC	Snoho	Lk Samm	Kent	Sumner	Pierce	Enumclaw	Pack Forest	Carus
FCC	0.000096	0.000100	0.000111	0.000081	0.000090	0.000099	0.000121	0.000114	0.000095
Snoho22	0.000100	0.000160	0.000162	0.000117	0.000151	0.000145	0.000165	0.000159	0.000140
LkSamm	0.000111	0.000162	0.000242	0.000156	0.000204	0.000202	0.000234	0.000227	0.000201
Kent	0.000081	0.000117	0.000156	0.000151	0.000167	0.000158	0.000161	0.000139	0.000140
Sumner	0.000090	0.000151	0.000204	0.000167	0.000232	0.000207	0.000210	0.000207	0.000190
Pierce	0.000099	0.000145	0.000202	0.000158	0.000207	0.000242	0.000222	0.000226	0.000195
Enumclaw	0.000121	0.000165	0.000234	0.000161	0.000210	0.000222	0.000287	0.000257	0.000231
Pack Forest	0.000114	0.000159	0.000227	0.000139	0.000207	0.000226	0.000257	0.000283	0.000227
Carus	0.000095	0.000140	0.000201	0.000140	0.000190	0.000195	0.000231	0.000227	0.000278

E Emissions Estimation

The following reports the steps taken to generate the total NO_x and VOC estimates used in the analysis. The data and documentation were provided by Sally Otterson, Washington Department of Ecology.

Western Washington and Oregon Historical Emissions Estimates, 1975-1996

provided by Sally Otterson, WA. Dept. of Ecology

Description of Project

Daily emissions estimates were calculated for western Washington and northwestern Oregon for June l to September 30 during the years 1975-1996. Ozone measurements and meteorological data over the same period will be analyzed with the emissions data to determine the effects of emissions on ozone concentrations.

Emissions were calculated using a 100 km grid system within the domain bounded by UTM East 350 – 650, and UTM North 5000 – 5400 (12 grid cells). Three additional grid cells were inventoried in the area bounded by UTM East 350 – 650, and UTM North 5400 – 5430 to allow for encompassing all of Washington State.

Emissions were calculated for five major source categories: onroad mobile, stationary area sources, nonroad mobile sources, large point sources, and biogenic sources. Four basic tasks were completed for each source category: 1) estimate an activity level, 2) adjust/allocate the activity (emissions) temporally, 3) allocate the activity (emissions) spatially, and 4) estimate emission rates per the activity level. Each of these tasks are described below for each source category.

ONROAD MOBILE SOURCES

1. Activity Level - Vehicle Miles Traveled

The Washington State Department of Transportation provided statewide estimates of vehicle miles traveled (VMT) data for the years 1974-1996.[1, 2] The data was used to determine growth factors that could be combined with spatially resolved VMT data for 1995.

The Washington State Department of Transportation (WSDOT) and several local transportation planning agencies provided VMT data for detailed roadway networks.[3, 4, 5, 6, 7] The VMT data is provided for each roadway segment (link). The following abbreviations are used: PSRC (Puget Sound Regional Council), SWWRTC (Southwest Washington Regional Transportation Council), TRPC (Thurston Regional Planning Council), and METRO (transportation planning agency for Portland, OR).

Several sources of summary VMT data were also obtained. WSDOT provided Highway Performance Monitoring System (HPMS) data, which is summary data over several urban and rural areas. HPMS differs from the state route link VMT because it includes county and city data. WSDOT also provided estimates of total VMT by county using the HPMS data. The county estimates were based in part on actual traffic counts, and are normally used for general informational purposes.[6]

The Cowlitz-Wahkiakum Council of Governments (CWCOG) provided summary data for the Kelso-Longview urban area. Skagit County provided county jurisdiction data .[8, 9]

Final Data Sources Chosen

Because of the overlap in data obtained, comparisons of average daily VMT estimates could be made (see below). In most of the counties, VMT from the transportation planning agencies was greater than that obtained from WSDOT. Data from the PSRC, SWWRTC and TRPC was used in King, Kitsap, Pierce, Snohomish, Thurston and Clark Counties. Data from METRO was used for Oregon. In all other areas, WSDOT's state route VMT was used.

For areas in Oregon outside of METRO's tracking area, VMT was estimated using the ratio of VMT to population within METRO's area multiplied by area population.

County	WSDOT VMT	local VMT	% diff
Clark	6,384,000	5,563,000	15
King	43,004,000	41,713,000	3
Kitsap	4,131,000	5,120,000	-19
Pierce	14,933,000	15,927,000	-6
Snohomish	12,787,000	14,913,000	-14
Thurston	5,421,000	6,833,000	-21
Total	86,661,000	90,069,000	-4

VMT Adjustments

Volume Adjustments In areas where WSDOT's state route VMT was used, VMT was increased over all links according to the ratio of total county HPMS VMT to county state route VMT.

2. Temporal Adjustments

All VMT data was supplied as average daily VMT (ADVMT).

Annual First, all VMT data was standardized to 1995. To do this, forward projections from 1994 to 1995 were made using 1994 and 1995 HPMS summary data for western WA. After standardizing, VMT data was projected backwards using historical estimates of statewide VMT provided by WSDOT.[1] VMT was projected to 1996 using 1996 HPMS data, also provided by WSDOT.[2]

ADVMT by County (in thousands)

Year	Clallam	Clark	Cowlitz	Grays Harbor	Island	Jefferson	King	Kitsap	Lewis	Mason	Pacific	Pierce	San Juan	Skagit	Skamania	Snohomish	Thurston	Wahkiakum	Whatcom
1975	551	2961	1381	802	481	371	19074	1883	1200	513	275	6705	41	1380	117	6017	2411	55	1605
1976	589	3164	1476	856	514	396	20378	2012	1282	548	294	7164	44	1474	125	6428	2576	59	1714
1977	632	3394	1583	919	552	425	21864	2159	1376	588	315	7686	48	1582	134	6897	2763	63	1839
1978	682	3666	1710	992	596	459	23614	2331	1486	635	340	8301	51	1708	144	7449	2985	68	1986
1979	704	3782	1764	1024	615	474	24362	2405	1533	655	351	8564	53	1762	149	7685	3079	71	2049
1980	682	3665	1709	992	596	459	23606	2331	1486	635	340	8299	51	1708	144	7447	2984	68	1986
1981	702	3774	1760	1021	613	473	24308	2400	1530	653	350	8545	53	1759	149	7668	3072	70	2045
1982	733	3940	1838	1066	640	494	25380	2506	1597	682	366	8922	55	1836	155	8006	3208	74	2135
1983	762	4097	1911	1109	666	513	26387	2605	1661	709	380	9276	57	1909	161	8324	3335	76	2220
1984	797	4282	1997	1159	696	537	27584	2723	1736	741	398	9697	60	1996	169	8702	3486	80	2320
1985	817	4391	2048	1188	714	550	28282	2792	1780	760	408	9942	61	2046	173	8922	3575	82	2379
1986	838	4505	2101	1219	732	565	29018	2865	1826	780	418	10201	63	2099	178	9154	3668	84	2441
1987	887	4768	2224	1291	775	598	30715	3033	1933	826	443	10798	67	2222	188	9689	3882	89	2584
1988	955	5132	2394	1389	834	643	33058	3264	2080	889	476	11621	72	2392	202	10428	4178	96	2781
1989	1012	5438	2537	1472	884	682	35030	3459	2204	942	505	12315	76	2534	214	11051	4427	101	2947
1990	1048	5630	2626	1524	915	706	36268	3581	2282	975	523	12750	79	2624	222	11441	4584	105	3051
1991	1086	5836	2722	1580	948	731	37591	3711	2366	1010	542	13215	82	2720	230	11858	4751	109	3162
1992	1140	6125	2857	1658	995	768	39454	3895	2483	1061	569	13870	86	2854	241	12446	4987	114	3319
1993	1142	6138	2863	1661	997	769	39537	3904	2488	1063	570	13899	86	2860	242	12473	4997	115	3326
1994	1121	6027	2811	1631	979	755	38820	3833	2443	1043	559	13647	84	2808	238	12246	4906	112	3266
1995	1155	6207	2895	1680	1009	778	39980	3947	2516	1075	576	14055	87	2892	245	12612	5053	116	3363
1996	1175	6314	2945	1709	1026	791	40673	4016	2560	1093	586	14298	88	2943	249	12831	5141	118	3421

Other Monthly and daily adjustments were made to the VMT data based on traffic recorder statistics supplied by WSDOT.[10, 11] The adjustments are presented in the tables below. The difference between local transportation agency data and WSDOT data in the day of week adjustment table is due to differences in defining "average" day VMT. The local transportation planning agencies' data was representative of Tuesday - Thursday traffic, and data supplied by WSDOT represented an average of all days.

Monthly Adjustment Factors

Month	Adj.
Jun	1.061
Jul	1.072
Aug	1.096
Sep	1.029

Day of Week Adjustment Factors

Day	Mon	Tue	Wed	Thu	Fri	Sat	Sun
WSDOT	1.013	1.037	1.044	1.052	1.148	0.933	0.775
Local	0.970	1.000	1.000	1.000	1.100	0.894	0.742

3. Spatial Allocation

Link geographic coordinates were used to spatially allocate VMT to the modeling grid system.

4. Emission Rates

The EPA's MOBILE model (version 5b) was used to generate emission rates for nitrogen oxides (NOx), and volatile organic compounds (VOC) in grams per mile.[12]

EPA used data collected from different categories of vehicles under different operating conditions to develop the model. The model is continuously updated as new information is gathered. The model may be tailored to account for local conditions (such as fleet registration mix, temperature, fuel parameters, inspection and maintenance programs (I/M), and speeds). The model can output results for several classes of gasoline and diesel powered vehicles. Organic emissions can be output both in total and with a detailed evaporative and exhaust emission breakdown.

For this study, local parameters were used for: speeds, daily maximum and minimum temperature, vehicle registration distributions, inspection and maintenance programs (I/M), anti-tampering programs, and Reid vapor pressure. Some detail on each parameter is presented below.

Speed

To determine an appropriate network speed for each pollutant, a detailed mobile source inventory was compiled using link-specific speeds in the Puget Sound area. Average VOC emissions occurred at approximately 29 mph, and average NOx at 49 mph.

Temperatures

The MOBILE model calculates emission rates based on inputs of daily maximum and minimum temperature. Daily maximum and minimum temperatures for each day from SeaTac and Portland International Airports were used in this study.[13] Portland temperatures were used for Oregon and Vancouver vehicle emissions calculations. SeaTac temperatures were used for all other areas.

Vehicle Registration Distributions

Vehicle registration distributions by model year were available for the years 1990 and 1995. The 1990 distribution was assigned to 1975-1992, and the 1995 distribution was used for 1993-1996. The distributions were derived from monthly registration statistics by model year available from the Department of Licensing.[14]

Inspection/Maintenance and Anti-Tampering Programs

Vehicles in several areas in the domain are required to be tested for emissions and/or tampering. The areas are: greater Seattle, greater Everett and Tacoma, Vancouver, and Portland. Detail on the program parameters and changes in the parameters[15, 16] over the 22-year period may be found in the MOBILE5b input files. No corrections were made for any vehicle not subject to inspection entering an I/M area.

Reid Vapor Pressure (RVP)

Prior to 1989, summertime RVP was not regulated. Studies by EPA and the Oregon Department of Environmental Quality showed a 1987 RVP of about 11.0.[17, 18] From 1989 to 1991, a limit of 10.5 was in effect for Washington and Oregon. In 1992, the limit for Oregon was lowered to 7.8 and the limit for Washington was lowered to 9.0. For this study, a safety margin of 0.3 was subtracted from all RVP limits except the 7.8 limit. Gasoline sold in Vancouver was assumed to come from Oregon suppliers per SWAPCA information.[19] The following table shows the RVP assignments.

Years	Portland-Vancouver	Washington (exc. Vancouver)
1975-88	11.0	11.0
1989-91	10.2	10.2
1992-96	7.8	8.7

STATIONARY AREA SOURCES

VOCs were inventoried for:

- Architectural Surface Coating
- Commercial/Consumer Products
- FIRFA products (mainly pesticides)
- Graphic Arts
- Autobody Surface Coating
- Industrial Surface Coating
- Surface Cleaning

1. Activity Level - Population

Population was used to estimate emissions from these sources. County population for each year was obtained from the Office of Financial Management for Washington and from the Bureau of the Census for Oregon. [20, 21] Counties and 1990 population are given below. For some counties, only a portion of the county (and population) was within the modeling domain.

ID#	County	1990 pop	ID#	County	1990 pop
WA-009	Clallam	54007	WA-059	Skamania	7191
WA-011	Clark	235295	WA-061	Snohomish	506610
WA-015	Cowlitz	79733	WA-067	Thurston	159124
WA-027	Grays Harbor	61574	WA-069	Wahkiakum	2887
WA-029	Island	58686	WA-073	Whatcom	124912
WA-031	Jefferson	18981	WA-077	Yakima	188823
WA-033	King	1456704			
WA-035	Kitsap	187999	OR-005	Clackamas	280910
WA-037	Kittitas	26725	OR-007	Clatsop	33428
WA-039	Klickitat	16616	OR-009	Columbia	37856
WA-041	Lewis	55783	OR-027	Hood River	16965
WA-045	Mason	35884	OR-051	Multnomah	586156
WA-049	Pacific	17374	OR-057	Tillamook	21644
WA-053	Pierce	573321	OR-065	Wasco	21778
WA-055	San Juan	9253	OR-067	Washington	314952
WA-057	Skagit	75989	OR-071	Yamhill	65985

2. Temporal Adjustments

Both month and day of week adjustments were made to data. Daily adjustments were made using EPA information.[22] Monthly adjustments were made using EPA adjustment factors for all categories except architectural surface coating and FIRFA products. Adjustments to those categories were made using total quarterly gross business income for standard industrial codes 523 “Paint, Glass and Wallpaper Stores” and code 526 “Retail Nurseries and Garden Stores.” Adjustment factors are shown below.

Category	Monthly Adjustments			
	June	July	August	September
Architectural	0.09	0.123	0.123	0.123
FIRFA	0.10	0.081	0.081	0.081
Comm/Cons	0.083	0.083	0.083	0.083
Graphic Arts	0.083	0.083	0.083	0.083
Autobody	0.083	0.083	0.083	0.083
Industrial	0.083	0.083	0.083	0.083
Surf Clean	0.083	0.083	0.083	0.083

Category	Day of Week Adjustments						
	Mon	Tue	Wed	Thu	Fri	Sat	Sun
Architectural	0.143	0.143	0.143	0.143	0.143	0.143	0.143
FIRFA	0.143	0.143	0.143	0.143	0.143	0.143	0.143
Comm/Cons	0.143	0.143	0.143	0.143	0.143	0.143	0.143
Graphic Art	0.200	0.200	0.200	0.200	0.200	0.000	0.000
Autobody	0.200	0.200	0.200	0.200	0.200	0.000	0.000
Industrial	0.200	0.200	0.200	0.200	0.200	0.000	0.000
Surf Clean	0.167	0.167	0.167	0.167	0.167	0.167	0.000

3. Spatial Allocation

1990 Census block population data was allocated to the 100 km grid system using geographical information system methods.[23] Each grid's population was subdivided by county. To estimate population for the remaining years, each grid's county subdivision population for the given year was multiplied by the ratio of the county's given yearly population to its 1990 population.

4. Emission Rates

No area specific information was gathered. All sources' emissions were based on national per capita factors.[24, 25] The per capita factors were multiplied by population estimates to calculate emissions. The following table lists the VOC factors in grams per person-yr.

Category	g/person-yr
Architectural Surface Coating – Solvent	1036
Architectural Surface Coating – Water	611
Commercial/Consumer Solvents	3556
Graphic Arts	590
Autobody Refinishing	1043
Industrial Surface Coating	3992
Surface Cleaning	1950

NONROAD MOBILE SOURCES

Emissions estimates for nonroad sources were calculated using EPA methodology.[26] Emissions of NOx and VOC were inventoried for several categories of nonroad mobile sources:

- Boats
- Construction Equipment
- Commercial Equipment
- Industrial Equipment
- Lawn and Garden Equipment
- Recreational Vehicles

1. Activity Level - Population

Population was used to estimate emissions from these sources. County population for each year was obtained from the Office of Financial Management for Washington and from the Bureau of the Census for Oregon.[20, 21] Counties within the modeling domain and their 1990 population are listed above under the Stationary Area Source section.

2. Temporal Adjustments

Both month and day of week adjustments were made using EPA adjustment factors.[22, 27] Percentage of activity for each month and day of week are shown below. Each of the categories in the tables are made up of many subcategories; the percentages shown are the most representative of the group. Individual subcategories may vary (such as snowblowers and snowmobiles).

Category	Monthly Percent of Activity			
	June	July	Aug	Sept
boats	19	19	19	6
construction	13	13	13	8
commercial	8	8	8	8
industrial	8	8	8	8
lawn and garden	13	13	13	10
recreational	14	14	14	7

Category	Day of Week Percent of Activity						
	Mon	Tues	Wed	Thur	Fri	Sat	Sun
boats	6	6	6	6	6	35	35
construction	17	17	17	17	17	17	0
commercial	17	17	17	17	17	17	0
industrial	17	17	17	17	17	17	0
lawn and garden	10	10	10	10	10	25	25
recreational	6	6	6	6	6	35	35

3. Spatial Allocation

1990 Census block population data was allocated to the 100 km grid system using geographical information system methods.[23] Each grid's population was subdivided by county. To estimate population for the remaining years, each grid's county subdivision population for the given year was multiplied by the ratio of the county's given yearly population to its 1990 population.

4. Emission Rates

Emission factors in grams per person-yr were taken from EPA's 1990 Nonroad Study for the Seattle-Tacoma ozone nonattainment area and are shown below.[27]

Category	Subcategory	NOx		VOC	
		diesel	gas	diesel	gas
Boats	Sailboat Aux. Inboard Engines	2.45	0.19	1.84	1.28
Boats	Sailboat Aux. Outboard Engines	0	0	0	0
Boats	Vessels w/Inboard Engines	75.87	93.1	10.76	561.38
Boats	Vessels w/Outboard Engines	0	13.57	0	1325.63
Boats	Vessels w/Sterndrive Engines	0	0	0	0

Category	Subcategory	diesel NOx	gas	diesel VOC	gas
Construction	Asphalt Pavers	17.36	0.24	1.06	0.69
Construction	Bore/Drill Rigs	28.74	0.84	3.85	3.17
Construction	Cement and Mortar Mixers	0.32	0.67	0.03	6.92
Construction	Concrete Pavers	9.24	0	1.06	0
Construction	Concrete/Industrial Saws	0.12	1.8	0.02	17.34
Construction	Cranes	267.85	0.52	34.48	1.33
Construction	Crawler Tractors	793.67	0	102.18	0
Construction	Crushing/Proc. Equipment	35.95	0.29	4.82	0.75
Construction	Dumpers/Tenders	0.04	0.09	0	0.85
Construction	Excavators	245.08	0	16.55	0
Construction	Graders	134.98	0	22.58	0
Construction	Off-Highway Tractors	250.71	0	54.02	0
Construction	Off-Highway Trucks	184.66	0	17.04	0
Construction	Other Construction Equipment	32.82	0.6	4.4	1.54
Construction	Paving Equipment	69.89	1.37	6.7	32.28
Construction	Plate Compactors	0.14	0.4	0.01	25.68
Construction	Rollers	42.77	0.67	3.89	7.74
Construction	Rough Terrain Forklifts	58.09	0.56	12.68	1.44
Construction	Rubber Tired Dozers	64.13	0	5.92	0
Construction	Rubber Tired Loaders	486.25	0.75	41.83	1.47
Construction	Scrapers	116.37	0	9.71	0
Construction	Signal Boards	3.18	0.02	0.5	0.23
Construction	Skid Steer Loaders	75.2	1.49	17.12	3.84
Construction	Surfacing Equipment	0	0.45	0	4.88
Construction	Tampers/Rammers	0	0.01	0	14.54
Construction	Tractors/Loaders/Backhoes	402.03	0.38	58.35	0.97
Construction	Trenchers	37.3	2.05	5.98	5.49
Commercial	Air Compressors < 50 HP	5.61	1.07	0.87	35.24
Commercial	Gas Compressors < 50 HP	0	1.34	0	1.49
Commercial	Generator Sets < 50 HP	26.67	6.07	4.15	367.38
Commercial	Pressure Washers < 50 HP	0.09	0.52	0.01	19.21
Commercial	Pumps < 50 HP	11.07	2.48	1.72	63.77
Commercial	Welders < 50 HP	22.91	1.61	3.57	51.68
Industrial	Aerial Lifts	13.35	12.49	1.55	26.43
Industrial	Forklifts	169.02	237.33	19.68	189.81
Industrial	Other General Industrial Equip	43.98	2.94	5.12	24.04
Industrial	Other Material Handling Equip	6.34	0.35	0.74	0.97
Industrial	Sweepers/Scrubbers	128.59	10.96	14.97	13.11

Category	Subcategory	NOx diesel	NOx gas	VOC diesel	VOC gas
Lawn & Garden	Chainsaws <4 HP	0	0.95	0	659.31
Lawn & Garden	Chippers/Stump Grinders	10.58	1.83	1.65	64.43
Lawn & Garden	Commercial Turf Equipment	0	9.76	0	289.96
Lawn & Garden	Front Mowers	0	0.32	0	15.89
Lawn & Garden	Lawn Mowers	0	8.85	0	1731.62
Lawn & Garden	Lawn/Garden Tractors	7.73	4.76	1.21	174.18
Lawn & Garden	Leaf Blowers/Vacuums	0	0.22	0	107.91
Lawn & Garden	Other Lawn/Garden Equipment	0.01	0.04	0	13.72
Lawn & Garden	Rear Engine Riding Mowers	0.09	1.16	0.01	44
Lawn & Garden	Shredders <5 HP	0	0.02	0	3.77
Lawn & Garden	Snowblowers	0	0.04	0	10.28
Lawn & Garden	Tillers <5 HP	0	0.4	0	55.13
Lawn & Garden	Trimmer/Edger/Brush Cutters	0	0.45	0	252.45
Lawn & Garden	Wood Splitters	0.01	0.08	0	10.9
Recreational	All Terrain Vehicles (ATV's)	0	0.84	0	96.64
Recreational	Golf Carts	0	0.94	0	149.03
Recreational	Minibikes	0	0.01	0	1.07
Recreational	Off-Road Motorcycles	0	0.16	0	39.42
Recreational	Snowmobiles	0	1.03	0	140.56
Recreational	Specialty Vehicle Carts	0.03	0.09	0.01	41.09

MAJOR STATIONARY SOURCES

1. Activity Level and Emission Rates

Large stationary sources are required to report annual emissions of NOx and VOC to their local air authority. The local air authorities, in turn, report the emissions to Ecology. The stationary source record began in 1977.[28, 29]

Emissions estimates of NOx and VOC are sometimes estimated using actual source measurements, but because of the cost involved, it is more common for sources to estimate emissions using production and emission factors in mass per production. EPA and industry organizations are constantly updating emission factors as better information becomes available. Because emission factors have changed over the years, emissions may not be comparable from year to year. This, coupled with the uncertainty of some historical production data and the large effort required to recalculate emissions, limited the direct use of the historical database for emissions estimates.

The procedure for estimating point source emissions made use of the historical database, but relied on current emissions methods and estimates for determining individual source emissions. The procedure consisted of four basic steps detailed below.

Step 1 – Determine Facility List

The most current year of record (1995) was queried for individual emission units within a facility with emissions above the following cutoffs: NOx = 9 tons, VOC = 4.5 tons. Emissions from the individual units were totaled for each facility. All facilities emitting under 50 tons per year were excluded.

The historical record was checked for any facilities that had been large emitters, but were no longer in operation. Emissions for these facilities were counted only for the years the facility was in operation. Four facilities were identified and are shown below.

Facility ID Number	Facility	Last Year of Record
S-027-0002	ITT Rayonier, Hoquaim	1991
S-061-0008	Weyerhaeuser, Everett	1991
E-011-0009	Carborundum, Vancouver	1986
C-053-0001	ASARCO, Tacoma	1984

The complete list of facilities used for this study is listed below.

C-033-0004 Ball-Foster Glass Container Corp
C-033-0006 Birmingham Steel Corp (West Seattle)
C-033-0013 Weyerhaeuser Co (Snoqualmie)
C-033-0015 Boeing Commercial Airplane (Auburn)
C-033-0017 Holnam, Inc., Ideal Division
C-033-0023 WA, Univ Of, Power Plant & Hospital
C-033-0037 Kenworth Truck Co (Paccar)
C-033-0048 Seattle Steam Co (Western Ave)
C-033-0052 Boeing Commercial Airplane (Renton)
C-033-0068 American National Can Co
C-033-0096 Kenworth Truck Company - Renton
C-033-0099 Ash Grove Cement Company (E Marg,)
C-033-0101 King Co Public Works (Cedar Hills)
C-033-0138 Metropolitan King Co. (West Point)
C-033-0157 Huntsman Design Products Corp
C-033-0161 American Millwork Inc
C-033-0199 Reynolds Metals Co-Seattle Can Plant
C-033-0285 Langendorf Baking Co Of Seattle Inc.
C-033-0873 Gai's Seattle French Baking Co
C-035-0003 Navshipyd Puget Sound
C-053-0001 ASARCO
C-053-0002 Occidental Chemical Corp
C-053-0012 Stone-Consolidated Corporation
C-053-0020 U S Army Fort Lewis
C-053-0022 U S Oil & Refining Co
C-053-0028 Puget Power (Frederickson)
C-053-0085 Girard Custom Coaters Inc
C-053-0178 Tacoma City Light
C-053-0548 Northwest Pipeline Corp (Sumner)
C-053-0820 Continental Lime Inc
C-061-0039 Boeing Commercial Airplane Grp(Evrt)
C-061-0080 US Marine
C-061-0222 BF Goodrich/Tramco Inc
C-061-0237 Canyon Creek Cabinets Dba Cascade
C-061-0763 Northwest Pipeline Corp (Echo Lake)
D-029-0003 Naval Air Station
D-057-0003 Texaco Inc
D-057-0005 Shell Oil
D-057-0044 Northwest Pipeline Corp
D-057-0045 March Point Cogeneration
D-073-0005 Tosco Refining Company
D-073-0007 Arco Cherry Pt Refinery
D-073-0028 Puget Power
D-073-0031 Northwest Pipeline
D-073-0032 Encogen NW Cogeneration Plant
D-073-0033 Sumas Cogeneration/Calpine
D-073-0037 Tenaska Washington Partners, LP
E-011-0003 Great Western Malting
E-011-0009 Carborundum Co.
E-011-0013 Boise Cascade
E-011-0064 Dewils Industries
E-011-0134 America Kotobuki
E-011-0143 Attbar Inc
E-011-0144 Northwest Pipeline Corp (Washougal)
E-015-0009 Kalama Chemical
E-041-0003 Cowlitz Stud Co (Morton)
E-041-0010 Pacific Power
E-041-0051 Northwest Pipeline Corp (Chehalis)
F-009-0004 K - Ply
F-009-0007 Daishowa America
F-027-0002 Grays Harbor Paper Lp
F-027-0059 Morton International
F-045-0002 Simpson Timber Co
F-049-0004 Weyerhaeuser Co
F-067-0008 Crown Cork & Seal Co Inc
F-067-0010 Lasco Bathware
S-009-0003 Rayonier Inc
S-011-0005 James River II
S-011-0011 Vanalco Inc
S-015-0002 Longview Fibre
S-015-0003 Weyerhaeuser Co
S-015-0015 Reynolds Metals
S-015-0044 Weyerhaeuser Co
S-027-0001 Weyerhaeuser Co
S-027-0002 ITT Rayonier
S-031-0001 Port Townsend Paper
S-053-0008 Simpson Tacoma Kraft
S-053-0019 Kaiser Aluminum & Chemical
S-061-0002 Kimberly Clark
S-061-0008 Weyerhaeuser
S-061-0008 Weyerhaeuser Co
S-073-0001 Intalco Aluminum

Step 2 – Incorporate any Major Changes

Facilities were checked for large changes in emissions over the historical record. For most facilities, the considerations listed above precluded using the historical record for year-to-year changes in emissions; however, for one facility (Kalama Chemical) VOC emissions were estimated using a combination of source measurements and material balances. In this case, since there was less uncertainty involved in the historical estimates, the individual years' estimates were used in the study.

Step 3 – Estimate Emissions For Each Year

Emissions estimates for the last full year of record for each facility were used to define emissions for each year backwards to 1975 (excepting Kalama Chemical). The historical record was examined for facilities that may have started up at some time after 1975. For those facilities, emissions were only backcast to the year the facility's record began. Because of possible lag time in inserting new facilities in the record, some of the dates may not be correct. Some discretion had to be used in defining facility start dates. Estimated start dates after 1975 are listed below.

Facility ID Number	Facility	First Yr of Record
C-033-0138	Municipality of METRO	1980
C-033-0161	American Millwork	1990
C-033-0199	Reynolds Metals, Seattle	1988
C-053-0085	Girard Custom Coaters	1980
C-061-0080	US Marine	1980
D-057-0044	Northwest Pipeline	1990
D-057-0045	March Point Cogeneration	1993
D-073-0028	Puget Power	1979
D-073-0031	Northwest Pipeline	1990
D-073-0032	Encogen Northwest	1993
D-073-0033	Sumas Cogeneration	1993
D-073-0037	Tenaska Washington	1994
E-011-0134	American Kotobuki	1990
E-011-0143	Attbar, Inc	1992
E-011-0144	Northwest Pipeline	1992
E-041-0051	Northwest Pipeline	1992
F-027-0059	Morton International	1991
F-067-0008	Crown Cork & Seal	1984
F-067-0010	LASCO Bathware	1988
S-015-0044	Weyerhaueser NORPAC	1994

Step 4 – Centralia Power Plant NOx Emissions

The Centralia Power Plant is the largest point source of NOx, approximately 5-6 times larger than the next largest source. For 1992-95, the plant estimated NOx emissions using actual source measurements. These four years of source test data were used to derive an emission rate in lbs NOx per ton of coal burned. This emission factor was then applied to coal consumption for each year where there was no source test data (1975-1991).

2. Temporal and Spatial Allocation

Sources were assumed to operate uniformly 365 days per year; therefore, daily emissions were assigned $1/365^{th}$ of the total annual emissions. Spatially, each facility was located in the appropriate grid according to its UTM coordinates.

BIOGENIC SOURCES

Much of the information here was excerpted from work done by Washington State University for an ozone formation study conducted for the Dept. of Ecology.[30]

Biogenic emissions were calculated for isoprene, terpenes and other VOCs. For each of these compound classes, the following formulation was used to calculate the emission flux (mass/area/time) for a given land use of vegetation class:

$$F = Fs \times CL \times CT$$

where Fs is the class specific emission flux for the specified compound class at 30 degC and 1000 umol/m2/sec PAR (photosynthetically active radiation), CL is a light correction factor, and CT is a temperature correction factor. To perform the daily emissions calculations, the standard emission

factors and correction factors were combined with vegetation species distributions. Each is discussed below.

Species Distribution

Recent US Forest Service tree inventory data were obtained for western Washington, and these data were used to determine the distribution of forest species within Washington and northwestern Oregon. These data included tree inventory information for approximately 2,000 plots within the state. For each plot the data included number of trees, species types, tree sizes, and crown area. Plots represented approximately 3 mi. x 3 mi. areas. The information from the plots was used to determine the species distributions for each grid where a plot occurred and to determine the fraction of the grid area accounted for by the total crown area.

The gridded plot data were then combined with gridded land use obtained from the National Research council of Canada. These data were the dominant land use type in each grid for the land use types.

To combine the land use and species plot data, for each grid with a plot, the species distribution was used directly and the balance of the land area within the grid was represented by the land use type. These plot data were then interpolated using an inverse distance squared routine where the existing land use type in a grid was modified according to the interpolation results for that grid. For example, given a grid with land use type equal to rangeland, the areal contribution of species from nearby plots was calculated and the rangeland area was reduced proportionally.

Standard Emission Factors

Emission factors for isoprene, terpenes and other VOCs from the Biogenic Emission Inventory System 2 (BEIS2) are given below for standard conditions of 30 degC and 1000 umol/m2/sec PAR.[31] Land use type average emission factors are also shown.[32]

genus	example	specid	isop	ovoc	terp	%area
Abies	fir	11	170	2775	5100	2
Abies	fir	17	170	2775	5100	1
Abies	fir	22	170	2775	5100	<1
Larix	larch	42	79.3	1295	1269.3	<1
Picea	Spruce	98	23800	2775	5100	<1
Pinus	pine	108	79.3	1295	2380	<1
Pinus	pine	119	79.3	1295	2380	<1
Pinus	pine	122	79.3	1295	2380	1
Pseudotsuga	Douglas fir	202	170	2775	2720	17
Taxodium	cypress	231	42.5	693.7	1275	<1
Thuja	w. red cedar	242	170	2775	1020	3
Tsuga	e. hemlock	263	79.3	1295	158.7	9
Tsuga	e. hemlock	264	79.3	1295	158.7	<1
Acer	maple	312	42.5	693.7	680	2
Alnua	alder	351	42.5	693.7	42.5	6
Alnus	alder	361	42.5	693.7	42.5	1
Betula	birch	376	42.5	693.7	85	<1
Cornus	dogwood	492	42.5	693.7	680	<1
Fraxinus	ash	542	42.5	693.7	42.5	<1
Populus	aspen	746	29750	693.7	42.5	<1
Populus	aspen	747	29750	693.7	42.5	<1
Prunus	cherry	760	42.5	693.7	42.5	<1
Quercus	oak	815	29750	693.7	85	<1
Misc	crops	999	7.6	11.4	19	<1
Urban		1100	188.2	453.84	440.4	4
Rangeland		1300	37.8	56.7	94.5	18
Forest		1400	718	1932	1650	8
Water		1500	0	0	0	26
Barren		1700	0	0	0	<1
Tundra		1800	2412	151	121	<1

Light Correction Factors

A modification of a canopy model developed by Dr. Brian Lamb of WSU was used to develop light correction factors for isoprene emissions. For terpenes and other VOC, there is no light effect. The model calculates a light correction factor based on eight different layers throughout the forest canopy. Inputs to the model are hourly PAR and canopy type (conifer, deciduous, none).

Each species was assigned to one canopy type. PAR was calculated for each day of the year for cloud covers ranging from 0% to 100% in 10% increments. Cloud cover data was not readily available for each day of the study period (June – September, 1975-1996). For all days except July – September 1996, percent possible sunshine was available. The effects of cloud cover become pronounced at approximately 80% cover. Using percent possible sunshine as an indication of cloud cover, days with less than 20% and greater than 10% possible sunshine were assigned a cloud cover of 80%. Days with less than 10% possible sunshine were assigned a cloud cover of 90%. For July – September 1996, a 0% cloud cover was assumed.

Temperature Correction Factors

Temperature correction factors were generated for isoprene and terpenes/other VOCs. The equations used are detailed in BEIS2. Temperature corrections are made on an hourly basis. Hourly temperatures were not readily available. Hourly temperatures were estimated using daily maximum

and minimum temperatures from the Portland and SeaTac international airports.[13] The hourly temperatures were estimated by fitting to a cosine curve where the mimimun temperature was assumed to occur at 3 am (pst) and the maximum at 3 pm (pst).[33] Portland temperatures were used for all area south of UTM 5100, and SeaTac for all area north of UTM 5100.

EMISSIONS SUMMARY

Graphical summaries of NOx and VOC emissions by year and major source category are shown below. Following each graph is a brief analysis of each source category. Abbreviations used in the graph legends are: ORM – onroad mobile, NRM – nonroad mobile, Area – stationary area sources, and Point – large stationary industrial/commercial facilities.

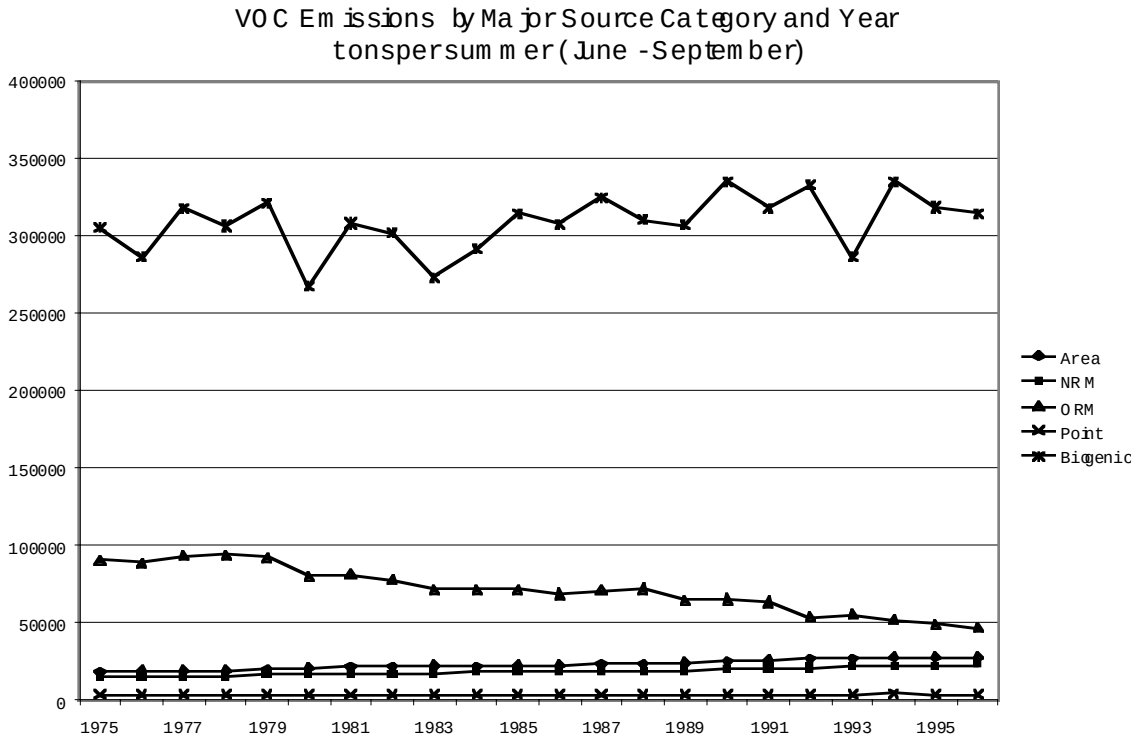

Biogenic emissions are dependent on temperature and, to a lesser degree, sunlight. The years with the lowest emissions also had lower average maximum temperatures, and the years with the highest emissions had the highest average maximum temperatures.

Onroad mobile sources VOC emissions generally decreased over the years, in spite of an increasing number of miles being driven. Federal new vehicle hydrocarbon emissions standards were set in 1975 and strengthened in 1981 and again in 1994. Fuel RVP was limited beginning in 1989 and tightened in 1992. The emissions standards and fuel RVP limits are largely responsible for the changes. Local I/M and anti-tampering programs also contributed to the downward trend.

Area and nonroad mobile source emissions were calculated based on per capita emission rates. Because of this, the emissions mirror the population trend. More specific data for these source categories could alter the trends.

Because of the uncertainty involved in the historical point source record, current point source VOC emissions were used for all years with only one exception (and it was not very significant). Any changes represent either the closure of facilities or the addition of new facilities over the years studied.

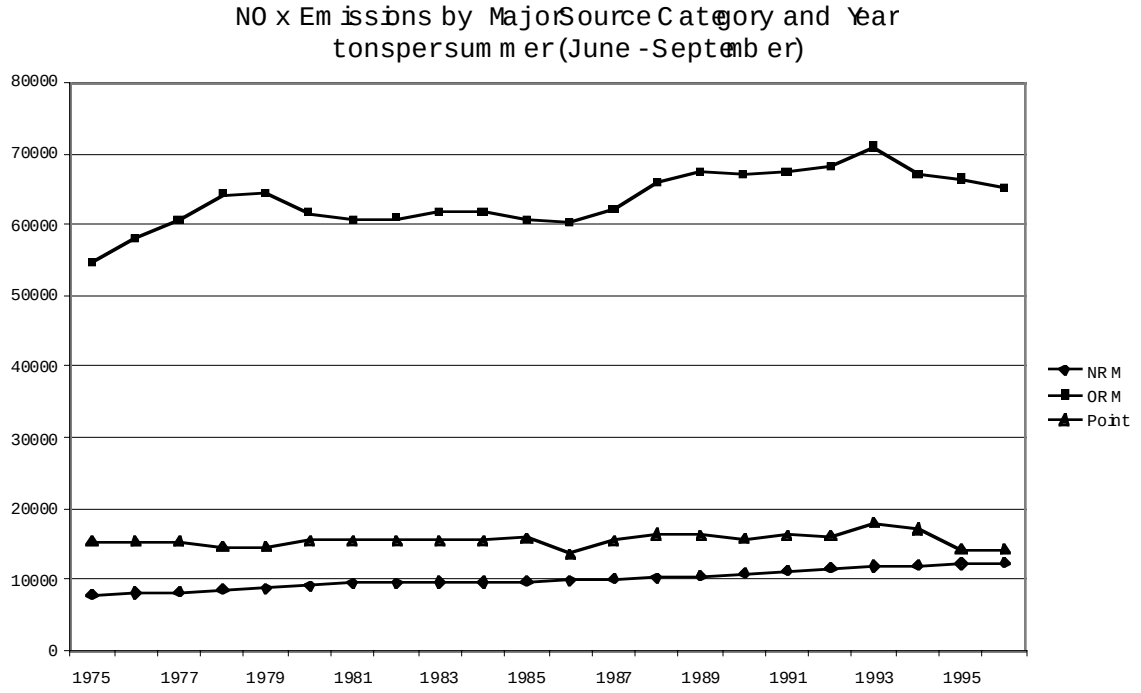

Onroad mobile source NOx emissions generally increased over the years as more miles were being driven. Federal new vehicle NOx emissions standards were set in 1981 and strengthened in 1994. The effects of the 1994 standards begin to be seen in 1995 with a reversing of the upward trend. Local I/M and anti-tampering programs were not designed to address NOx, although it is reasonable to assume that the programs would have a small NOx benefit through better vehicle maintenance.

The amplitude of the onroad mobile peak in 1993 is almost certainly exaggerated, and may actually have occurred after 1993. There are two reasons for this: 1) fleet turnover results in lower emission rates, i.e. as older vehicles are replaced with vehicles required to meet tighter standards, the emissions per vehicle decrease; however, the replacement rate has been slowing – vehicles are lasting longer. The 1990 registration distribution, used for 1975-1992 emissions calculations had a higher turnover rate than the 1995 distribution, which was used beginning in 1993. If distributions had been available for each year, the trend would have been smoother. 2) In 1994 WSDOT made changes to traffic counting methods that resulted in lowering the estimates. Examination of the miles driven data shows fewer miles driven in 1994 than 1993, which probably was not the case. If the peak proves troublesome, work could be done to normalize the 1975-93 data to the 1994-96 data.

Area and nonroad mobile source emissions were calculated based on per capita emission rates. Because of this, the emissions mirror the population trend. More specific data for these source categories could alter the trends.

Because of the uncertainty involved in the historical point source record, current point source NOx emissions were used for all years with only one exception, the Centralia power plant. Most of the variation in the point source emissions are attributable to changes in the power plant's emissions. For example, the larger decreases in the graph represent years where less coal was burned. Smaller

changes are due to either the closure of facilities or the addition of new facilities over the years studied.

REFERENCES

1 “Forecast of Fuel, Vehicles, and Related Data Through 2019”. Washingt
Transportation. Rick Judd 360-705-7937.

2 “1996 HPMS Mileage and Daily Travel Summary”. Washington State Depart
Transportation. Pat Whittaker 360-664-9681.

3 Puget Sound Regional Council, VMT data via Sierra Research.

4 Regional Transportation Council. VMT data. 1351 Officers' Row; Vancou
98661. Steve Kelley. 360-737-6067.

5 Thurston Regional Planning Council. VMT data. 2404 Heritage Court So
Washington 98502-6031. Paula Reeves. 360-786-5480.

6 Washington State Department of Transportation. VMT data from TRIPS, H
systems. Elizabeth Church (TRIPS), Pat Whitaker (HPMS), Marci Mitchel
(GIS), Lloyd Fergestrom (MPO liaison).

7 METRO. 600 Northeast Grand Avenue; Portland, Oregon 97232-2736. VMT
Peterson and Jean Alleman. 503-797-1772.

8 Cowlitz-Wahkiakum Council of Governments. VMT data. Administration A
Fourth Avenue; Kelso, Washington 98626-4195. Cecil Chen. 360-577-30

9 Skagit County Public Works Department. VMT data. Dave Baltz. 360-33

10 "Adjustment Factors for Vehicle Miles Traveled." Washington State De
Transportation. Barbara Hertzog and Hank Borden. July 1992.

11 Annual Traffic Report. Washington State Department of Transportation
(monthly traffic count data).

12 MOBILE5b. Model and User's Guide. Environmental Protection Agency, O
Sources. September 1996.

13 National Climatic Data Center. National Oceanic and Atmospheric Admi
available through internet NCDC homepage. Daily Summary data for Seat
AP, Portland International Airport. (Actually got data from Tim 1975-
Safety section June-Sep. 1996.)

14 “Motor Vehicle Registrations by Year w/n Class.” Department of Licens
1990 and July 1994 – June 1995.

15 John Raymond. Washington State Department of Ecology, I/M program d

16 Stan Sumich. Oregon Department of Environmental Quality, I/M and Anti
data. 503-731-3050, ext. 231.

17 “Final Regulatory Impact Analysis and Summary and Analysis of Comment
Gasoline Volatility Regulations. May 1990. USEPA.

18 Interoffice Memorandum from John Kowalczyk and Nick Nikkila to Merlyn
Gasoline Volatility and Stage II information. Sept. 30, 1988.

19 Jennifer Brown, Southwest Air Pollution Control Authority. 360-574-3

20 Bureau of the Census homepage. Oregon population data by county for

21 Population Trends. State of Washington Office of Financial Management
1979, 1990, 1996 (data for years 1975-1996).

22 Procedures for the Preparation of Emission Inventories for Carbon Mon
Ozone. Volume I, table 5.8.1; and Volume II, table 6-11. EPA-450/4-9
EPA-454/R-92-026, March 1992 (vol. II).

23 Population Census gridded into 5 km grids. Tom Schuettke, Washington
Ecology.

24 Procedures for the Preparation of Emission Inventories for Carbon Mon
Ozone. Volume I, tables 4.3-4. EPA-450/4-91-016, May 1991.

25 Area Source Chapter documents. Prepared by Radian Corporation for Ar
of the STAPPA-ALAPCA Emission Inventory Improvement Program (EIIP): Ar
Surface Coating (Final 11/95), Consumer and Commercial Solvent Use (Fir
Refinishing (External Draft 7/96), Graphic Arts (Final 11/96), Industri
(External Draft 7/96).

26 Procedures for Emission Inventory Preparation, Vol. IV: Mobile Sources
(Revised), Section 4.0.

27 Nonroad Engine Emission Inventories for CO and Ozone Nonattainment Bou
Tacoma. Energy and Environmental Analysis, Inc. Arlington, Virginia.
Spreadsheets dated Aug. 25 and 26, 1992 (seasonal-monthly adjustments)

28 Washington Emissions Data System, 1977-1995.

29 Aerometric Information Retrieval System Facility Subsystem.

30 An Evaluaton of the Impact of Vehicle Refueling Emissions on Ozone For
Washington. Part One: Methodology (Draft). Department of Ecology, Ju

31 Biogenic Emissions Inventory System 2. Computer Model and User's Gui
EPA.

32 Dr. Brian Lamb, Washington State University.

33 From examination of 9 days of hourly temperature data during July-Sep
days had been candidates for ozone modeling for the stage 2 vapor reco